NASA Contractor Report 4226

A Variable-Gain Output Feedback Control Design Methodology

Nesim Halyo, Daniel D. Moerder,
John R. Broussard, and Deborah B. Taylor
Information & Control Systems, Incorporated
Hampton, Virginia

Prepared for
Langley Research Center
under Contract NAS1-17493

National Aeronautics and
Space Administration
Office of Management
Scientific and Technical
Information Division

1989

TABLE OF CONTENTS

LIST OF FIGURES

LIST OF TABLES

I. INTRODUCTION

In designing control laws, the usual first step is to describe the plant at a given operating point and then to develop a control law with a satisfactory performance for that plant model. In this case, an important property of a satisfactory control law is that its performance should not deteriorate in a material way when 'small' variations in the operating condition occur; i.e., the control law should be robust, or insensitive to small variations in the, usually unmeasured, parameters describing the operating condition.

However, the design of most control systems of practical interest further requires control laws which maintain high performance in the presence of large changes in the operating point parameters. For example, the motion of an aircraft at a fixed airspeed can be described by well-known mathematical models [1]. However, the parameters of this model can vary considerably over a range of airspeeds. When dealing with large variations in the plant model parameters, a single constant-gain control law, no matter how robust, cannot attain the level of performance of a control law with variable gains. Thus, variable-gain control laws provide a class of controllers which can maintain high performance over a wide range of operating conditions. In Section II, we will formulate an optimal control problem for the design of variable-gain output feedback control laws.*

Conventional gain scheduling techniques have provided a method of designing variable-gain control systems which can accommodate significant variations in the plant operating point parameters while continuing to make use of the accumulated knowledge and experience in the design of linear systems. The ability to use the well-established theory and

*The variable-gain output feedback problem was formulated in 1983: Halyo, N., "Modern Control System Design Using Optimal Gain Scheduling,"ICS TM-83-011, Information & Control Systems, Incorporated, 28 Research Dr., Hampton, VA, 1983.

accumulated experience in the design of linear systems, while extending its use and applicability to control nonlinear systems makes the concept of variable-gain control laws highly attractive. However, the straight-forward application of the gain scheduling concept to complex systems can lead to unacceptable control system designs with deficiencies ranging from unsatisfactory performance to instability, as is discussed in the following.

Conventional Gain Scheduling

In its broadest form, the concept of gain scheduling can be applied to control systems designed using a classical frequency approach as well as a modern control approach. Modern and classical designs for practical systems using specific simple forms of gain scheduling are not uncommon; e.g., [2], [3]. Figure 1 shows a simple schedule where only one gain is programmed as a function of one parameter. Currently, the use of any type of gain scheduling in modern control system designs is less common, [4], [5], probably due to the fact that few such systems are designed for practical applications, where the need for gain scheduling becomes apparent.

The conventional approach to the design of control systems using gain scheduling consists of the following steps.

1) A small number of operating points covering the operating range are selected; the method of selection is largely arbitrary, but the designer will use his intuition and previous experience in his choice.
2) For each operating condition selected, a satisfactory linear design with the same basic structure is obtained using any available design technique.
3) Using interpolation techniques, the control system gains are expressed as a linear function (i.e., a schedule) of the parameters describing the operating conditions, so that the schedule evaluated at any of the selected operating conditions is as "close" as possible to the design made in Step 2 for that operating condition.

While the approach outlined above may result in satisfactory designs of variable-gain control systems (usually after a considerable amount of trial-and-error), some of the

problems encountered in this approach are immediately apparent from the steps outlined. Some of these problems are given below:

a) The selection of the points covering the operating range is quite arbitrary. Different selections can result in significantly different gain-scheduled control laws with differing performance characteristics. In general, the selected points are represented in the gain-schedule, while other points are not represented at all.

b) The amount of effort involved in designing a satisfactory system for each operating point can be considerable. Particularly, if many points have to be selected to cover the operating range, this effort may become impractical.

c) No matter what interpolation technique is used in Step 3, the gain schedule will not be the same as the system designed meticulously in Step 2 for the selected operating points, with the possible exception of unusual situations. Thus, even at the operating points selected, the gain-scheduled control system may not have a satisfactory performance. In fact, as demonstrated by the example below, the gain-scheduled system may even be unstable at one or more of the operating points selected.

d) There is no guarantee that the conventional gain scheduling approach outlined will result in a satisfactory or even stable (!) gain-scheduled control law over the operating range even when such a system exists.

e) The three basic steps outlined lack a control theory framework which provides insight into the solution of the problem resulting in an integrated variable-gain control law. In other words, each step is largely independent of the others; e.g., the systems designed for the particular operating conditions selected may be excellent designs for those conditions, but may collectively result in a very poor fit or an unacceptable gain-schedule.

Conventional gain scheduling is essentially a curve fitting or interpolation problem rather than a control law design problem. The shortcomings of the current approach listed above are based not only on analytical observations, but also on the experience of the

authors in the design of gain-scheduled control laws for complex and practical applications. An example of some actual problems encountered can be found in [5] which considers a gain-schedule with respect to the parameters of angle of attack, airspeed and normal acceleration for a fighter aircraft. Figure 2 shows the closed-loop mapped eigenvalues of two gain-schedules obtained using a conventional gain scheduling approach. The individual operating point designs were obtained using modern control techniques. The interpolation method used selects the fit of the control gains which maximizes the correlation coefficient of the scheduled gains and the individual designs. From Figure 2, it is seen that Schedule 1 results in an unsatisfactory, in fact unstable, design at one of the operating points selected, for the eigenvalues attributed to $\Delta\beta$ command. Schedule 2, a simpler schedule in functional form, is seen to remain stable within the complete operating range. It is interesting to note, however, that the Schedule 1 gains are closer to the original design gains for the operating point considered than the Schedule 2 gains, as can be seen in Figure 3. Yet the closer gains are unacceptable from a stability standpoint.

This example illustrates some of the remarks mentioned earlier. However, possibly a more important aspect is apparent here. The "closeness" of the schedule to the originally designed gains is not an appropriate criterion in the design of a variable-gain control system. Two gains may be "close" in most metrics (e.g., euclidean distance), but have very different stability characteristics, while gains which are not close can have more desirable and similar stability characteristics.

Thus, the use of an arbitrary interpolation technique, based on minimizing a metric defined on the control gains, is seen to be inappropriate. A design methodology which, at least directly considers the stability of the gain-scheduled systems or, if possible, guarantees the stability of the scheduled system, would clearly be superior to the current heuristic approach. Furthermore, while stability is necessary for a control system to be acceptable, a satisfactory system must usually possess further desirable characteristics which depend on the particular control tasks to be performed. Thus, a design methodology for variable-

gain control system which addresses such desirable characteristics, at every point in the operating range, while guaranteeing that the resulting closed-loop system is stable in that operating range would eliminate the major problems discussed above. Such a control system design methodology will be proposed in the following sections in the context of modern digital control theory.

II. VARIABLE-GAIN OUTPUT FEEDBACK _ FORMULATION

In this section, we will formulate an optimal control problem to design variable-gain output feedback control laws. The objective is to develop a control theory framework for the design of variable-gain controllers within which the shortcomings of conventional gain scheduling described in the preceding section can be overcome. In turn, this approach will result in a method of extending the operating range of the control law while continuing to use established linear control design and analysis techniques; i.e., a method of designing a controller for a nonlinear system using linear theory.

Consider a nonlinear system linearized at a given operating condition defined by the parameter vector, p.

$$\dot{x}(t,p) = A(p)\,x(t,p) + B(p)\,u(t,p) + w(t,p) \qquad , \tag{1}$$

$$y(t,p) = C(p)\,x(t,p) + v(t,p) \qquad , \tag{2}$$

where p is a q-vector of parameters describing the system operating point, $x(t,p)$ is a n-vector describing the plant state perturbation at time t for the given operating condition p, $y(t,p)$ is a m-vector describing the measurements or the feedback variables at time t; $w(t,p)$ and $v(t,p)$ are vector random processes of appropriate dimensions describing the plant and measurement noises, respectively, at the operating condition p, and $A(p)$, $B(p)$, $C(p)$ are matrices of appropriate dimensions which define the significant plant dynamics at the operating condition p.

As we are interested in digital controllers, we will adopt a sampled-data control approach to the problem. Thus, the control commands, $u(t,p)$, will be assumed to remain constant over the sampling interval with a duration of T seconds.

$$u(t,p) = u(k,p) \quad , \quad kT \leq t \leq (k+1)T \tag{3}$$

The continuous stochastic system described by (1), (2) and (3) can now be described by the discrete stochastic system [6].

$$x(k+1,p) = \phi(p)\, x(k,p) + \Gamma(p)\, u(k,p) + w(k,p) \quad , \tag{4}$$

$$y(k,p) = C(p)\, x(k,p) + v(k,p) \quad , \tag{5}$$

where $x(k,p)$ is the continuous state at the sampling instant kT; i.e.,

$$x(k,p) = x(kT,p) \quad , \tag{6}$$

$w(k,p)$ is the discrete plant noise sequence which is obtained from the continuous plant noise $w(t,p)$ [6], and $\phi(p)$, $\Gamma(p)$, $C(p)$ are the discretized versions of the continuous plant dynamics in (1) and (2). Note that if the control is of the form given in (3), then the discrete system in (4) describes the continuous state at the sampling instants, kT, with no approximation, as indicated by (6).

When the continuous plant noise, $w(t,p)$, is white, it can be shown that [6] the discrete plant noise is a sequence of uncorrelated random vectors; i.e., discrete white noise. In the following, we will assume that the discrete plant and measurement noises are both white sequences with zero mean; i.e.,

$$E[w(k,p)] = 0 \quad , \quad E[v(k,p)] = 0 \tag{7}$$

$$E[w(k,p)\, w^T(j,p)] = W(p)\, \delta_{k-j} \tag{8}$$

$$E[v(k,p)\, v^T(j,p)] = V(p)\, \delta_{k-j} \tag{9}$$

where δ_k is the Kronecker delta and the superscript " ^{T} " denotes the matrix transpose. Furthermore, it will be assumed that the plant and measurement noises and the initial state are uncorrelated; i.e.,

$$E[w(k,p)\, v^T(k,p)] = 0 \quad , \tag{10}$$

$$E[w(k,p)\, x^T(0,p)] = 0 \quad , \quad E[v(k,p)\, x^T(0,p)] = 0 \tag{11}$$

The control law structure of interest is the class of variable-gain output feedback controllers which may be described by

$$u(k,p) = -K(p)\, y(k,p) \tag{12}$$

where $y(k,p)$ given by (5) represents the variables which have been selected for feedback by the designer and $K(p)$ is the variable gain for the operating point, p. This controller structure is a simple extension of the 'constant gain' output feedback case treated previously [7], [8].

In many cases, performance requirements make it desirable for the controller to use dynamic compensation in the feedback loop. Therefore, it is important to note that the output feedback control structure in (12) includes control laws with dynamic compensation; e.g., consider the controller structure

$$z(k+1,p) = \phi_z(p)\, z(k,p) + \Gamma_z(p)\, y(k,p) \tag{13}$$

$$u(k,p) = -K_z(p)\, z(k,p) - K_y(p)\, y(k,p) \tag{14}$$

which contains the dynamic compensator (13) driven by the feedback vector $y(k,p)$. The control law feeds back the compensator state $z(k,p)$ as well as the feedback vector $y(k,p)$.

This controller structure is depicted in the functional block diagram in Figure 4. In this case, the matrices $\phi_z(p)$, $\Gamma_z(p)$, $K_z(p)$ and $K_y(p)$ are the control law gains to be determined in the optimization of the controller.

Select an open loop (pre-design) dynamic compensator

$$z(k+1,p) = \phi_{zo}(p)\, z(k,p) + \Gamma_{zo}(p)\, y(k,p) + u_z(k,p) \tag{15}$$

where $\phi_{zo}(p)$ and $\Gamma_{zo}(p)$ are arbitrarily selected by the designer to achieve a desired objective through the cost function. For example, $\phi_{zo}(p)$ and $\Gamma_{zo}(p)$ can simply be selected as the appropriately dimensioned zero matrices. The vector $u_z(k,p)$ is the compensator control. Augmenting the state equations in (4) by the dynamic compensator in (15), the state vector $x(k,p)$ by $z(k,p)$, the feedback vector $y(k,p)$ by $z(k,p)$ and the control vector by $u_z(k,p)$, it can be shown that

$$\begin{pmatrix} u(k,p) \\ u_z(k,p) \end{pmatrix} = - \begin{pmatrix} K_y(p) & K_z(p) \\ \Gamma_{zo}(p) - \Gamma_z(p) & \phi_{zo}(p) - \phi_z(p) \end{pmatrix} \begin{pmatrix} y(k,p) \\ z(k,p) \end{pmatrix} \tag{16}$$

is the output feedback control law for the augmented system which produces the dynamic compensator control structure given by (13) and (14). Thus, this control structure is included in the output feedback structure of (12) by augmenting the system.

Since some systems cannot be stabilized by instantaneous output feedback, the case of variable-gain dynamic compensator feedback is an important class of control laws. In the following, we will assume that the necessary augmentation to accommodate dynamic compensation has already been included in the system described by (4), (5) and (12).

At a given operating point, p, the control structure (12) corresponds to the discrete stochastic output feedback formulation of [8]. However, in the current formulation, the quantity to be optimized is not a single control gain matrix for a particular operating point, but rather it is the global control law defined by the collection of control gains over the total operating range, $\{K(p), p \epsilon \mathcal{R}\}$, where $\mathcal{R}$ is the collection of all operating points,

p, of interest for the design under consideration. Therefore, the relationship of the control gains at different operating points must be an integral part of the optimal control problem we are formulating.

Consider a linear functional relationship between the gain and the operating point parameters, i.e.,

$$K(p) = K_o + \sum_{i=1}^{q} p_i K_i \quad , \quad p \epsilon \mathcal{R} \qquad , \tag{17}$$

where the coefficient matrices $K_o, K_1, \cdots, K_q$ determine the variable-gain control law over the total operating range.

It should be noted that, since it is not feasible to compute the gain, $K(p)$, at every point of $\mathcal{R}$, it is necessary to select some type of functional relationship between the gain and the parameters, whether linear or nonlinear. While the relation in (17) is linear in the operating point parameters, p_i, these parameters can be selected as nonlinear functions of the physical variables of the plant. Thus, the linearity constraint in (17) is considerably less restrictive than is at first apparent, but provides a structure which can be handled more easily in both analytical development and actual implementation. Nevertheless, a controller structure which can handle nonlinear relationships between the control gain and the parameter vector, p, more directly will be given below.

The significant difference between the conventional gain scheduling approach and the variable-gain output feedback approach formulated here is that the latter approach does not design local control laws, but rather determines the global control law $\{K(p), p \epsilon \mathcal{R}\}$ by optimizing a control objective over many operating points. If some operating points have less stability margin than others, the optimization automatically places greater emphasis on those operating conditions.

Nonlinear relationships between the control gain and the operating condition parameters can be treated in the following manner. Let $H_i(p)$ be a $r \times r$ matrix of real functions of p, for each $i = 1, 2, \cdots, q$. As in (17), K_i is a $r \times m$ matrix for $i = 0, 1, \cdots, q$. Now

consider the relation

$$K(p) = K_o + \sum_{i=1}^{q} H_i^T(p)\, K_i \quad , \quad p \in \mathcal{R} \quad . \tag{18a}$$

The elements of the matrices $H_i(p)$ are arbitrarily selected integrable functions of p which may contain nonlinearities in terms of p. We will refer to this relation as a separable form, since the operating point parameter, p, and the gain coefficient matrices, K_i, are separately expressed. The dual form

$$K(p) = K_o + \sum_{i=1}^{q} K_i\, G_i(p) \quad , \quad p \in \mathcal{R} \tag{18b}$$

where $G_i(p)$ is a $m \times m$ matrix of real functions of p will also be considered.

It should be noted that the linear relationship in (17) is a special case of the separable form in (18). The following selection of $H_i(p)$ in (18) results in (17),

$$H_i(p) = p_i\, I \quad , \quad 1 \leq i \leq q \quad . \tag{19}$$

Thus, the variable-gain output feedback control law structure will be defined by (12) and (18), resulting in a feedback law of the form

$$u(k,p) = -\left[K_o + \sum_{i=1}^{q} H_i^T(p)\, K_i\right] y(k,p) \quad , \quad p \in \mathcal{R} \quad . \tag{20}$$

Following the optimal quadratic sampled data formulation, consider a cost or objective function of the form

$$J_{\ell c}(K(p),p) = \lim_{t_f \to \infty} \frac{1}{t_f} \int_o^{t_f} E\{x(t,p)^T Q_c(p)\, x(t,p) + u(t,p)^T R_c(p)\, u(t,p)\}\, dt \tag{21}$$

where E denotes the expectation operator. We will refer to $J_{\ell c}$ as the local continuous objective function as it expresses the objective at the operating point, p. It can be shown

that the local continuous objective function $J_{\ell c}$ is equivalent to a local discrete objective function [6]. In this study, we will use the form

$$J_\ell(K(p),p) = \lim_{N\to\infty} \frac{1}{2(N+1)} \sum_{k=0}^{N} E\{x(k+1,p)^T Q(p)\, x(k+1,p) + u(k,p)^T R(p)\, u(k,p)\} \tag{22}$$

as the local objective function for the discrete optimization problem. For simplicity, cross-terms between state and control are not included in the objective functions (21) and (22).

Since the parameter vector, p, has q components, the operating range, $\mathcal{R}$, is a subject of R^q, where R denotes the reals. The operating range may be defined by the constraints

$$a_i \le p_i \le b_i \quad , \quad 1 \le i \le q \tag{23}$$

where p_i is the i^{th} component of the parameter vector p, a_i and b_i are the minimum and maximum values of that i^{th} component, respectively. For notational convenience, we will express (23) by

$$a \le p \le b \tag{24}$$

where in (20) "$\le$" is a partial ordering on R^q.

In this formulation, the quantity to be optimized is not a single control gain for a particular operating point, but rather it is the global control law defined by the collection of control gains over the total operating range $\{K(p), p \in \mathcal{R}\}$. Similarly, the objective or cost function for the design problem is not a local objective corresponding to the system performance at a single operating point, but a global objective with performance specifications over the complete operating range, $\mathcal{R}$. Thus, the cost function for the design problem can be selected as

$$\bar{J} = \int_{a_1}^{b_1} \cdots \int_{a_q}^{b_q} f(p)\, J_\ell(K(p), p)\, dp_q \cdots dp_1 = \int_a^b f(p) J_\ell(K(p), p)\, dp \qquad (25)$$

where $f(p)$ is an non-negative scalar function of p selected by the designer to allow greater weighting of certain regions of the operating range over other regions. The shorthand notation on the right-hand-side of (25) uses a single integral sign from the vector a to b to denote q scalar integrals.

In general, the operating range, $\mathcal{R}$, need not be of the form of (23) and (24). Thus, in general, the desired global objective function for the variable-gain output feedback problem is

$$\bar{J}(K) = \int_{\mathcal{R}} f(p)\, J_\ell(K(p), p)\, dp \qquad (26)$$

where the local cost functions $J_\ell(K(p), p)$ are weighted over the operating range, and

$$K = \begin{pmatrix} K_o \\ K_1 \\ \vdots \\ K_q \end{pmatrix} \qquad (27)$$

The notation on the left-hand-side of (26) simply recognizes that for the feedback structure selected, the global cost is determined by the choice of K.

A discrete version of the global cost $\bar{J}$ can be expressed as

$$J(K) = \sum_{j=1}^{M} f_j\, J_\ell(K(p^j), p^j) \qquad , \qquad (28)$$

where J_ℓ is defined by (22), f_j is the discrete weighting for the j^{th} operating point p^j and $\{p^j, j = 1, 2, \cdots, M\}$ correspond to the plant operating points of interest for the design. This version of the cost function may also be considered an Euler approximation of the continuous cost function in (27).

The variable-gain output feedback control law design can now be posed as a stochastic optimal control problem. The optimization consists of finding a variable-gain control law,

$K(p)$, over the design operating range $\mathcal{R}$, which minimizes the cost function $\bar{J}$ or the discrete version J, subject to the constraints of (4) - (12) and (18).

The optimal control approach taken here puts the variable-gain design problem into a firm theoretical setting. The desired characteristics of the controller are specified from the outset. No interpolation or curve fitting of local control laws arises in this approach. Since an instability at an arbitrary operating point would result in an infinite cost locally and globally for most practical systems, the optimal variable-gain control law will stabilize all the operating points considered in the design. Finally, the problem is formulated in a modern control setting for direct-digital-design and is compatible with previous developments on stochastic output feedback [8], [9], [10], [11], [12], [13], [14].

III. NECESSARY CONDITIONS AND INCREMENTAL COST

In this section, we will obtain the necessary conditions for optimality of the variable-gain output feedback control problem posed in the previous section. Rather than using the Lagrangian approach and differentiating the augmented cost function to obtain the necessary conditions, we will follow the approach initiated in [8] of obtaining the incremental cost. From the latter, as in the stochastic output feedback and decentralized control cases, the necessary conditions will be apparent.

At a given operating condition specified by the parameter vector, p, the system has the form of the standard stochastic output feedback problem defined by (4) - (12).

Following [8], define the symmetric non-negative definite matrix P evaluated at the gain $K(p)$ as the solution of the discrete Lyapunov equation

$$\begin{aligned} P(K(p)) =& \phi^T(K(p),p)\, P(K(p))\, \phi(K(p),p) \\ &+ C^T(p)\, K^T(p)\, R(p)\, K(p)\, C(p) + Q(p) \quad , \quad p \in \mathcal{R} \end{aligned} \tag{29}$$

where

$$\phi(K(p),p) = \phi(p) - \Gamma(p)\, K(p)\, C(p) \quad , \quad p \in \mathcal{R} \tag{30}$$

is the closed-loop transition matrix at the operating point, p.

From Lemma 1 in [8], it is known that for all gains $K(p)$ which stabilize the closed-loop plant, i.e.,

$$\rho(\phi(K(p),p)) < 1 \tag{31}$$

the Lyapunov equation (29) has a non-negative definite solution, $P(K(p))$.* In (31), $\rho(\phi)$ denotes the spectral radius of the matrix, ϕ; i.e., the value of the largest magnitude among the eigenvalues of ϕ.

Furthermore, it can be shown that the local cost $J_\ell(K(p),p)$ at the operating condition, p, given in (22) can be expressed in terms of the non-negative definite matrix $P(K(p))$ when the closed-loop system is stabilized by the output feedback gain matrix, $K(p)$.

LEMMA 1.

If $\rho(\phi(K(p),p)) < 1$, then the local cost $J_\ell(K(p),p)$ defined in (22) is finite and is given by

$$J_\ell(K(p),p) = \frac{1}{2}\mathrm{tr}\left\{P(K(p))\,W(p)\right\} + \frac{1}{2}\mathrm{tr}\left\{K^T(p)\left[\Gamma^T(p)\,P(K(p))\,\Gamma(p) + R(p)\right]\,K(p)\,v(p)\right\} \tag{32}$$

where $P(K(p))$ is the solution of (24).

This results if a direct consequence of Lemma 2 in [8] and will not be proved here. It states that if the output feedback gain matrix $K(p)$ stabilizes the open loop plant at p, then the limit in (22) converges to a finite cost $J_\ell(K(p),p)$. When the plant $(\phi(p),\Gamma(p),C(p)$ is output stabilizable at p, then some gain, $K(p)$, stabilizes the plant and achieves a finite cost. If the plant is output stabilizable at all operating points of interest in $\mathcal{R}$, then some variable-gain $\{K(p), p \in \mathcal{R}\}$ will achieve a finite global cost for finite selections of $\mathcal{R}$.

*Note that P depends both on the feedback gain $K(p)$ as well as the operating condition p. For notational convenience, the dependence on p is not explicitly shown in the above, to avoid writing $P(K(p),p)$.

We will define the stability sets

$$S(p) = \{K | \rho(\phi(K,p)) < 1\} \quad , \quad p \in \mathcal{R} \tag{33}$$

$$S = \{\{K(p), p \in \mathcal{R}\} | K(p) \in S(p) \,, \ \forall p \in \mathcal{R}\} \tag{34}$$

Thus, $S(p)$ is the set of all output feedback gains matrices, K, which stabilize the plant at the operating point, p. Whereas S is the collection of variable-gain output feedback matrices which stabilize the plant at every operating point in $\mathcal{R}$. Clearly, the plant must be output stabilizable for all operating points of interest for S to be nonnull.

To obtain the global cost functions given by (26) and (28), it is sufficient to integrate or sum the local cost in (32) over the appropriate points. Thus,

$$\begin{aligned} \bar{J}(K) = & \frac{1}{2} \int_{\mathcal{R}} f(p) \operatorname{tr} \{P(K(p)) W(p)\} \, dp \\ & + \frac{1}{2} \int_{\mathcal{R}} f(p) \operatorname{tr} \left\{ K^T(p) \, \hat{P}(K(p)) \, K(p) \, V(p) \right\} dp \end{aligned} \tag{35}$$

$$\begin{aligned} J(K) = & \frac{1}{2} \sum_{j=1}^{M} f_j \Big[\operatorname{tr} \{P(K(p^j)) W(p^j)\} \\ & + \operatorname{tr} \left\{ K^T(p^j) \, \hat{P}(K(p^j)) \, K(p^j) \, V(p^j) \right\} \Big] \end{aligned} \tag{36}$$

where

$$\hat{P}(K(p)) = \Gamma^T(p) \, P(K(p)) \, \Gamma(p) + R(p) \quad , \quad p \in \mathcal{R} \quad . \tag{37}$$

Note that, following the notation used for $P(K(p))$, we neglect to explicitly show the dependence of $\hat{P}$ on p, but show the dependence on $K(p)$, for notational convenience.

In (35), the integration is over a subset of R^q, namely over $\mathcal{R}$, and may be interpreted as q scalar integrals. In (36), the points $\{p^j, j = 1, 2, \cdots, M\}$ represent the operating points of special interest in $\mathcal{R}$.

At this point, the optimization of the variable-gain output feedback control is one of minimizing the global cost functions in (35) and (36) over the gains K which stabilize the closed-loop system. Since matrix Lyapunov equation solvers are readily available, the integrand in (35) and (36) can be computed at the desired values to perform the integration or summation. However, as the order of the systems considered increases, the numerical aspects of the optimization can be cumbersome.

The incremental cost refers to the change in the cost due to a change in the control gains. For the local cost function $J_\ell(K(p),p)$, the incremental cost at a given operating condition will be denoted by $\Delta J(K(p),\Delta K(p),p)$ and will be defined as

$$\Delta J_\ell(K(p),\Delta K(p),p) = J_\ell(K(p)+\Delta K(p),p) - J_\ell(K(p),p) \quad , \quad p \in \mathcal{R} \quad , \tag{38}$$

where $\Delta K(p)$ is the change in the gain for the operating condition p.

Let $K(p)$ and $K(p)+\Delta K(p)$ belong to $S(p)$. Then, the incremental cost can be shown to be

$$\begin{aligned}\Delta J_\ell(K(p),\Delta K(p),p) = \frac{1}{2}\mathrm{tr}\Big\{2\Delta K^T(p)\Big[&\hat{P}(K(p)+\Delta K(p))\,K(p)\hat{S}(K(p)) \\ &- \Gamma^T(p)\,P(K(p)+\Delta K(p))\,\phi(p)\,S(K(p))\,C^T(p)\Big] \\ &+ \Delta K^T(p)\,\hat{P}(K(p)+\Delta K(p))\,\Delta K(p)\,\hat{S}(K(p))\Big\} \quad , \quad p \in \mathcal{R}\end{aligned} \tag{39}$$

where $S(K(p))$ is the solution to the Lyapunov equation.

$$\begin{aligned}S(K(p)) = &\,\phi(K(p),p)\,S(K(p))\phi^T(K(p),p) \\ &+ \Gamma(p)\,K(p)\,V(p)\,K^T(p)\,\Gamma^T(p) + W(p) \quad ,\end{aligned} \tag{40}$$

$$\hat{S}(K(p)) = C(p)\,S(K(p))\,C^T(p) + V(p) \quad . \tag{41}$$

As for P and $\hat{P}$, S and $\hat{S}$ depend on $K(p)$ and p, although the dependence to the latter is explicitly shown. It is interesting to note that $S(K(p),p)$ is the steady-state covariance of the state $x(k,p)$ when the control law $K(p)$ closes the loop; i.e.,

$$S(K(p),p) = \lim_{k\to\infty} E\left\{x(k,p)\, x^T(k,p)\right\} \quad . \tag{42}$$

To obtain the global incremental cost it is necessary to integrate (39) over the operating points of interest. However, before taking that step, note that the variable-gain output feedback control structure which we have selected is of the form of (18). Now, let us form the matrix

$$H(p) = \begin{pmatrix} I \\ H_1(p) \\ \vdots \\ H_q(p) \end{pmatrix} \quad , \quad p \in \mathcal{R} \tag{43}$$

Then,

$$K(p) = H^T(p)\, K \quad , \quad p \in \mathcal{R} \quad . \tag{44}$$

$$\Delta K(p) = H^T(p)\, \Delta K \quad , \quad p \in \mathcal{R} \quad . \tag{45}$$

Now, substituting (44) and (45) into (39), and combining the result with the global cost function in (35), we obtain

$$\Delta \bar{J}(K, \Delta K) = \bar{J}(K + \Delta K) - \bar{J}(K) \tag{46}$$

$$\begin{aligned} &= \frac{1}{2}\mathrm{tr}\left\{2\Delta K^T \int_{\mathcal{R}} f(p)\, H(p) \Big[\hat{P}(K(p) + \Delta K(p))\, K(p) \hat{S}(K(p)) \right. \\ &\left. - \Gamma^T(p)\, P(K(p) + \Delta K(p))\, \phi(p)\, S(K(p))\, C^T(p)\Big]\, dp \right. \\ &\left. + \Delta K^T \int_{\mathcal{R}} f(p)\, H(p)\, \hat{P}(K(p) + \Delta K(p))\, \Delta K(p)\, \hat{S}(K(p))\, dp \right\} \end{aligned} \tag{47}$$

Similarly, the incremental cost for the discrete cost function in (28) can be found to result in

$$\Delta J(K,\Delta K) = J(K+\Delta K) - J(K) \tag{48}$$

$$\begin{aligned} &= \frac{1}{2}\mathrm{tr}\left\{ 2\Delta K^T \sum_{j=1}^{M} H(p^j)\Big[\hat{P}(K(p^j)+\Delta K(p^j))\,K(p^j)\hat{S}(K(p^j)) \right. \\ &- \Gamma^T(p^j)\,P(K(p^j)+\Delta K(p^j))\,\phi(p^j)\,S(K(p^j))\,C^T(p^j)\Big] \\ &\left. +\Delta K^T \sum_{j=1}^{M} f_j\,H(p^j)\,\hat{P}(K(p^j)+\Delta K(p^j))\,\Delta K(p^j)\,\hat{S}(K(p^j)) \right\} \end{aligned} \tag{49}$$

It should be noted that the expressions obtained in (48) and (49) are not approximations such as first or second order variations of the cost, but rather represent the total change in the cost. Also note that the separable form selected for the gain in (18) is partially responsible for the form of the global incremental cost.

From these expressions, the necessary conditions for optimality are easily obtained. Due to the form of the incremental cost, the gradient of the global cost due to a small change in the control gains, ΔK, can be obtained by observation.

$$\begin{aligned} \frac{\partial \bar{J}}{\partial K}(K) = \int_{\mathcal{R}} H(p)\Big[&\hat{P}(K(p))\,K(p)\,\hat{S}(K(p)) \\ &- \Gamma^T(p)\,P(K(p))\,\phi(p)\,S(K(P))\,C^T(p)\Big]\,f(p)\,dp \end{aligned} \quad , \tag{50}$$

where $K(p)$ and $\Delta K(p)$ are given by (44) and (45).

Setting the gradient to zero results in the necessary conditions. It may be of interest to partition the necessary conditions in the form:

$$\int_{\mathcal{R}} H_i(p)\,\hat{P}(K(p))\,K(p)\,\hat{S}(K(p))\,f(p)\,dp$$
$$= \int_{\mathcal{R}} H_i(p)\Gamma^T(p)\,P(K(p))\,\phi(p)\,S(K(p))\,C^T(p)\,f(p)\,dp \quad ,$$
$$i = 0, 1, \cdots, q \tag{51}$$

where

$$H_o(p) = I \quad . \tag{52}$$

The necessary conditions for the linear case can be obtained simply by substituting (19) into (51). The gradient and necessary conditions for the discrete global cost function can be obtained following the same procedure explained above, resulting in

$$\frac{\partial J}{\partial K}(K) = \sum_{j=1}^{M} H(p^j)\Big[\hat{P}(K(p^j))\,K(p^j)\,\hat{S}(K(p^j))$$
$$- \Gamma^T(p^j)\,P(K(p^j))\,\phi(p^j)\,S(K(p^j))\,C^T(p^j)\Big]\,f_j \tag{53}$$

$$\sum_{j=1}^{M} H_i(p^j)\,\hat{P}(K(p^j))\,K(p^j)\,\hat{S}(K(p^j))\,f_j$$
$$= \sum_{j=1}^{M} H_i(p^j)\,\Gamma^T(p^j)\,\hat{P}(K(p^j))\,\phi(p^j)\,S(K(p^j))\,C^T(p^j)\,f_j \quad ,$$
$$i = 0, 1, \cdots, q \quad . \tag{54}$$

The solution of the necessary conditions would provide a potential solution to the optimal control problem, since any critical point of the global cost function will satisfy these conditions. Using the expressions developed for the gradient, it is possible to use standard gradient-based minimization techniques to obtain the optimal solution.

However, in the following section, we will show that the variable-gain output feedback problem can be embedded into the Multi-Configuration Control (MCC) problem which ICS has solved previously, and use the MCC algorithm to obtain the optimal gain.

IV. EMBEDDING INTO MULTI-CONFIGURATION CONTROL AND ALGORITHM DEVELOPMENT

In this section, we will obtain a solution for the optimal control problem posed using the discrete cost function (28) by embedding it into an already solved problem, namely, the Multi-Configuration Control (MCC) problem [9]. While standard minimization techniques can be applied using the expressions for the gradient obtained in the last section, these would not make use of any special knowledge about the form of the cost or incremental cost function. Whereas the approach used here makes use of some of the known characteristics of the cost function.

From the familiar form of the expressions developed in the last section, it may be conjectured that the solution of the variable-gain output feedback problem may be simplified. In fact, the similarities among the standard stochastic output feedback problem [8], the MCC problem [9], the decentralized control problem [9] and the variable-gain output feedback problem investigated here are largely due to the fact that the incremental cost function can be expressed in a similar form for each of these problems.

Multi-Configuration Control

First we will describe the Multi-Configuration Control (MCC) problem. The motivation for the MCC problem is the development of a modern control technique for the design of highly robust output feedback control systems; e.g., a single control law that can control a plant which has many configurations or many operating points. In comparison to the variable-gain controller, the MCC technique produces a constant-gain control law whose performance does not deteriorate as much as others when the plant operating points change without notice. Clearly, a variable-gain control law can provide better performance than a constant-gain control law when the operating point parameters are measured or estimated with sufficient accuracy.

Consider the plant described by (4) and (5). Suppose that we want to design a constant-gain output feedback control law which can operate not only at one nominal operating condition, but also at several other operating conditions. The form of the control law is given by

$$u(k,p) = -K\, y(k,p) \qquad , \qquad p \epsilon \{p^j, j = 1,2,\cdots,M\} \tag{55}$$

where it is seen that the control gains do not depend on the operating condition. Therefore, the controller must perform satisfactorily, but at least be stable, at all the operating conditions considered.

The optimal control problem posed by the global cost function given in (28), the plant (4)-(11) and the control structure (55), is referred to as the Multi-Configuration Control (MCC) or the Multiple Model Control problem [9]. The MCC problem has been treated and an algorithm to obtain the optimal MCC design has been presented in [9] and will not be repeated here.

As can be seen from the formulations of the MCC and the variable-gain output feedback control problems, the essential difference is in their control structures (55) and (12). Thus, to embed the latter into the former problem is a question of accommodating the control structures of these problems.

Embedding into MCC

The selection of the separable forms for the variable-gain control structure given in (18) provide the needed step for embedding. First, we will consider the separable form in (18a). For this case, recall that the gain can be written as

$$K(p) = H^T(p)\, \mathcal{K} \qquad , \qquad p \epsilon \mathcal{R}$$

where $H(p)$ is defined in (43) and $\mathcal{K}$ in (27).

Now, define the augmented control vector, $\bar{u}(k,p)$, which is constrained to feed back only the variables $y(k,p)$ through constant gains; i.e.,

$$\bar{u}(k,p) = -\mathcal{K}\, y(k,p) = -\begin{pmatrix} K_o \\ K_1 \\ \vdots \\ K_q \end{pmatrix} y(k,p) \tag{56}$$

Note that the augmented control vector $\bar{u}(k,p)$ has $(q+1)r$ components.

In the same vein, define the augmented control effectiveness matrix, $\bar{\Gamma}(p)$, as

$$\bar{\Gamma}(p) = \Gamma(p)\, H^T(p) = \begin{pmatrix} \Gamma(p) & \Gamma(p)H_1^T(p) & \cdots & \Gamma(p)H_q^T(p) \end{pmatrix} \tag{57}$$

With these definitions, note that

$$\bar{\Gamma}(p)\, \bar{u}(k,p) = -\Gamma(p)\, H^T(p)\, \mathcal{K}\, y(k,p) \qquad , \tag{58}$$

$$x(k+1,p) = \phi(p)\, x(k,p) + \bar{\Gamma}(p)\, \bar{u}(k,p) + w(k,p) \tag{59}$$

Thus, the plant state remains the same, while the control vector is augmented but still restricted to the feedback vector, $y(k,p)$, given by (5).

Finally, define the augmented control cost matrix, $\bar{R}(p)$, by

$$\bar{R}(p) = H(p)\, R(p)\, H^T(p) = \begin{pmatrix} R(p) & R(p)H_1^T(p) & \cdots & R(p)H_q^T(p) \\ H_1(p)R(p) & H_1(p)R(p)H_1^T(p) & & \\ \vdots & & & \\ H_q(p)R(p) & & & H_q(p)R(p)H_q^T(p) \end{pmatrix} \tag{60}$$

It follows that the local, hence global, cost functions in (22) and (28), can be expressed in terms of the augmented control vector in a quadratic form.

$$J_\ell(K(p),p) = \lim_{N\to\infty} \frac{1}{2(N+1)} \sum_{k=o}^{N} E\left\{x(k+1,p)^T\, Q(p)\, x(k+1,p) + \bar{u}(k,p)^T\, \bar{R}(p)\, \bar{u}(k,p)\right\} \tag{61}$$

$$J(\mathcal{K}) = \sum_{j=1}^{M} f_j\, J_\ell(K(p^j),p^j) \tag{62}$$

The augmented plant model (59), the feedback vector (5), the constant-gain control law of (56) and the global cost in (62) define a Multi-Configuration Control design problem, which can be solved using the MCC algorithm. The optimal control gain matrix, say $\mathcal{K}^*$, obtained for this problem also provides the optimal variable-gain control law, say $K^*(p)$, for the problem posed in Section II through the relation

$$K^*(p) = H^T(p)\, \mathcal{K}^* \tag{63}$$

The dual of the previous development is obtained when the separable form in (18b) is used as the control structure. In this case, rather than augmenting the control vector, the feedback vector is augmented. Thus, let

$$\bar{\mathcal{K}} = (K_o\, K_1 \cdots K_q) \quad , \tag{64}$$

$$G(p) = \begin{pmatrix} I \\ G_1(p) \\ \vdots \\ G_q(p) \end{pmatrix} \quad , \tag{65}$$

$$K(p) = \bar{\mathcal{K}}\, G(p) \quad . \tag{66}$$

Define the augmented feedback vector, $\bar{y}(k,p)$, as

$$\bar{y}(k,p) = G(p)\, y(k,p) = \bar{C}(p)\, x(k,p) + \bar{v}(k,p) \quad , \tag{67}$$

$$\bar{C}(p) = G(p)\, C(p) = \begin{pmatrix} C(p) \\ G_1(p)C(p) \\ \vdots \\ G_q(p)C(p) \end{pmatrix} \quad , \tag{68}$$

$$\bar{v}(k,p) = G(p)\, v(k,p) \tag{69a}$$

$$\bar{V}(p) = E\{\bar{v}(k,p)\, \bar{v}^T(k,p)\} \tag{69b}$$

$$\bar{V}(p) = G(p)\, V(p)\, G^T(p) = \begin{pmatrix} V(p) & V(p)G_1^T(p) & \cdots & V(p)G_q^T(p) \\ G_1(p)V(p) & & & \\ \vdots & & & \\ G_q(p)V(p) & & & G_q(p)V(p)G_q^T(p) \end{pmatrix} \tag{70}$$

$$u(k,p) = -\bar{K}\, \bar{y}(k,p) \quad . \tag{71}$$

The plant model given by (4), the feedback vector given by (67)-(70), the control constraint given by (71) and the cost function in (28) pose an optimal Multi-Configuration Control problem whose solution, say $\bar{K}^*$, provides the optimal variable-gain output feedback control law in the form of

$$K^*(p) = \bar{K}^*\, G(p) = K_o^* + \sum_{i=1}^{q} K_i^*\, G_i(p) \quad . \tag{72}$$

The optimal variable-gain output feedback problem has thus been embedded in the MCC problem whose solution can be obtained by the algorithm described in the following when the original problem is augmented as described above. It should be noted that this development has been obtained at the expense of augmenting the control or feedback vectors according to which form is used, which increases the dimension of the corresponding vector. This increase in dimension is proportional to the number of elements used in the separable form (18) of the control law. Thus, the complexity of the selected variable-gain

control law proportionally determines the dimension, hence the numerical complexity, of the problem to be solved.

Algorithm Development

As described in the preceding, the variable-gain output feedback problem must first be transformed into a Multi-Configuration Control (MCC) problem. Then, the MCC output feedback algorithm can be used to obtain a critical point of the global cost function. The following algorithm can be used to obtain the gain $\bar{K}^*$ defined by (64).

Variable-Gain Output Feedback Algorithm

1. Embed the variable-gain problem into the MCC form by augmentation, using the augmented constant gain $\bar{K}$.
2. Select an initial stable gain $\bar{K}_o$, $\alpha_o = 1, z > 1, i = 0$.
3. Solve the Lyapunov equations $j = 1, 2, \cdots, M$.

$$\phi_j(\bar{K}_i) = \phi(\bar{K}_i\, G(p)\, p^j) \quad , \quad \Gamma_j = \Gamma(p^j) \quad , \quad C_j = \bar{C}(p^j)$$

$$Q_j = Q(p^j) \quad , \quad R_j = R(p^j) \quad , \quad W_j = W(p^j) \quad , \quad V_j = \bar{V}(p^j)$$

$$P_j(\bar{K}_i) = \phi_j(\bar{K}_i)^T P_j(\bar{K}_i)\, \phi_j(\bar{K}_i) + C_j^T \bar{K}_i^T R_j\, \bar{K}\, C_j + Q_j$$

$$S_j(\bar{K}_i) = \phi_j(\bar{K}_i) S_j(\bar{K}_i)\, \phi_j(\bar{K}_i)^T + \Gamma_j\, \bar{K}_i\, V_j\, \bar{K}_i^T\, \Gamma_j^T + W_j$$

If $P_j(\bar{K}_i)$ or $S_j(\bar{K}_i)$ is not non-negative definite, go to 6.

4. Solve for the direction $d(\bar{K}_i)$

$$\sum_{j=1}^{M} f_j\, \hat{P}_j(\bar{K}_i)\, d(\bar{K}_i)\, \hat{S}_j(\bar{K}_i) = -\frac{\partial J}{\partial \bar{K}}(\bar{K}_i)$$

where $\hat{P}_j(\bar{K}_i)$, $\hat{S}_j(\bar{K}_i)$ and $\frac{\partial J}{\partial \bar{K}}(\bar{K}_i)$ are given in (37), (41) and (53), respectively and f_j is the discrete weighting of the jth operating point in (28); now compute the new gain

$$\bar{K}_{i+1} = \bar{K}_i + \alpha_i\, d(\bar{K}_i)$$

5. Compute the cost $J(\bar{K}_i)$. If $i = 0$, set $i = 1$, go to 3. If

$$J(\bar{K}_i) - J(\bar{K}_{i-1}) < 0$$

then go to 7.*

6. Reduce step

$$\alpha_i = \alpha_i / z \quad , \quad (\bar{K}_i) = (\bar{K}_{i-1}) \quad , \quad d(\bar{K}_i) = d(\bar{K}_{i-1})$$

$$(\bar{K}_{i-1}) = (\bar{K}_i) + \alpha_i\, d(\bar{K}_i) \quad , \quad \alpha_{i+1} = \alpha_i \quad , \quad i = i + 1 \quad , \quad \text{go to 3.}$$

7. Check convergence criteria; if not converged, go to 3.

The algorithm described above was coded for the case of linear relationship between gain and operating conditions; namely, $G_i(p) = p_i, i = 1, 2, \cdots, q$. When the number of controls and the number of feedback variables in the problem are large, solving for the iterative direction, $d(\bar{K}_i)$, in step 4 is quite difficult and computationally costly. In variable-gain output feedback problems, these dimensions are often large due to the augmentation in transforming the problem into the MCC form.

*This condition may be replaced by the alternative condition
$J(\bar{K}_i) - J(\bar{K}_{i-1}) < \frac{\alpha_{i-1}(2 - \alpha_{i-1})}{4} \sum_{j=1}^{M} f_j \text{ tr} \left\{ d(\bar{K}_{i-1})^T \hat{P}_j(\bar{K}_{i-1})\, d(\bar{K}_{i-1})\, \hat{S}_j(\bar{K}_{i-1}) \right\}$,
which would produce a greater improvement per iteration in the absence of numerical errors.

To increase the speed and accuracy of the algorithm, a new method of solving the direction $d(\bar{K})$ was developed. First, note that the equation can be rewritten in terms of Kronecker products, $\otimes$:

$$\left[\sum_{j=1}^{M} f_j \, \hat{S}_j(\bar{K}) \otimes \hat{P}_j(\bar{K})\right] v\{d(\bar{K})\} = -v\left\{\frac{\partial J}{\partial \bar{K}}(\bar{K})\right\} \tag{73}$$

where $v\{\cdot\}$ is the column vector form of the gain matrix in brackets. Thus, obtaining $d(\bar{K})$ requires the inversion of a large matrix in brackets in (73). To reduce the computational load involved, first we will make the following approximation by minimizing

$$\| \sum_{j=1}^{M} f_j \, \hat{S}_j \otimes \hat{P}_j - \tilde{S} \otimes \tilde{P} \|^2 \quad , \tag{74}$$

where the argument $\bar{K}$ has been dropped for convenience. When $\tilde{S}$ and $\tilde{P}$ are known, the required inverse is easily obtained by noting that

$$\left(\tilde{S} \otimes \tilde{P}\right)^{-1} = \tilde{S}^{-1} \otimes \tilde{P}^{-1} \tag{75}$$

After considerable manipulation, it can be shown that $\tilde{S}$ and $\tilde{P}$ satisfy

$$\tilde{S} = \frac{1}{\| \tilde{P} \|^2} \sum_{j=1}^{M} f_j \, \hat{S}_j \, \mathrm{tr}\{\hat{P}_j \, \tilde{P}\} \tag{76}$$

$$\tilde{P} = \frac{1}{\| \tilde{S} \|^2} \sum_{j=1}^{M} f_j \, \hat{P}_j \, \mathrm{tr}\{\hat{S}_j \, \tilde{S}\} \tag{77}$$

Numerical experience indicates that iterating on (76) and (77) results in robust and rapid convergence to a solution which is a sufficiently good approximation. However, even with this approach, inverting $\tilde{S}$ and $\tilde{P}$ can be difficult when $\tilde{S}$ is obtained by augmentation from the variable-gain problem. $\tilde{S}$ is then dimensioned $(q+1)m \times (q+1)m$. To alleviate this problem, we minimize

$$\|\tilde{S} - \tilde{S}_1 \otimes \tilde{S}_2\|^2 \tag{78}$$

where $\tilde{S}_1$ is dimensioned $(q+1) \times (q+1)$ and $\tilde{S}_2$ is dimensioned $m \times m$.

We will use the following notation. The i,j element of any matrix A will be denoted by $[A]_{ij}$. The $(q+1)m \times (q+1)m$ matrix $\tilde{S}$ will be partitioned as shown below:

$$\tilde{S} = \begin{pmatrix} \tilde{S}(1,1) & \tilde{S}(1,2) & \cdots & \tilde{S}(1,q+1) \\ \tilde{S}(2,1) & & & \\ \vdots & & & \\ \tilde{S}(q+1,1) & & & \end{pmatrix} \tag{79a}$$

For given i and j, $\tilde{S}(i,j)$ is a $m \times m$ matrix; so that $\{\tilde{S}(i,j),\ 1 \le i,\ j \le q+1\}$ determines all the elements of $\tilde{S}$. In the same vein, for given k and ℓ, define $T(k,\ell)$ as the $(q+1)\times(q+1)$ matrix given by

$$[T(k,\ell)]_{ij} = [\tilde{S}(i,j)]_{k\ell} \quad , \quad 1 \le i,\ j \le q+1 \quad , \quad 1 \le k,\ \ell \le m \tag{79b}$$

Now iterating alternately on (80) and (81) results in $\tilde{S}_1$ and $\tilde{S}_2$ which provides an approximation to $\tilde{S}$.

$$[\tilde{S}_1]_{ij} = \frac{1}{\|\tilde{S}_2\|^2} \operatorname{tr}\{\tilde{S}_2\, \tilde{S}(i,j)\} \quad , \quad 1 \le i,\ j \le q+1 \quad , \tag{80}$$

$$[\tilde{S}_2]_{k\ell} = \frac{1}{\|\tilde{S}_1\|^2} \operatorname{tr}\{\tilde{S}_1\, T(k,\ell)\} \quad , \quad 1 \le k,\ \ell \le m \quad , \tag{81}$$

It should be noted that $\tilde{S}^{-1}$ can be obtained by directly inverting $\tilde{S}$ whenever desired or by using the approximation described above coupled with

$$\tilde{S}^{-1} \simeq \tilde{S}_1^{-1} \otimes \tilde{S}_2^{-1}$$

Withe these improvements, the impact of high dimensionality can be significantly alleviated, making even high-order variable-gain output feedback design problems solvable with reasonable effort.

V. APPLICATION TO RECONFIGURABLE AIRCRAFT CONTROL

The design methodology and algorithm developed in the preceding sections was applied to a high-performance aircraft reconfiguration problem arising from a control surface failure. The failure of a control surface, a control actuator or servo, or the failure of a sensor in the feedback loop provide excellent examples to illustrate the control design methodology developed, although numerous other applications to control system design are possible. Restructuring and reconfiguring aircraft flight control law has received some attention [15], [16], [17].

The high-performance aircraft considered in this application is the AFTI F16 shown in Figure 5. The objective is to design a reconfigurable digital control law in which a failure in the horizontal tail is accommodated by the automatic reconfiguration of the flight control law as soon as the failure is detected. While the detection of the failure is an integral part of the process, here we concentrate on the design methodology for the control law.

As the AFTI F16 has static instability, the design of the control law and its reconfiguration strategy gain more importance, since a failure can easily bring the aircraft back to instability with catastrophic consequences. The objective of designing a digital reconfigurable controller will be attempted using the variable-gain output feedback design methodology developed in this investigation.

The AFTI F16 aircraft rigid-body dynamics and servoactuators were simulated on a digital computer. The reconfigurable control system design was formulated as an optimal variable-gain output feedback control problem. A reconfigurable design was obtained using the algorithm developed in the last section. Finally, the closed-loop reconfigurable aircraft/controller system was simulated to evaluate its behavior.

The simulation of the aircraft and its servoactuators was done using a linearization about a Mach number of 0.8 and an altitude of 5000 ft. with the aircraft in nominal

straight and level flight. At this flight condition, the aircraft has a static instability in the short period mode at +0.3172. Furthermore, since the aircraft uses a single engine, the gyroscopic effects are not negligible and produce a roll/yaw coupling. As a result, even the case of no control failure contains significant coupling between the lateral and longitudinal modes. These effects are readily apparent in the coupled (A, B) matrix model shown in Table 1. These A and B matrices were obtained by linearizing the NASA Langley Research Center AFTI F16 nonlinear simulation.

The aircraft control surfaces can be seen in Figure 5. The independently movable controls consist of the rudder, left horizontal tail, right horizontal tail, left and right flaperons, left and right vertical canards and the throttle position. The leading-edge flaps and the speed brake were not used in this simulation. Detailed integrated servoactuator models were used to simulate the dynamics of the control surfaces. A first order model with a 0.5 sec. time constant was used to model the throttle command to actual throttle position. The remaining model transfer functions are shown in Table 2. The control effector simulation uses both rate and maximum/minimum position limits which are shown in Table 3.

The simulation uses a 3^{rd}-order Adams-Bashforth numerical integration algorithm to update the aircraft variables. The simulation update or sampling rate is 40 Hz. The complete rigid-body dynamics and servoactuator simulation model is of 33^{rd} order.

To design a variable-gain output feedback control law for the aircraft, first requires building a design model. The design model determines the structure of the control law as well as the values of the control gains which are used. We start building the design model with the aircraft rigid-body state and control variables.

$$x^T = (u_B \quad w_B \quad q_B \quad \theta \quad v_B \quad p_B \quad r_B \quad \phi \quad \psi) \tag{82}$$

where u_B, v_B, w_B are the linear velocity components along body x_B, y_B, z_B axes, q_B, p_B, r_B are the pitch, roll and yaw rates expressed in the body axes, and θ, ϕ, ψ are the pitch, roll

and yaw angles.

The control effector position vector will be denoted by δ with the following order of variables.

$$\delta^T = (\delta R \quad \delta htl \quad \delta htr \quad \delta fl \quad \delta fr \quad \delta vel \quad \delta ver \quad \delta th) \tag{83}$$

where δR denotes the rudder position, δhtl and δhtr the left and right horizontal tails, δfl and δfr the left and right flaperons, δvel and δver the left and right vertical canards, and δth the throttle position. For a variety of reasons (e.g., see [13], [10]), we select a control rate command structure for the controller by augmenting the design model by the following equations.

$$\delta_{k+1} = \delta_k + u_k \quad , \tag{84}$$

where u_k is the control vector for the design model and represents the change in the corresponding control effector position from one sample to the next. A sampling rate of 10 Hz is used for the purpose of obtaining the control law design.

Finally, to obtain a reconfigurable design with type-1 steady-state characteristics, integral feedback of the command variables is added. The command state vector, z is selected as

$$z^T = (u_B \quad \theta \quad \phi \quad \psi) \quad , \tag{85a}$$

$$z_c^T = (u_{Bc} \quad \theta_c \quad \phi_c \quad \psi_c) \tag{85b}$$

where the subscript " c " denotes the commanded value of the variable. The integral error, or more correctly accumulated error, is obtained by

$$I_{k+1} = I_k + \Delta t(z_k - z_{ck}) \tag{86}$$

The complete design model state, X, is the augmented state shown below

$$X^T = (x^T \quad \delta^T \quad I^T) \quad , \tag{87}$$

with the control vector being denoted by u. The discretized equations for the aircraft dynamics, augmented by the (84) and (86) forms the design model state equations.

$$X_{k+1} = \begin{pmatrix} x_{k+1} \\ \delta_{k+1} \\ I_{k+1} \end{pmatrix} = \begin{pmatrix} \phi & \Gamma(p) & 0 \\ 0 & I & 0 \\ \Delta t H_x & 0 & I \end{pmatrix} \begin{pmatrix} x_k \\ \delta_k \\ I_k \end{pmatrix} + \begin{pmatrix} 0 \\ I \\ 0 \end{pmatrix} u_k - \begin{pmatrix} 0 \\ 0 \\ \Delta t z_{ck} \end{pmatrix} \tag{88}$$

$$\Gamma(p) = \Gamma_o - \Gamma_1 p_1 - \Gamma_2 p_2 \quad , \quad 0 \leq p_i \leq 1 \quad , \quad i = 1,2 \tag{89}$$

In the equations above, the parameter vector p has two components, with p_1 and p_2 representing the fractional surface effectiveness loss for the left and right horizontal tail surfaces. In (89), Γ_o is the standard matrix obtained by discretizing the continuous aircraft perturbation equations when all the controls are operating normally. Γ_1 is a null matrix with the exception that its 2^{nd} column (i.e., the column corresponding to the left horizontal tail) has been replaced by the 2^{nd} column of Γ_o. Similarly, Γ_2 is a null matrix with the exception that its 3^{rd} column (i.e., the column corresponding to the right horizontal tail) has been replaced by the 3^{rd} column of Γ_o. Thus, $p_i = 0$ corresponds to zero effectiveness loss or a normally operating control surface; whereas a value of $p_i = 1$ corresponds to 100% loss of effectiveness such as a centered surface.

The variable-gain control law is of the form

$$K(p) = K_o + K_1 p_1 + K_2 p_2 \tag{90}$$

$$u_k = -K(p)\, X_k \tag{91}$$

Figures 6 and 7 show the simulations of the reconfigurable control law obtained with the design model described and using the conditions where 1) all controls working normally ($p_1 = p_2 = 0$), 2) the left horizontal tail is centered ($p_1 = 1, p_2 = 0$), and 3) the right horizontal tail is centered ($p_1 = 0, p_2 = 1$). Table 4 shows the gain matrices used in the simulations.

The command in these simulations is a total pitch angle of 15°, while the commanded roll and yaw angles are zero, and the commanded speed is Mach .8. In Figure 6, the case where no failures occur is simulated. Figure 7 shows the simulation for the case where the left horizontal tail is centered at 1.8 sec. into the simulation while the commanded maneuver is in progress. The simulation assumes that the failure is immediately detected and isolated; so that the parameter vector, p, immediately reconfigures the flight control law. While a more realistic FDI simulation would be desirable, as long as the FDI correctly isolates the failure, the difference from the results shown here would be in the transient behavior while the steady-state results would be the same [18], at least for linear simulations.

In Figure 6, with no failures occurring, the aircraft pitch angle rapidly increases from its trim value at straight and level flight, slightly overshoots the commanded 15° and then smoothly settles to its commanded value.

The maneuver is largely achieved by the horizontal tail producing a positive pitching moment. The pitch-up results in more drag and a correspondingly small drop in speed which is then controlled by an increase in the thrust. However, the coupling between the thrust and the rolling and yawing moments produces a slight response in the lateral modes. This coupling produces a maximum of 0.09° of roll and 0.03° of yaw with an oscillatory behavior which is quickly damped out. Further experimentation with the design would be needed to eliminate this transient effect.

When during the initial stages of the commanded maneuver, at 1.8 sec., the left horizontal tail fails and is automatically centered, the variable-gain controller has to reconfigure its strategy in order to accommodate this condition. Despite this failure, the

reconfigured control law easily meets its objective of 15° pitch with no steady-state roll or yaw. Although the response in pitch is different, it is just as fast as before. The roll and yaw angles go through a larger transient, but are firmly brought back to their commanded values after the reconfiguration in the control law.

The failure of the left horizontal tail (but not the right) produces a large coupling between the lateral and longitudinal dynamics. The control law reconfiguration strategy is to use the operational right horizontal tail to produce and maintain the pitching moment necessary to achieve the commanded pitch, while nulling the cross-coupling moments with the flaperons and vertical canards. The thrust profile seems only slightly changed.

After the failure, the large deflection in the right horizontal tail, now unbalanced, produces a significant amount of positive rolling moment as well as positive yawing moment. The sudden onset of these moments, produce the positive roll and yaw transients mentioned earlier. The reconfigured control law is seen to bring and maintain the roll at zero mainly by using the flaperons to counteract the rolling moment, and by using the rudder to counteract the yawing moment. The vertical canards are used to shape and improve the transient behavior.

Overall, the reconfigured control strategy is seen to handle the failure of the left horizontal tail with relative ease. Alternately, the design methodology of optimizing a variable-gain output feedback controller has produced a reconfigurable control design which accommodates the control surface failure considered with relative ease.

VI. CONCLUSIONS AND RECOMMENDATIONS

The main contribution of the investigation described in this report has been the formulation, development and solution of the variable-gain output feedback problem in the form of an optimal stochastic control problem. This approach provides a control theory framework within which the operating range of a control law can be significantly extended. Furthermore, the approach avoids the major shortcomings of the conventional gain-scheduling techniques.

The optimal variable-gain output feedback control problem is solved by embedding into the Multi-Configuration Control (MCC) problem, previously solved at ICS. An algorithm to compute the optimal variable-gain output feedback control gain matrices has been developed. The algorithm is a modified version of the MCC algorithm improved so as to handle the large dimensionality which arises particularly in variable-gain control problems.

The design methodology developed was applied to a reconfigurable aircraft control problem. A variable-gain output feedback control problem was formulated to design a flight control law for an AFTI F16 aircraft which can automatically reconfigure its control strategy to accommodate failures in the horizontal tail control surface. Simulations of the closed-loop reconfigurable system show that the approach produces a control design which can accommodate such failures with relative ease.

While the example considered is an important illustration of the power of this new design methodology, applications to a large variety of current problems is desirable. In particular, it is possible to extend the flight regime of most aircraft by appropriate application of the methodology. For example, superagility characteristics can be achieved by using angle-of-attack and airspeed as components of the operating condition parameter, p. Sensor failure accommodation can also be achieved using the methodology. Numerous

other applications to a variety of control problems remain for future investigation. Two important areas for study are: 1) the development of new algorithms that have better numerical convergence characteristics for high dimensional problems, and 2) the extension of the variable-gain output feedback approach to the feedforward control law design.

Finally, it should be noted that digital control design methodologies for nonlinear systems are rare at present. Until such nonlinear techniques and analysis tools able to handle the theoretical and, more importantly, practical requirements of complex control systems can be developed and demonstrated, the variable-gain output feedback approach presented here provides the control system engineer with a design methodology for aerospace control problems.

REFERENCES

1. Etkin, B., *Dynamics of Atmospheric Flight*, John Wiley & Sons, Inc., New York, 1972.
2. Halyo, N., "Flight Tests of the Digital Integrated Automatic Landing System (DIALS)," NASA CR-3859, December 1984.
3. Broussard, J. R., "ATOPS B-737 Inner Loop Control System Linear Model Construction and Verification," NASA CR-166055, February 1983.
4. Broussard, J. R. and N. Halyo, "Active Flutter Suppression Using Optimal Output Feedback Digital Controllers," NASA CR-165939, May 1982.
5. Berry, P. W., Broussard, J. R. and S. Gully, "Validation of High Angle-of-Attack Analysis Methods," ONR-CR 215-237-3F, U.S. Navy, September 1979. (Available from DTIC as AD A087 621).
6. Halyo, N. and A. K. Caglayan, "A Separation Theorem for the Stochastic Sampled-Data LQG Problem," *Int. J. Control*, Vol. 23, No. 2, pp. 237-244, February 1976.
7. Halyo, N. and J. R. Broussard, "A Convergent Algorithm for the Stochastic Infinite-Time Discrete Optimal Output Feedback Problem," *Proc. 1981 JACC*, U. of Virginia, Charlottesville, VA, Vol. 1, June 17-19, 1981.
8. Halyo, N. and J. R. Broussard, "Investigation, Development, and Application of Optimal Output Feedback Theory – Volume I: A Convergent Algorithm for the Stochastic Infinite-Time Discrete Optimal Feedback Problem," NASA CR-3828, August 1984.
9. Halyo, N. and J. R. Broussard, "Algorithms for the Output Feedback, Multiple Model and Decentralized Control Problems," NASA Aircraft Controls Research – 1983, NASA CP-2296, October 25-27, 1983.
10. Hueschen, R. M., "The Design, Development, and Flight Testing of a Modern-Control-Designed Autoland System," American Control Conference, Boston, MA, June 1985.

11. Broussard, J. R. and N. Halyo, "Investigation, Development, and Application of Optimal Output Feedback Theory – Volume II: Development of an Optimal Limited State Feedback Outer-Loop Digital Flight Control System for 3-D Terminal Area Operation," NASA CR-3829, August 1984.

12. Halyo, N., "A Combined Stochastic Feedforward and Feedback Control Design Methodology with Application to Autoland Design," NASA CR-4078, July 1987.

13. Halyo, N., "Investigation, Development, and Application of Optimal Output Feedback Theory – Volume IV: Measures of Eigenvalue/Eigenvector Sensitivity to System Parameters and Unmodeled Dynamics," NASA CR-4108, December 1987.

14. Ostroff, A. and R. Hueschen, "Investigation of Control Law Reconfigurations to Accommodate a Control Element Failure on a Commercial Airplane," *Proc. ACC*, San Diego, CA, June 1984.

15. Ostroff, A., "Techniques for Accommodating Control Effector Failures on a Mildly Statically Unstable Airplane," *Proc. ACC*, Boston, MA, June 1985.

16. Moerder, D. D., Halyo, N., Broussard, J. R. and A. K. Caglayan, "Application of Precomputed Control Laws in a Reconfigurable Aircraft Flight Control System," ICS TM-86-102 presented at the *American Control Conf.*, Seattle, WA, June 1986.

17. Caglayan, A. K., Rahnamai, K., Moerder, D. D. and N. Halyo, "A Hierarchical Reconfiguration Strategy for Aircraft Subjected to Actuator Failure/Surface Damage," AFWAL-TR-87-3024, May 1987.

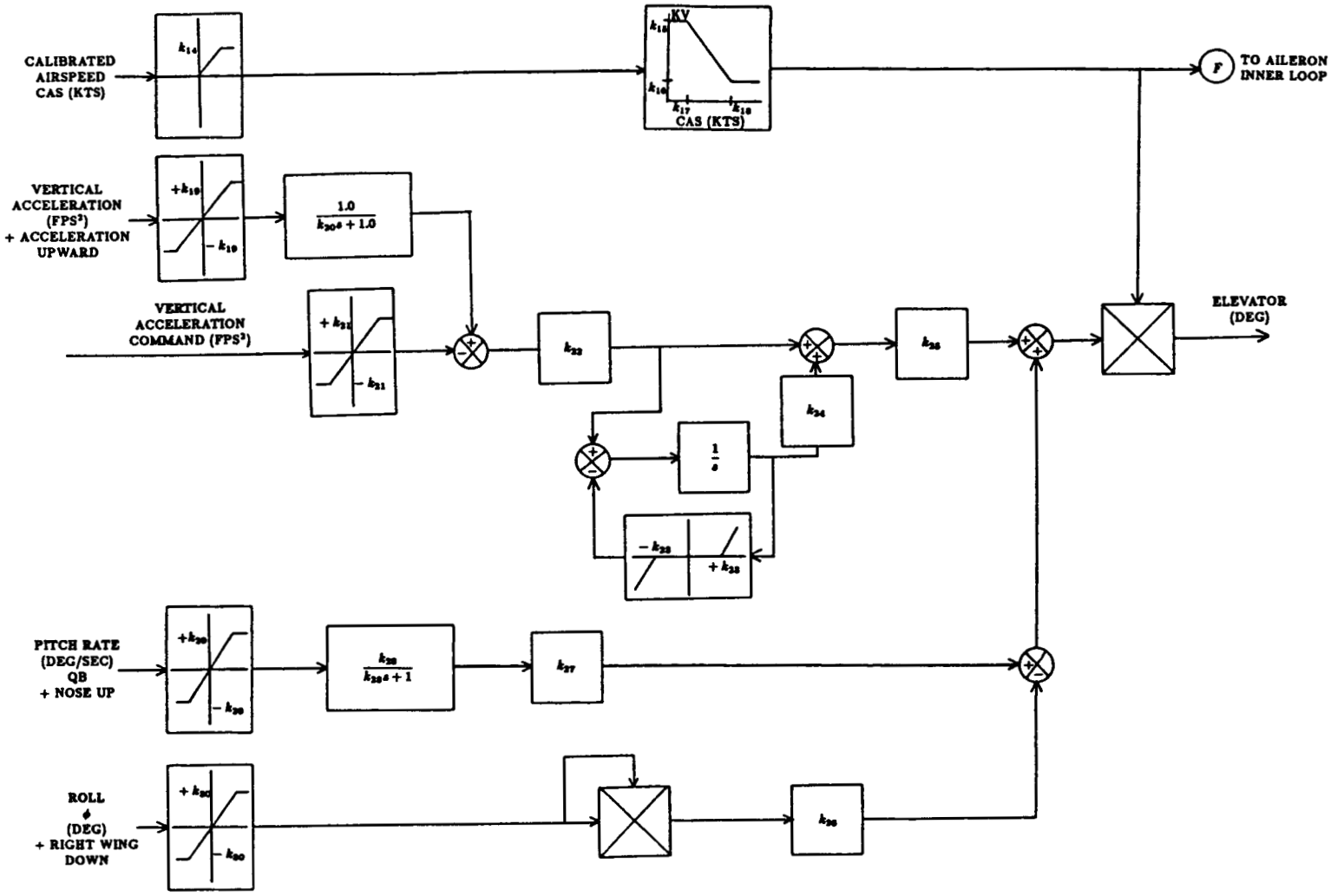

Figure 1. Elevator Inner-loop Control System Diagram

ORIGINAL PAGE IS
OF POOR QUALITY

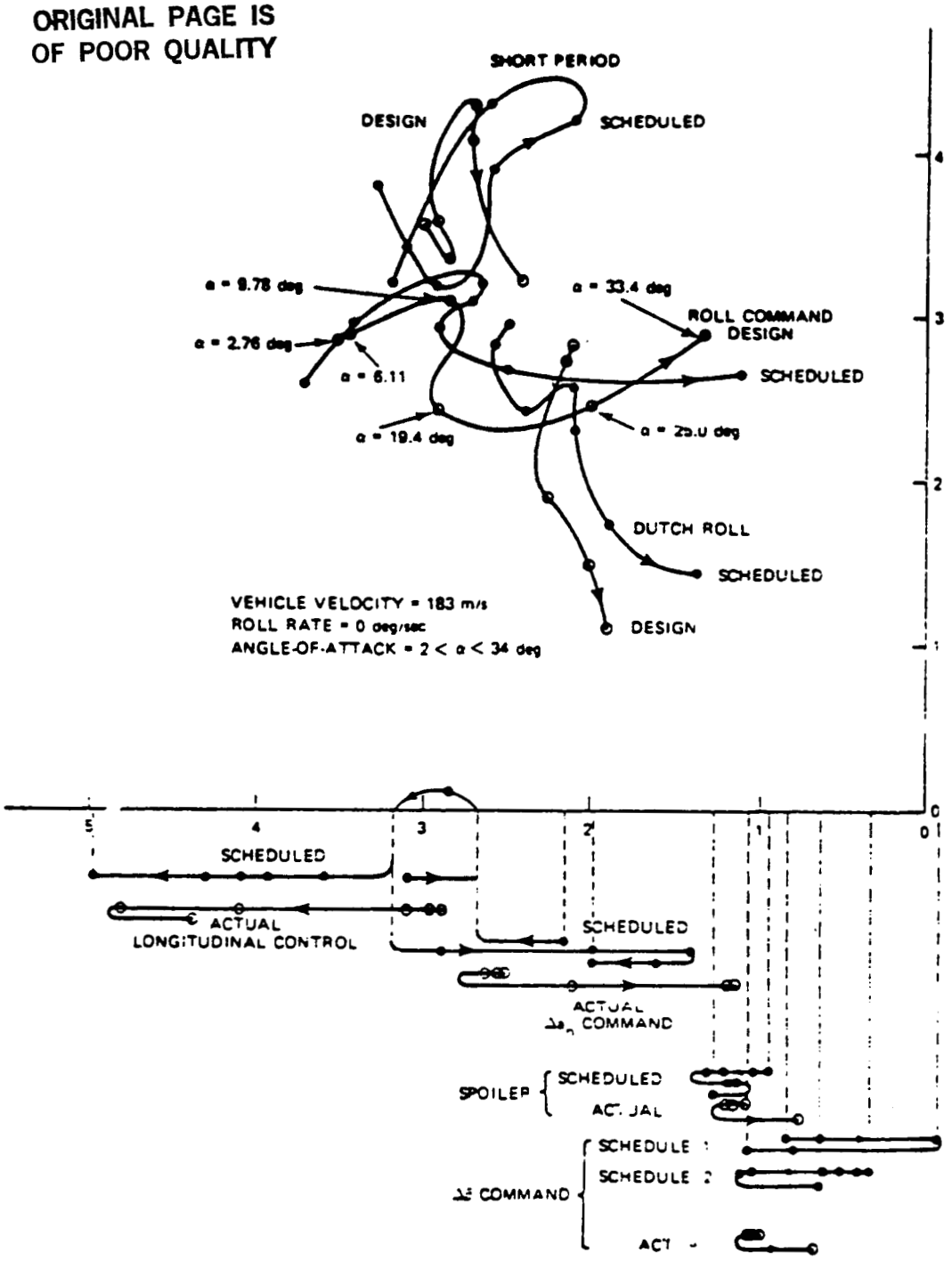

Figure 2. Effects of the Gain Scheduled on Closed-loop Type 0 DFCS Mapped Eigenvalues

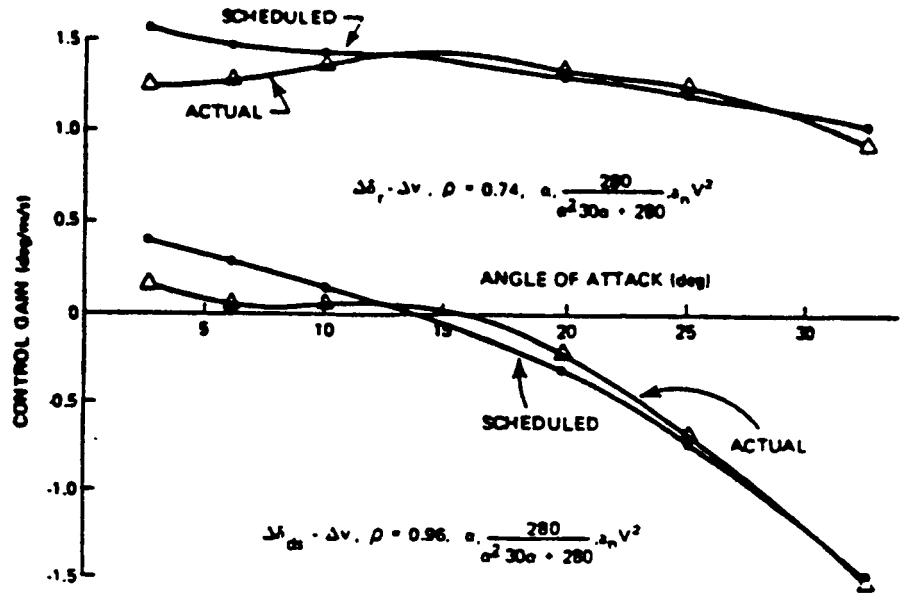

a) Type 1 DFCS

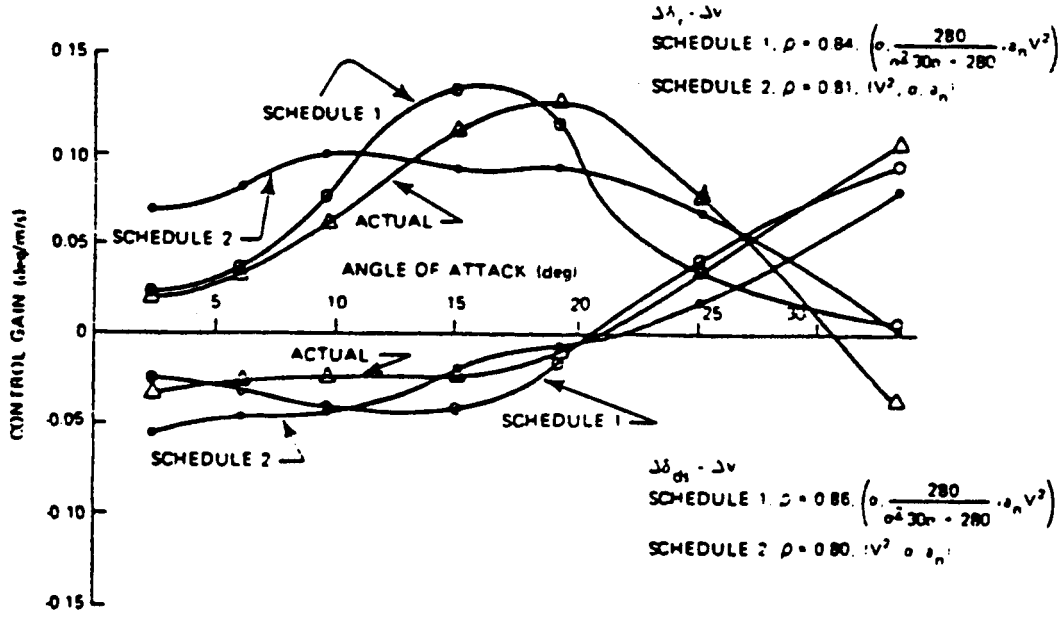

b) Type 0 DFCS

Figure 3. Control Gain Variation with Angle of Attack (V = 183 m/s (600 fps), $p_{w_o} = 0$ deg/sec)

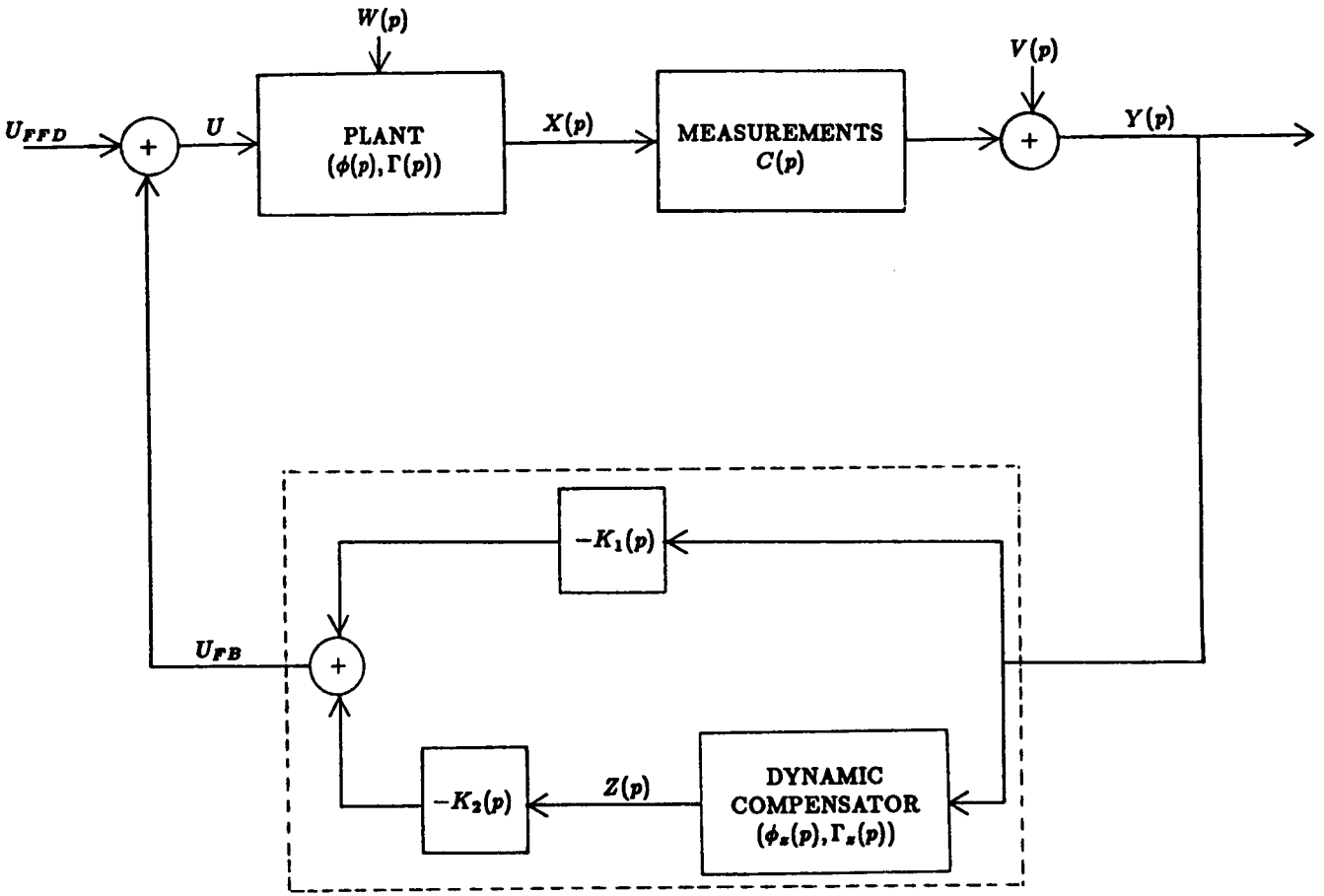

Figure 4. Variable-gain Output Feedback with Dynamic Compensation

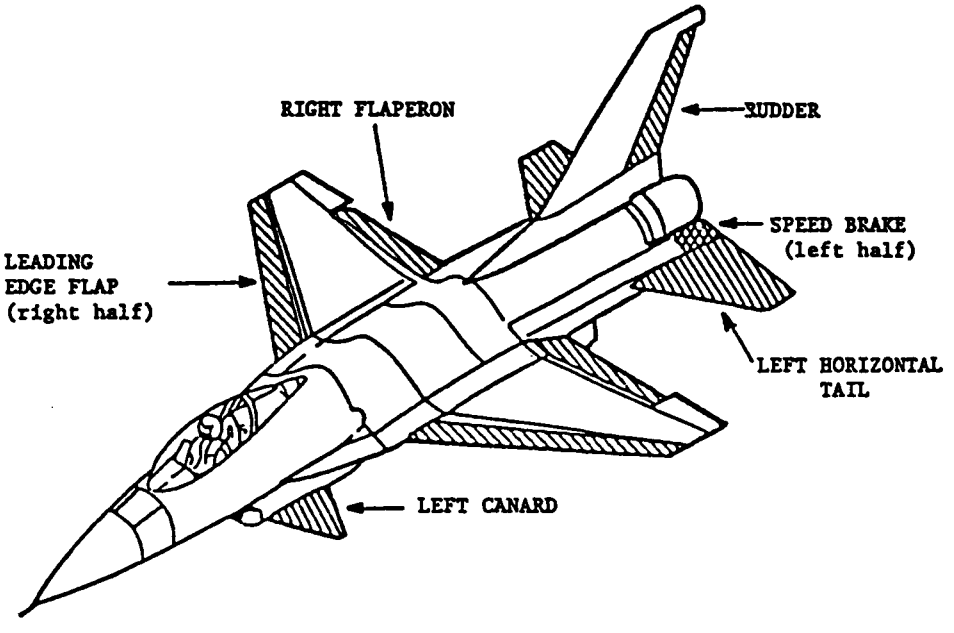

- HORIZONTAL TAILS
- FLAPERONS
- CANARDS

} EACH SIDE INDEPENDENTLY ACTUATED

- LEADING EDGE FLAPS
- SPEED BRAKES

} SYMMETRIC MOTION ONLY

Figure 5. AFTI F16 Aircraft Control Surface Configuration

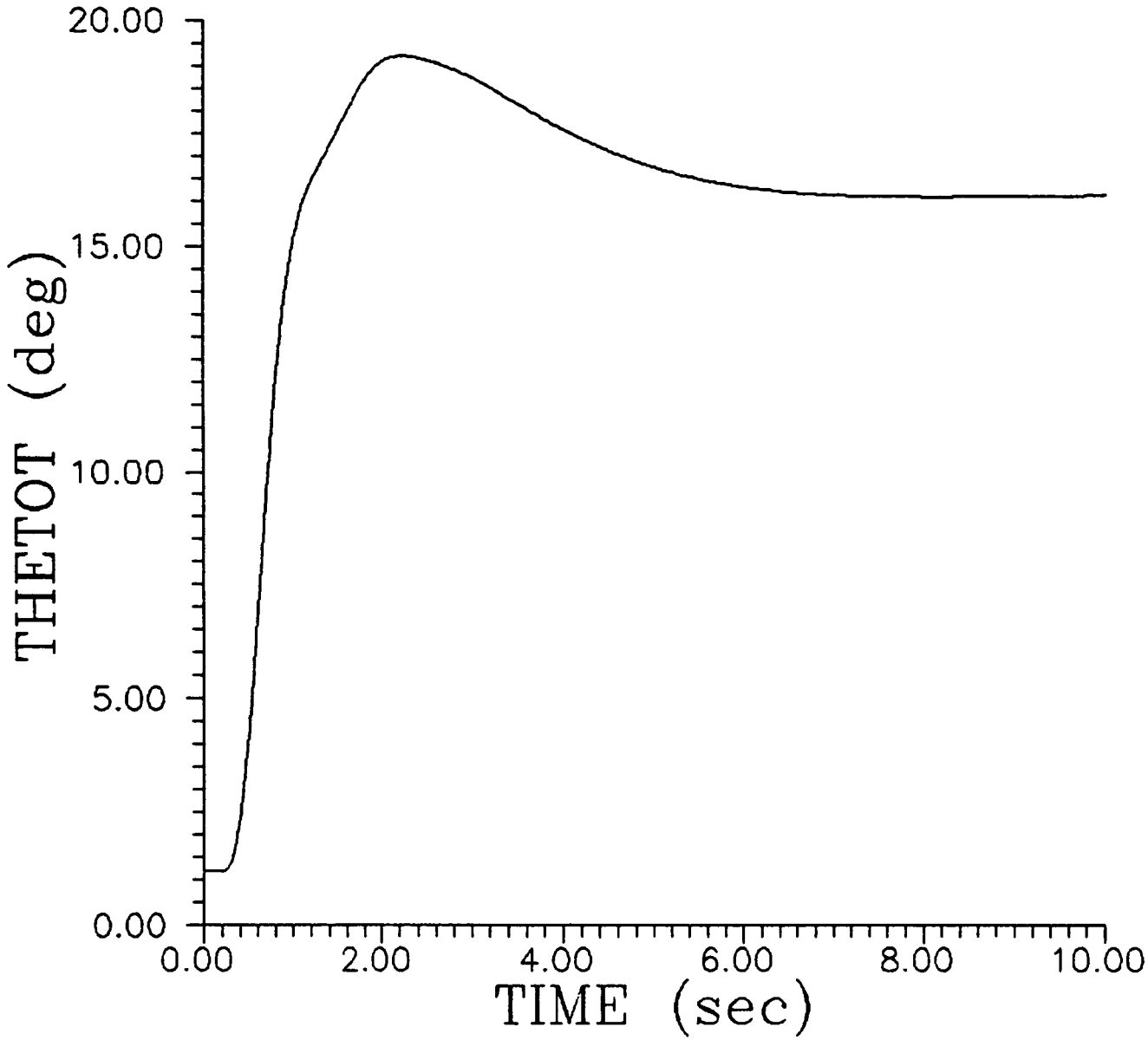

Figure 6.a. Simulation of Nominal (No Failure) Closed-loop System

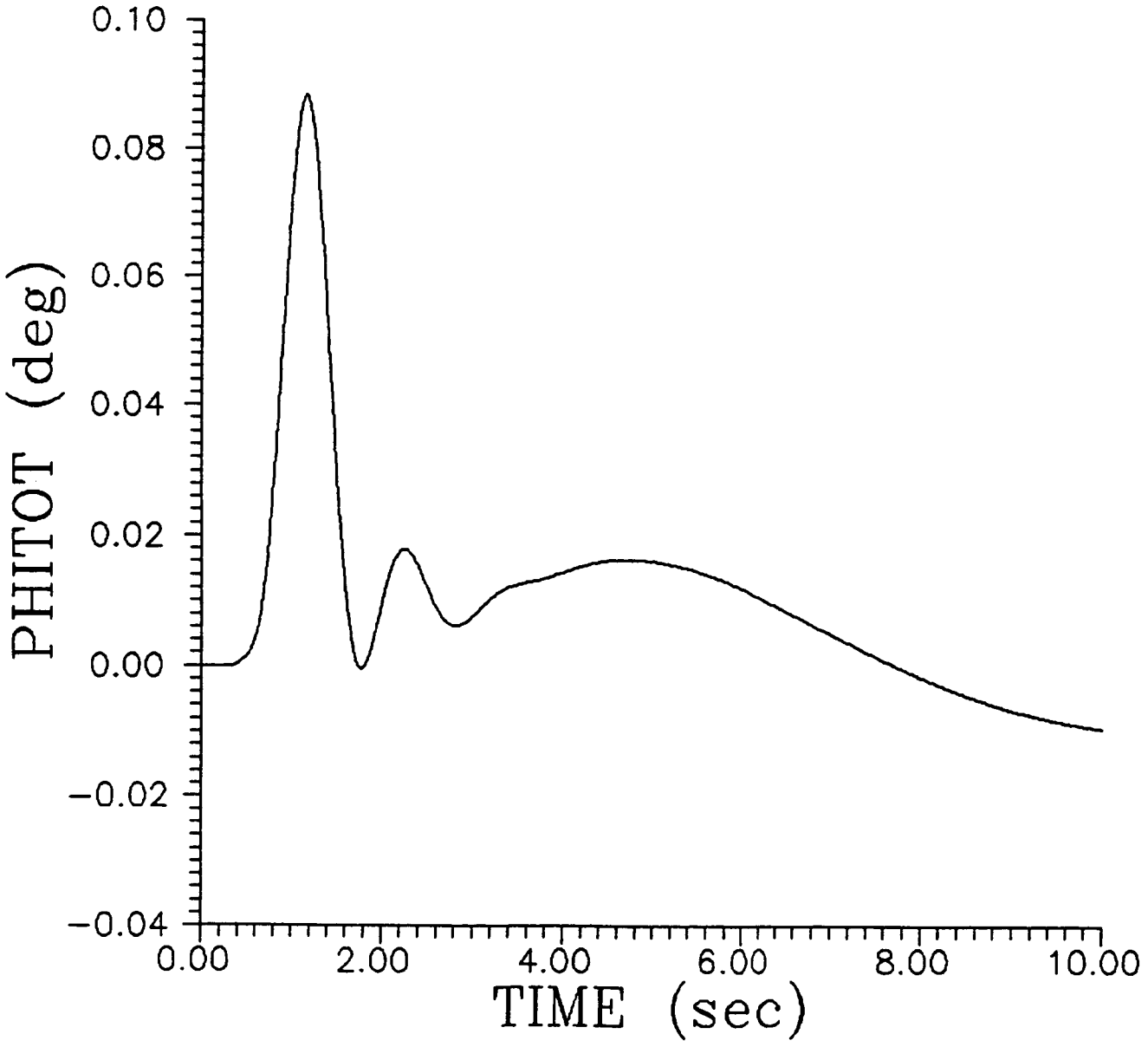

Figure 6.b. Simulation of Nominal (No Failure) Closed-loop System

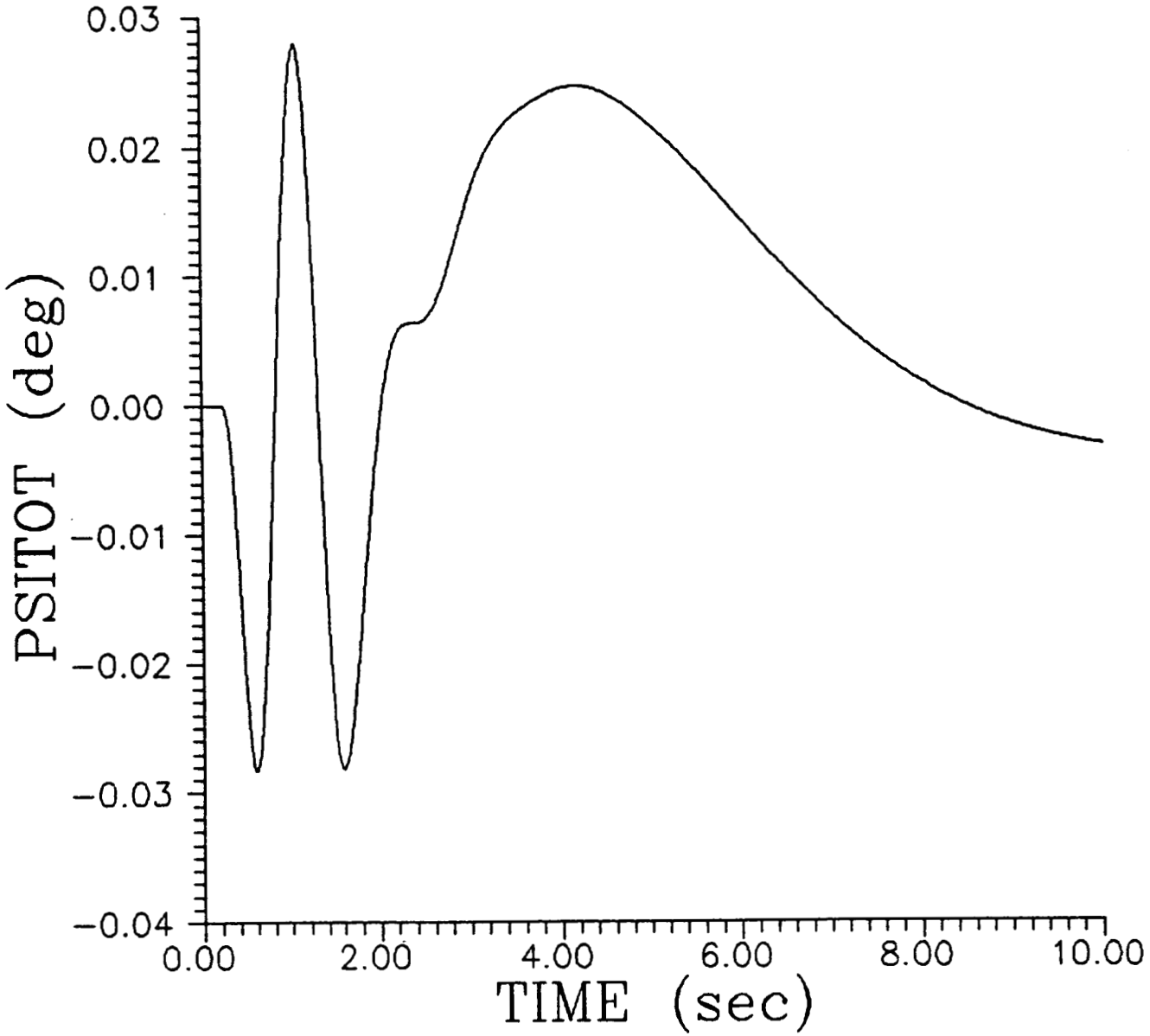

Figure 6.c. Simulation of Nominal (No Failure) Closed-loop System

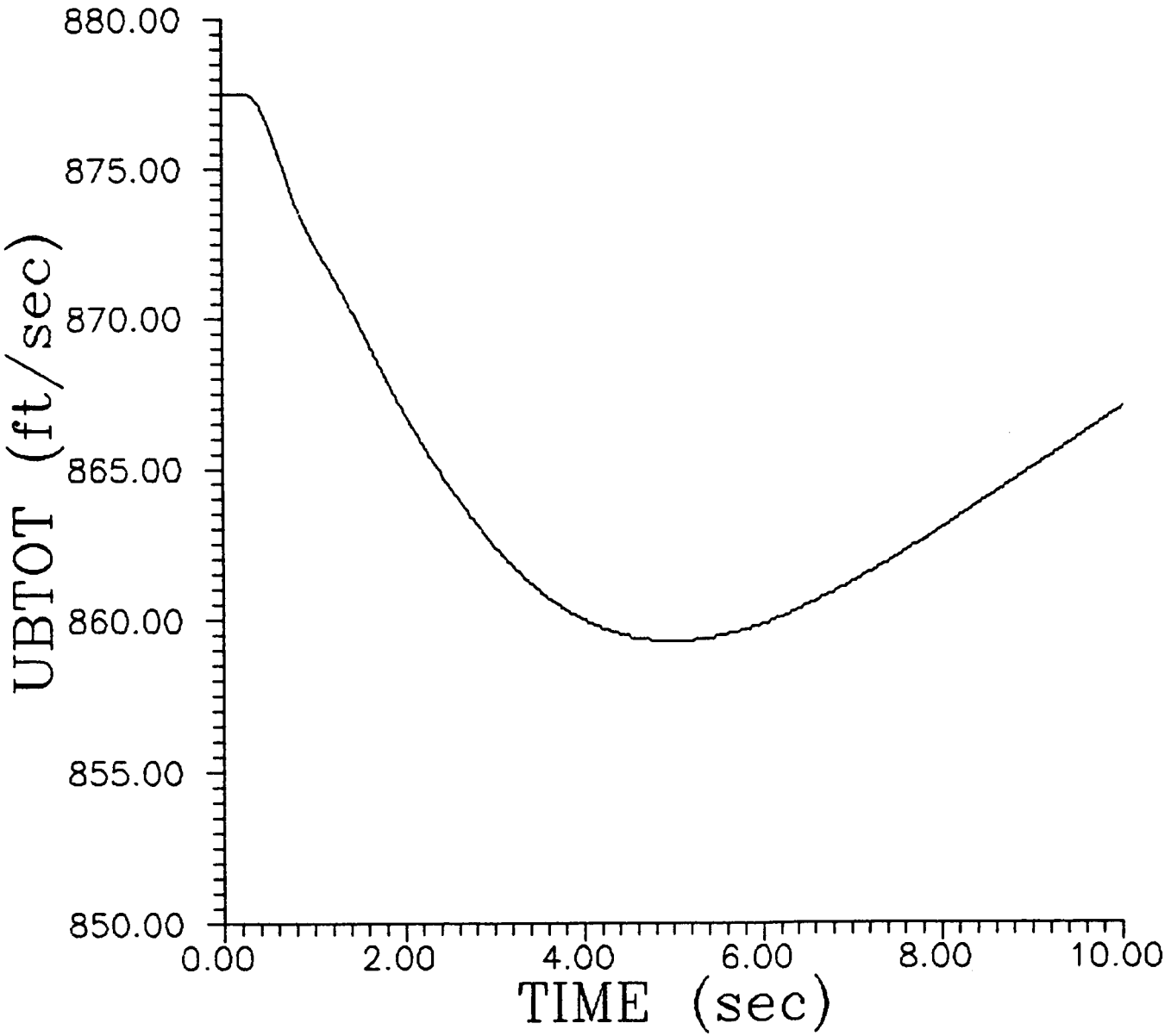

Figure 6.d. Simulation of Nominal (No Failure) Closed-loop System

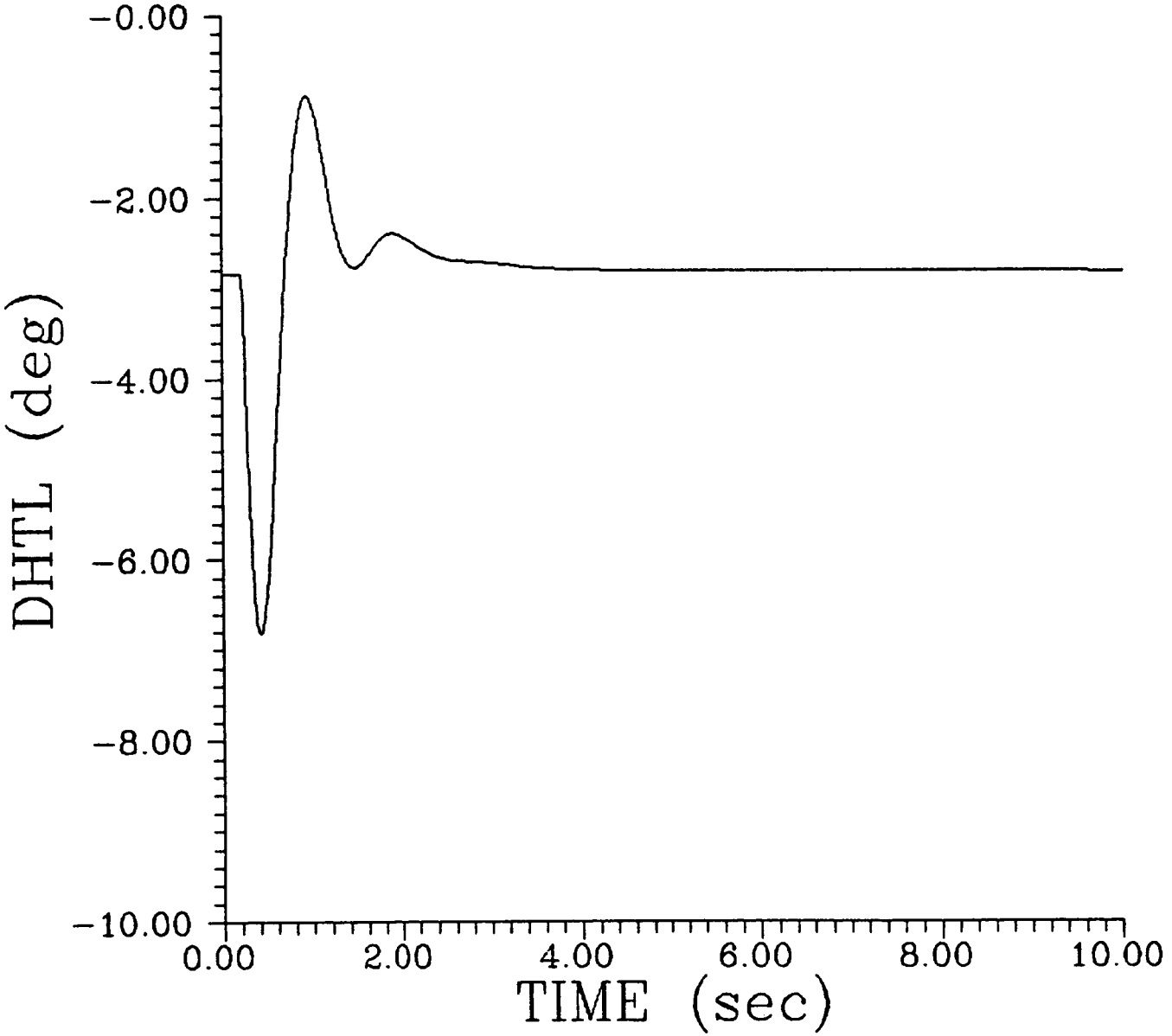

Figure 6.e. Simulation of Nominal (No Failure) Closed-loop System

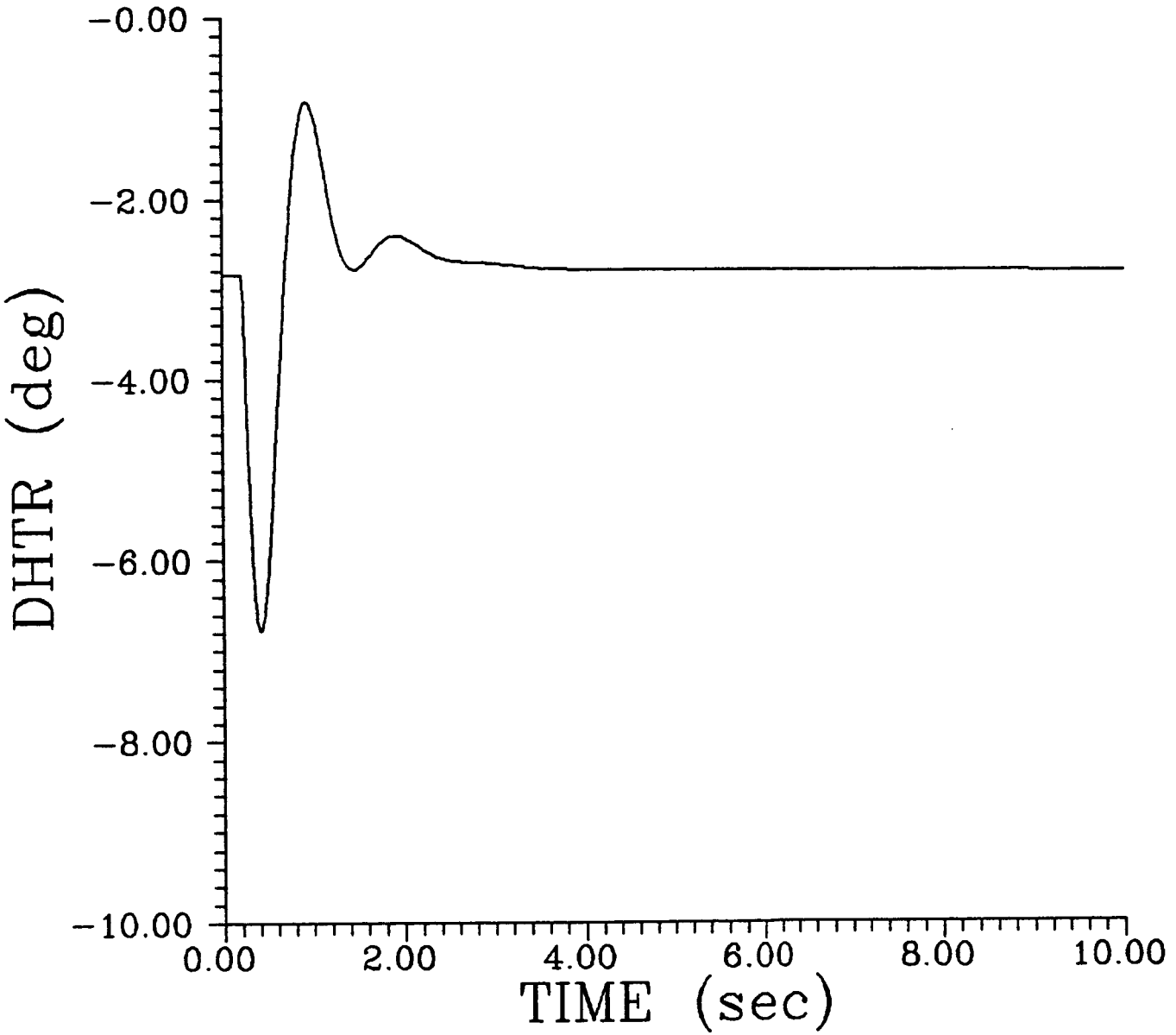

Figure 6.f. Simulation of Nominal (No Failure) Closed-loop System

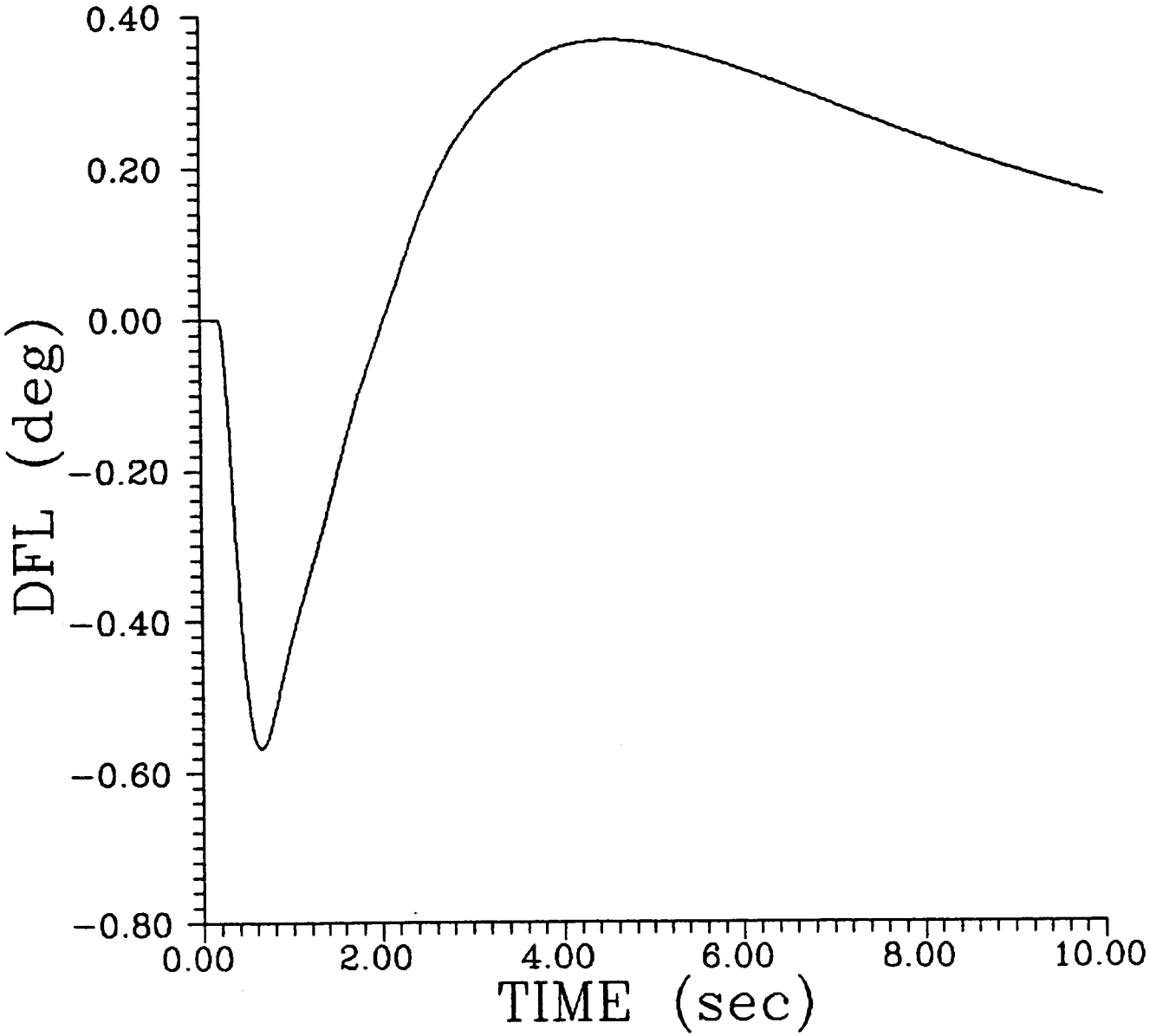

Figure 6.g. Simulation of Nominal (No Failure) Closed-loop System

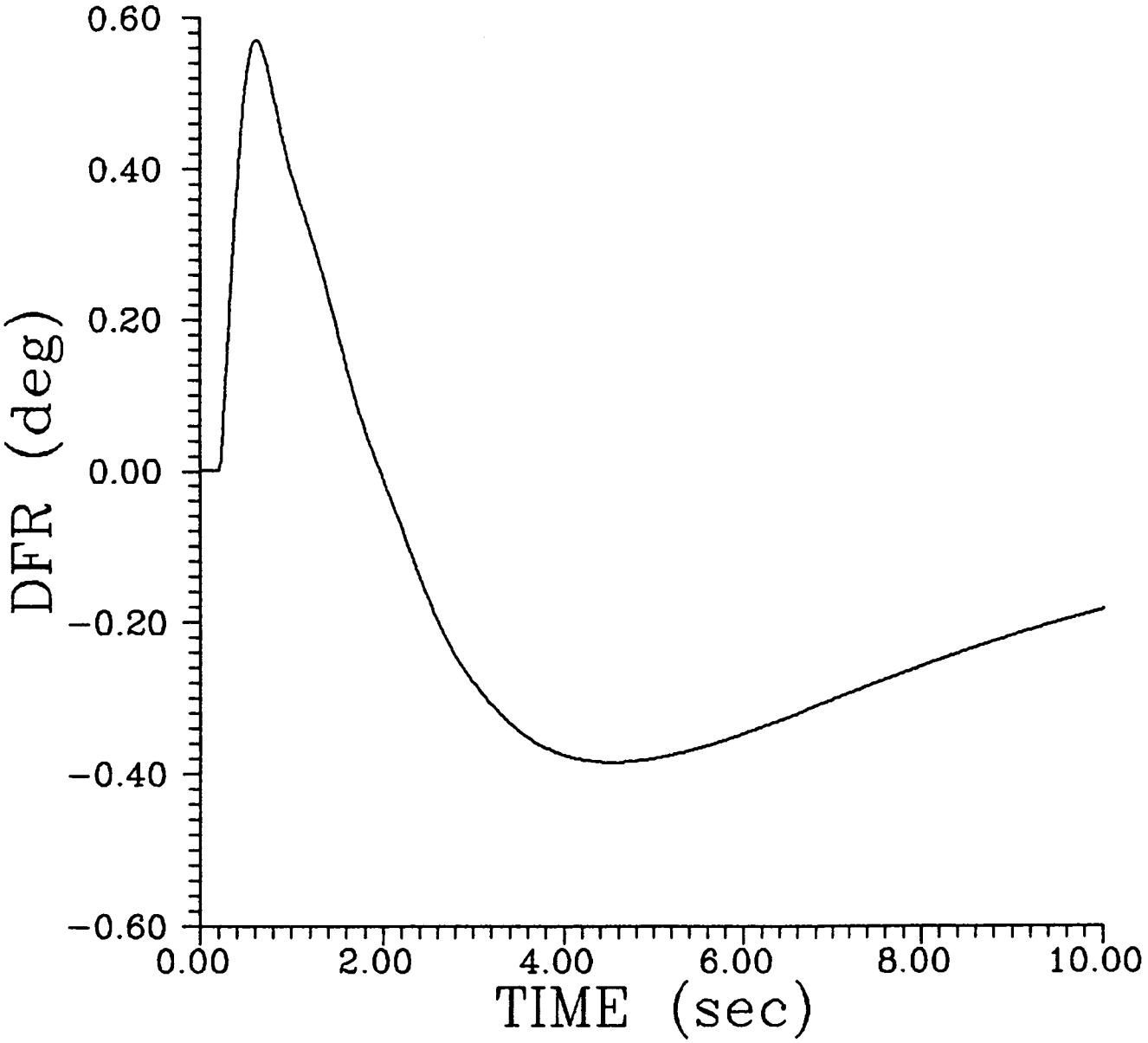

Figure 6.h. Simulation of Nominal (No Failure) Closed-loop System

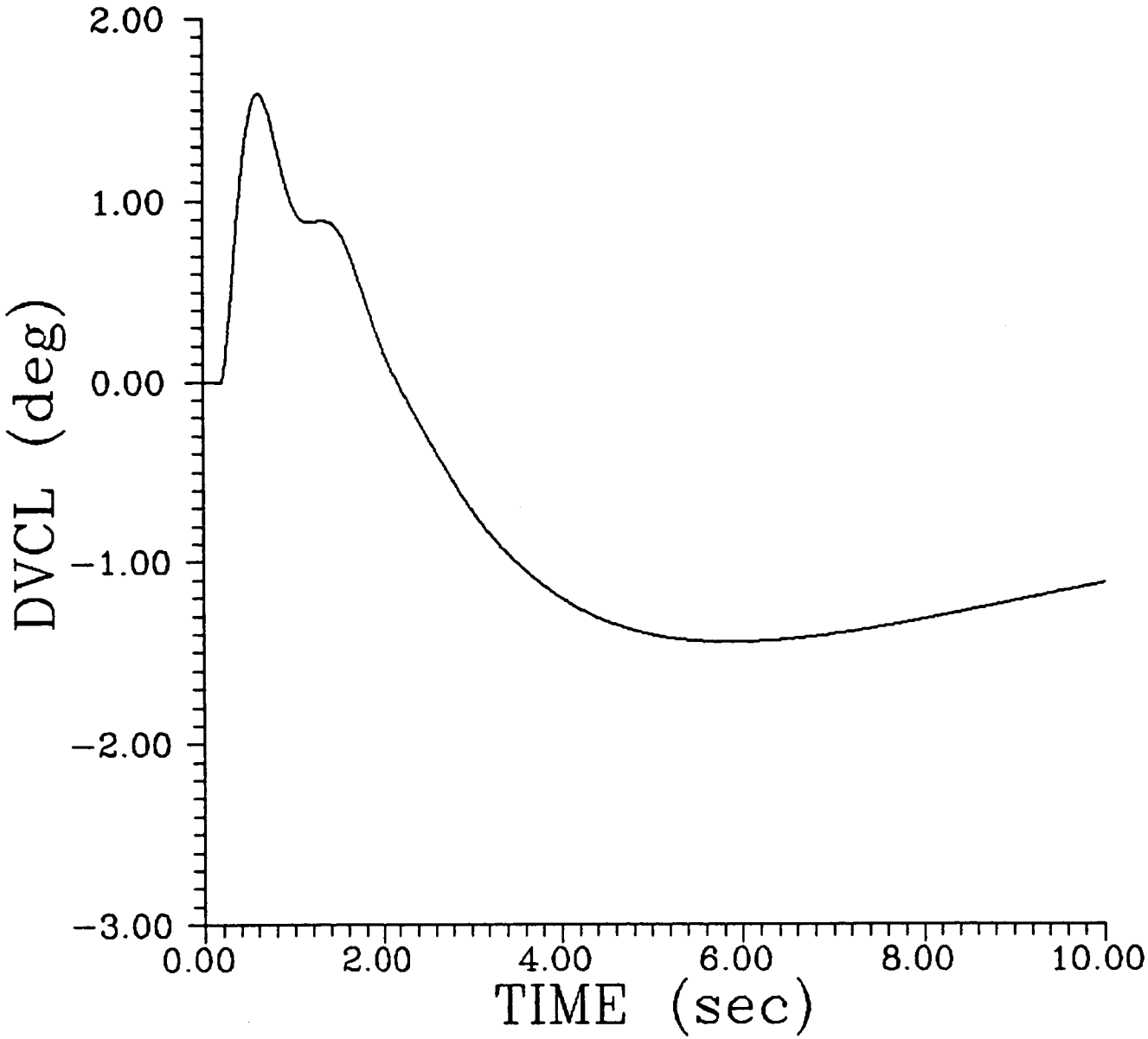

Figure 6.i. Simulation of Nominal (No Failure) Closed-loop System

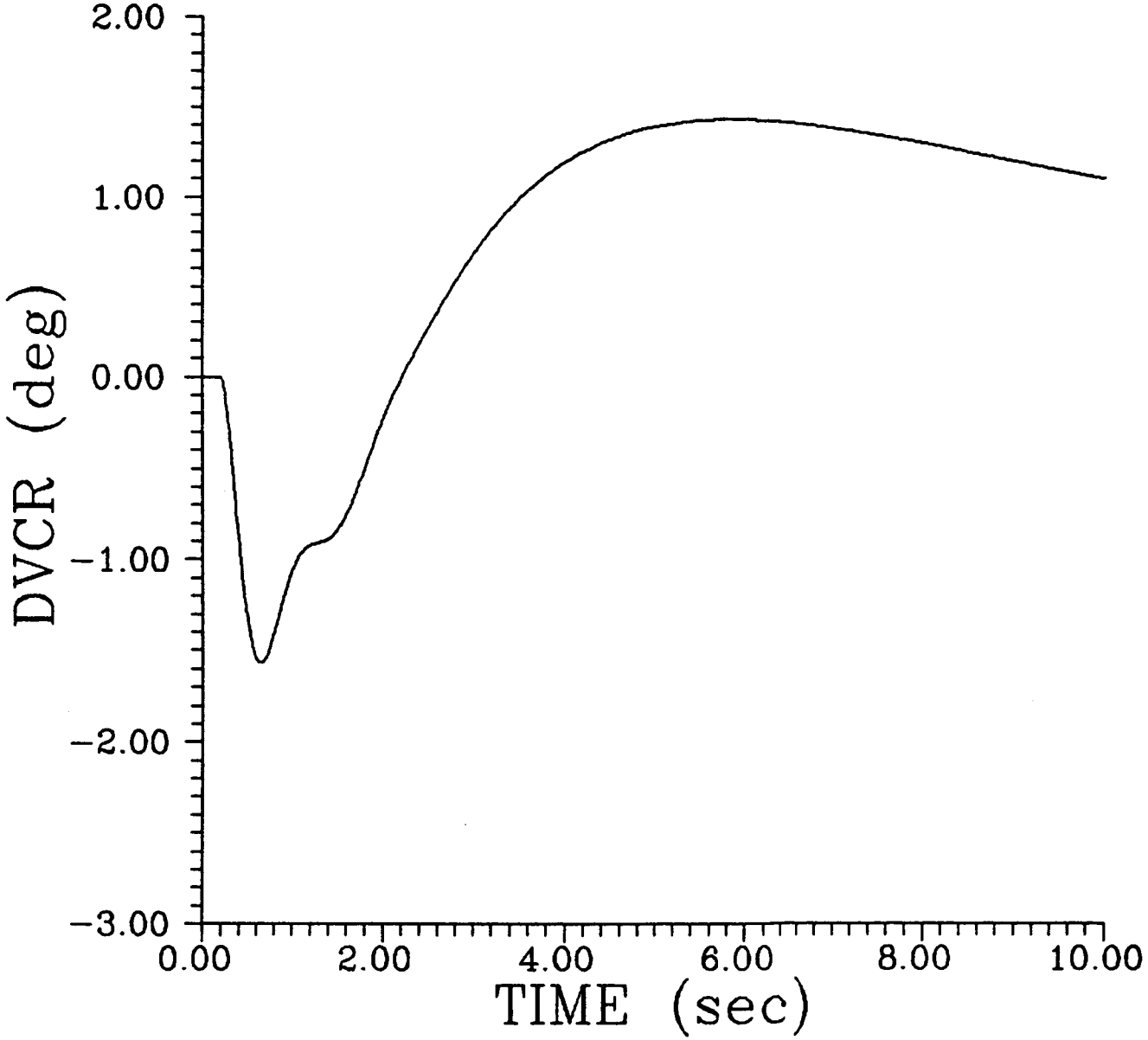

Figure 6.j. Simulation of Nominal (No Failure) Closed-loop System

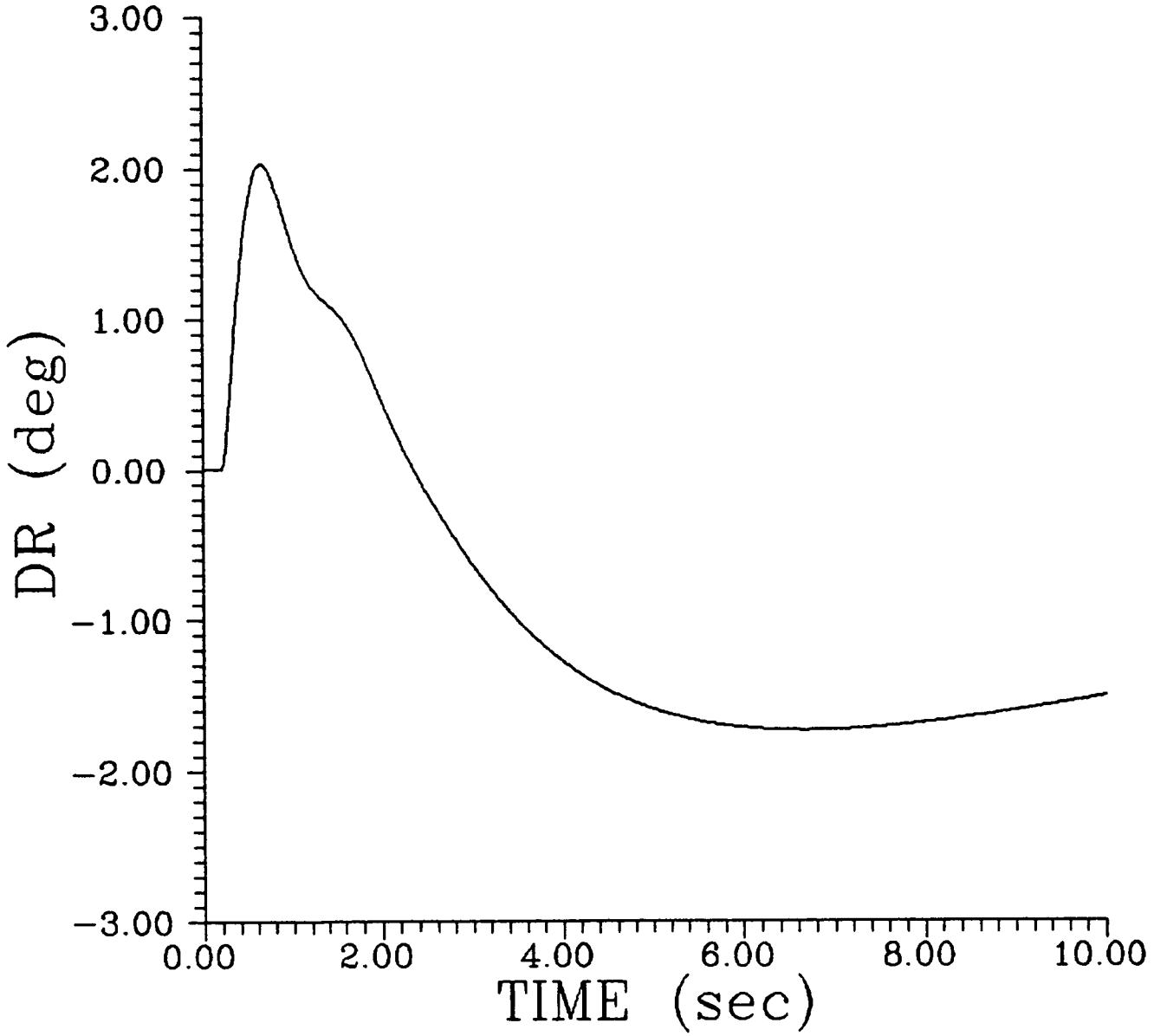

Figure 6.k. Simulation of Nominal (No Failure) Closed-loop System

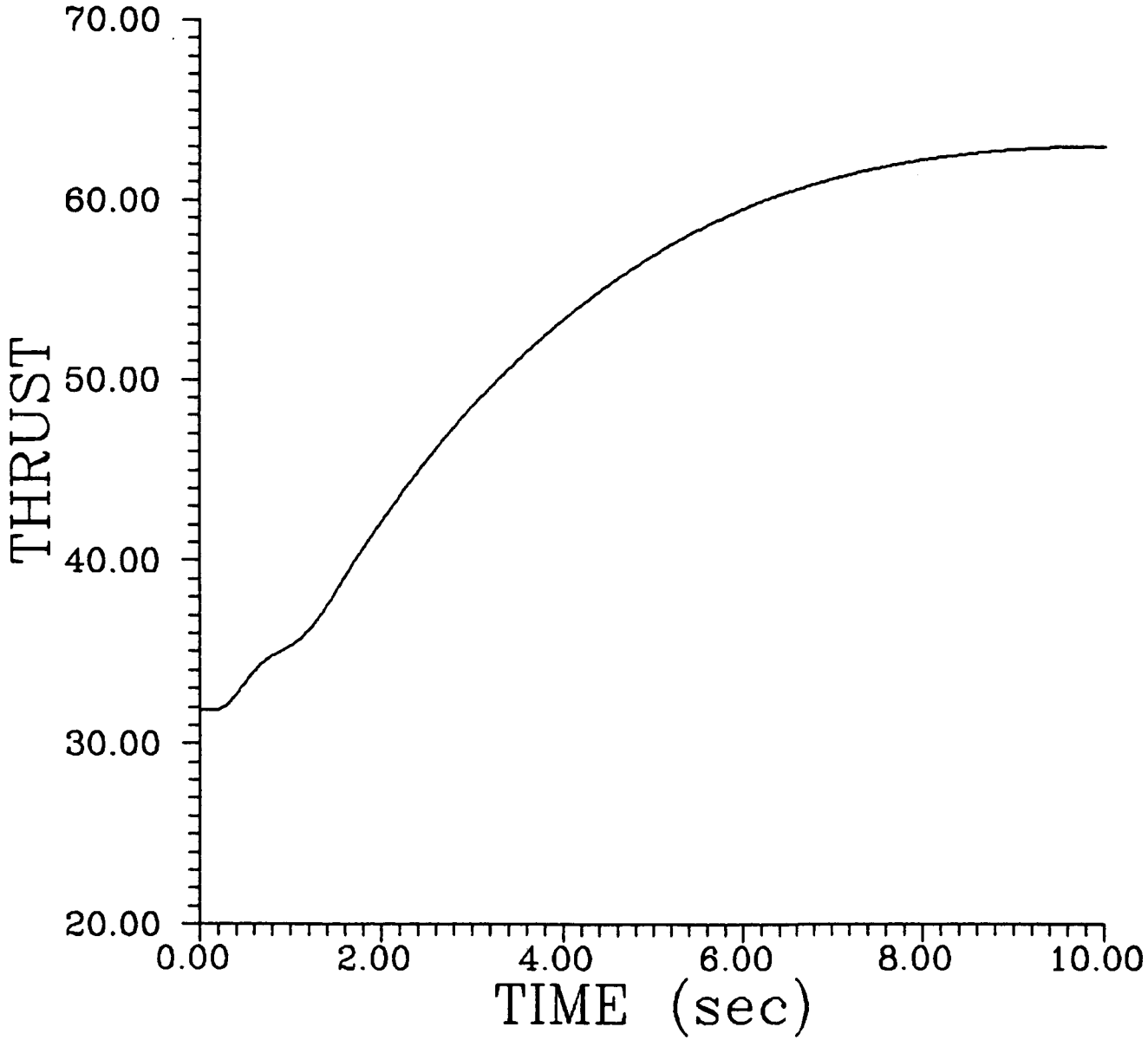

Figure 6.1. Simulation of Nominal (No Failure) Closed-loop System

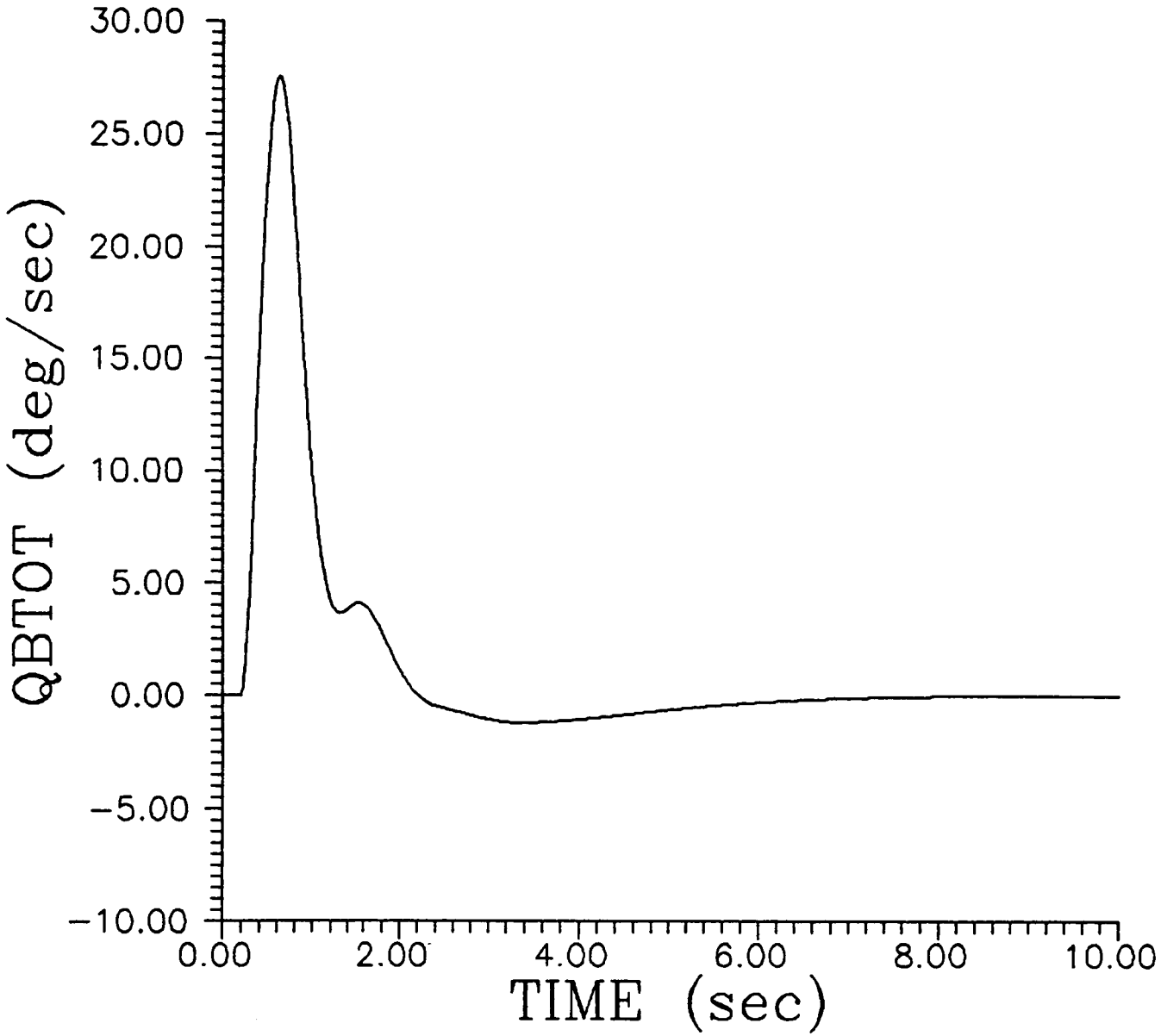

Figure 6.m. Simulation of Nominal (No Failure) Closed-loop System

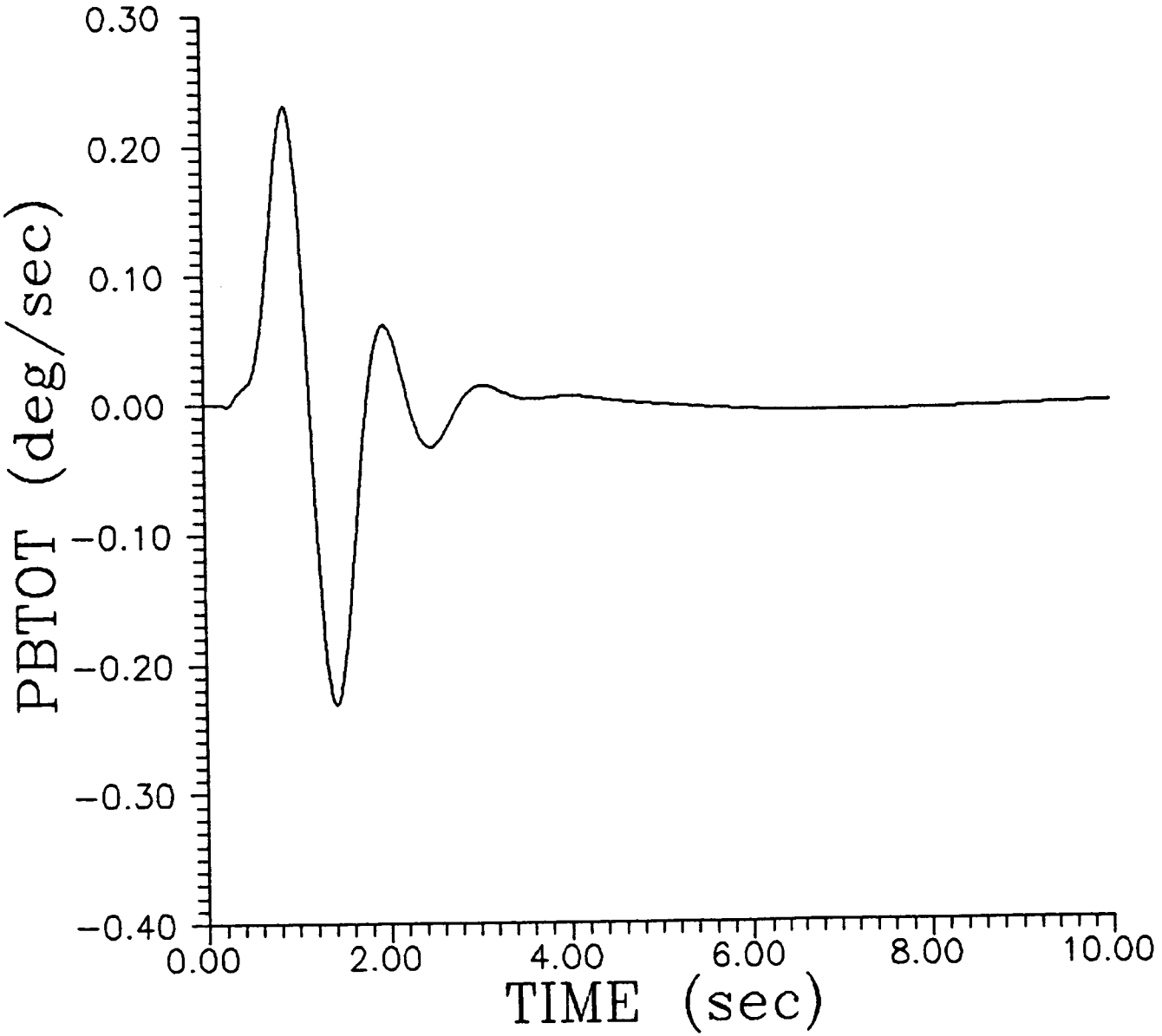

Figure 6.n. Simulation of Nominal (No Failure) Closed-loop System

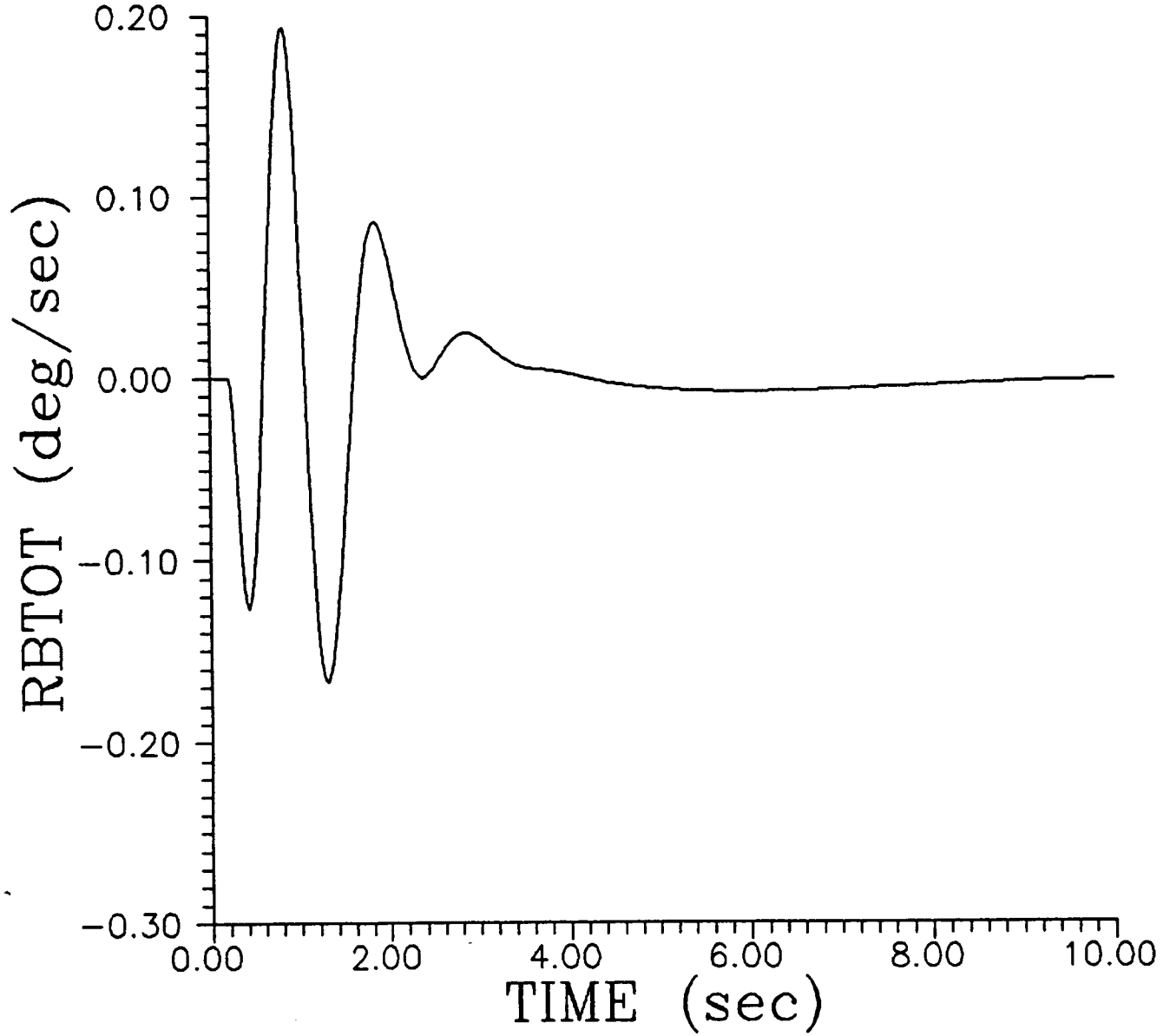

Figure 6.o. Simulation of Nominal (No Failure) Closed-loop System

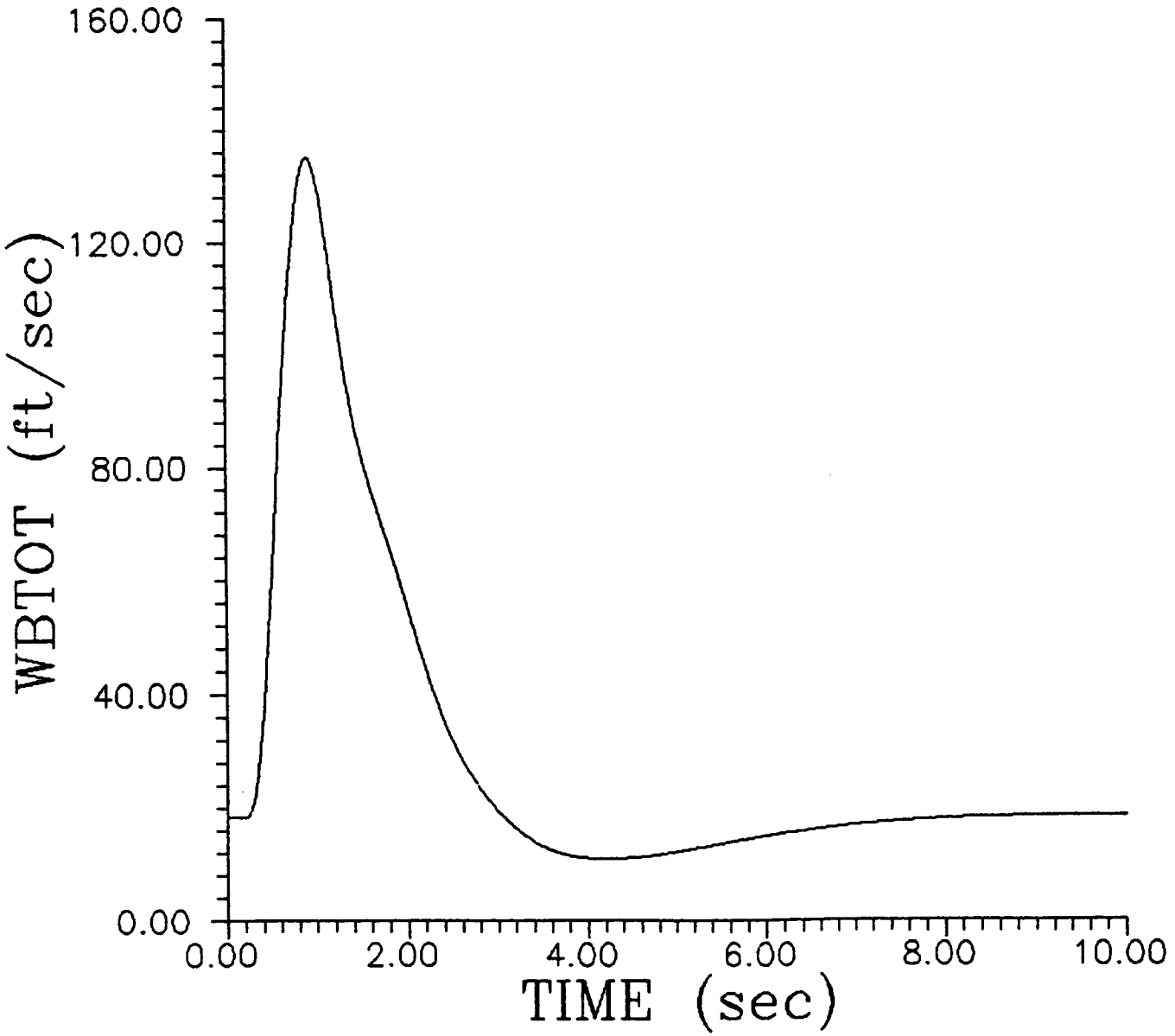

Figure 6.p. Simulation of Nominal (No Failure) Closed-loop System

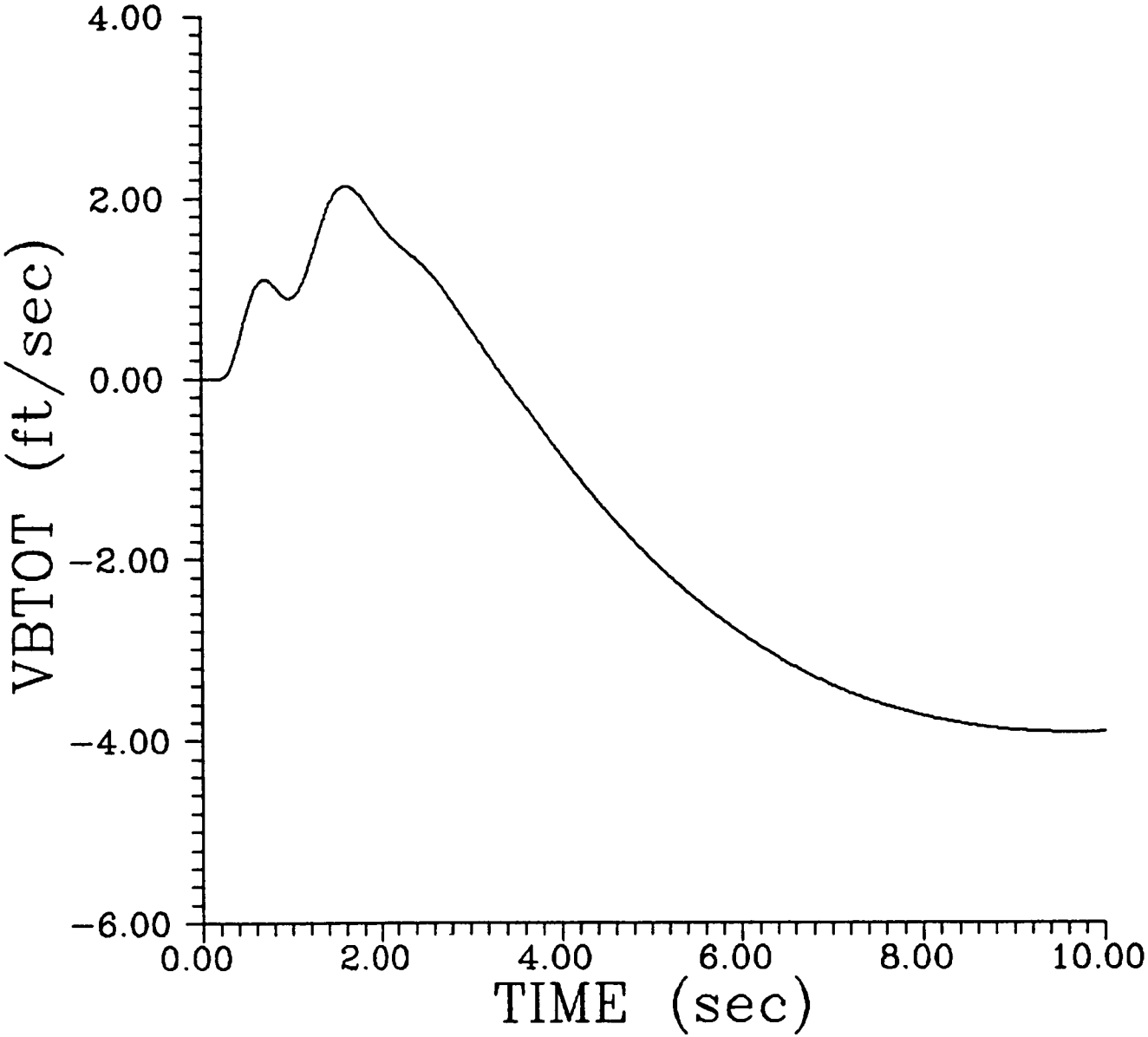

Figure 6.q. Simulation of Nominal (No Failure) Closed-loop System

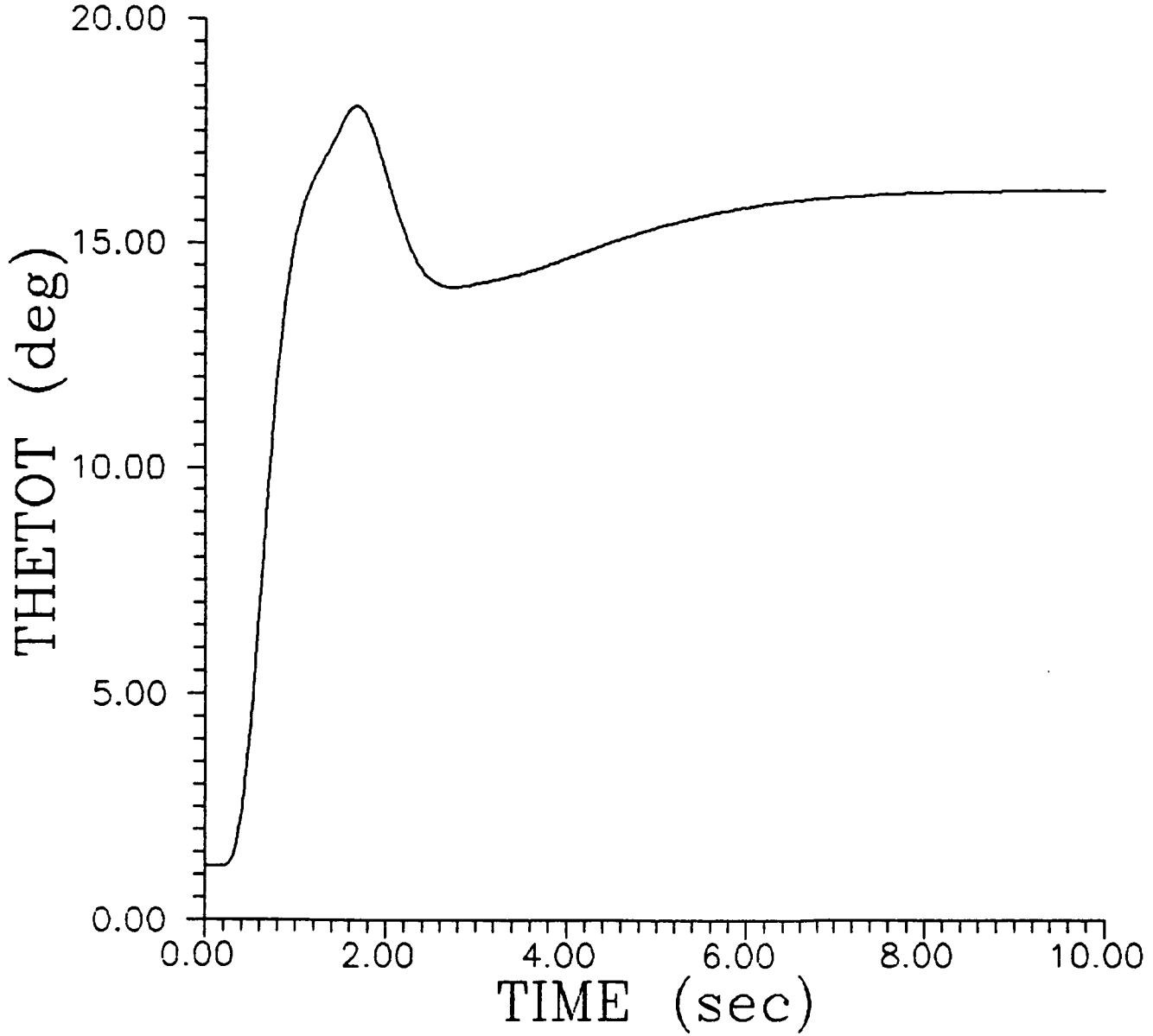

Figure 7.a. Simulation of Centered Left Horizontal Tail and Reconfigured Control Law

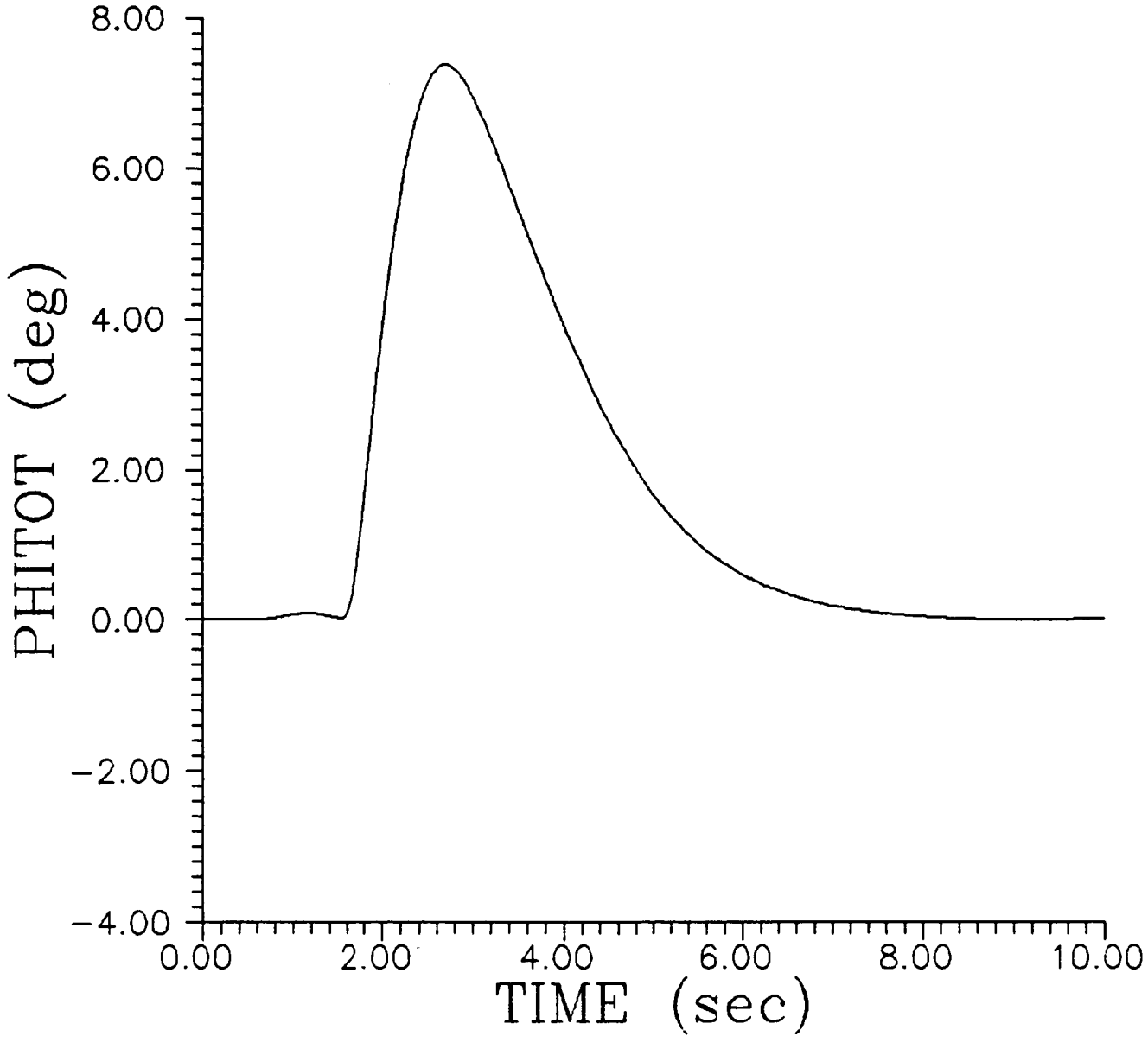

Figure 7.b. Simulation of Centered Left Horizontal Tail and Reconfigured Control Law

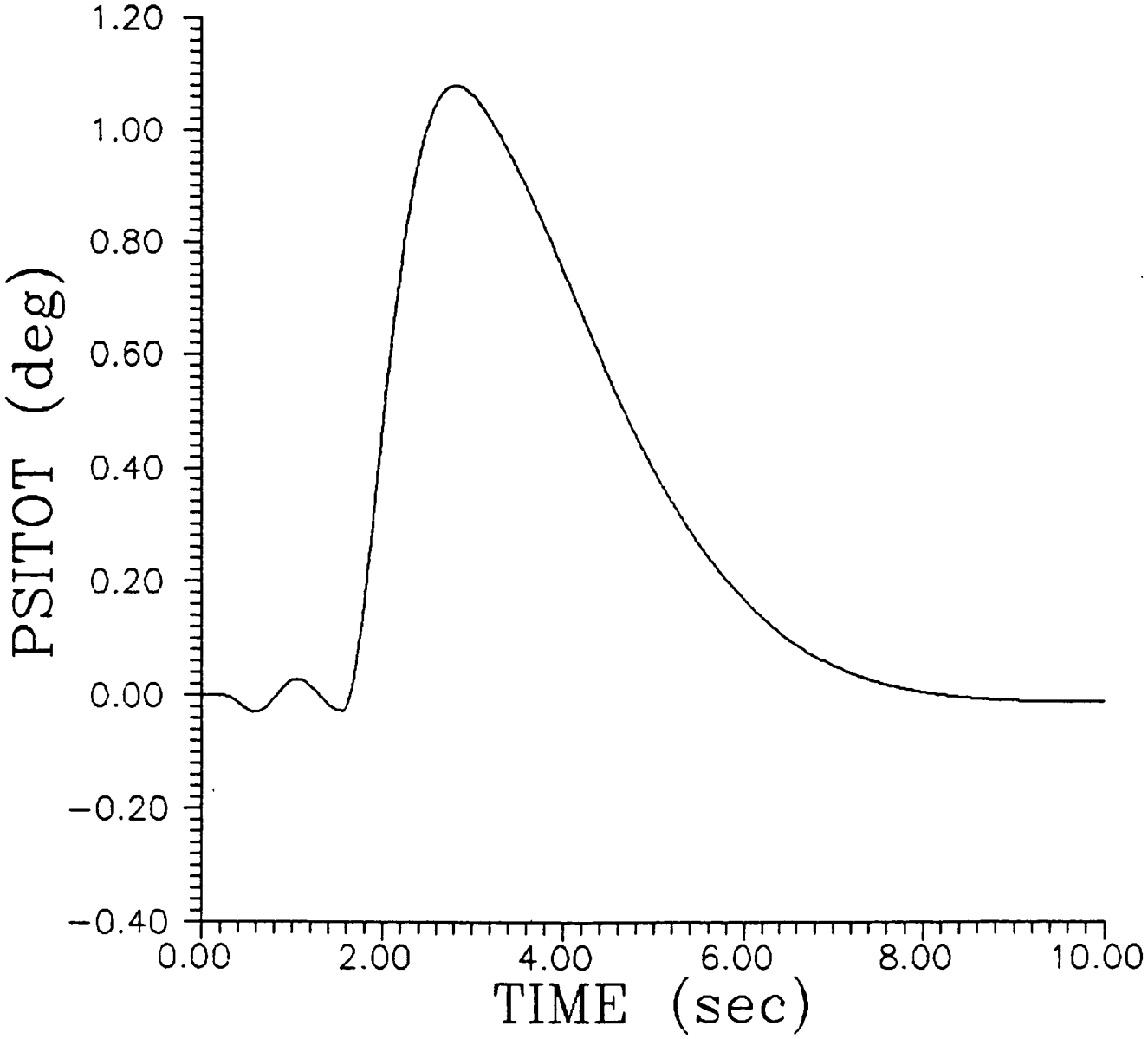

Figure 7.c. Simulation of Centered Left Horizontal Tail and Reconfigured Control Law

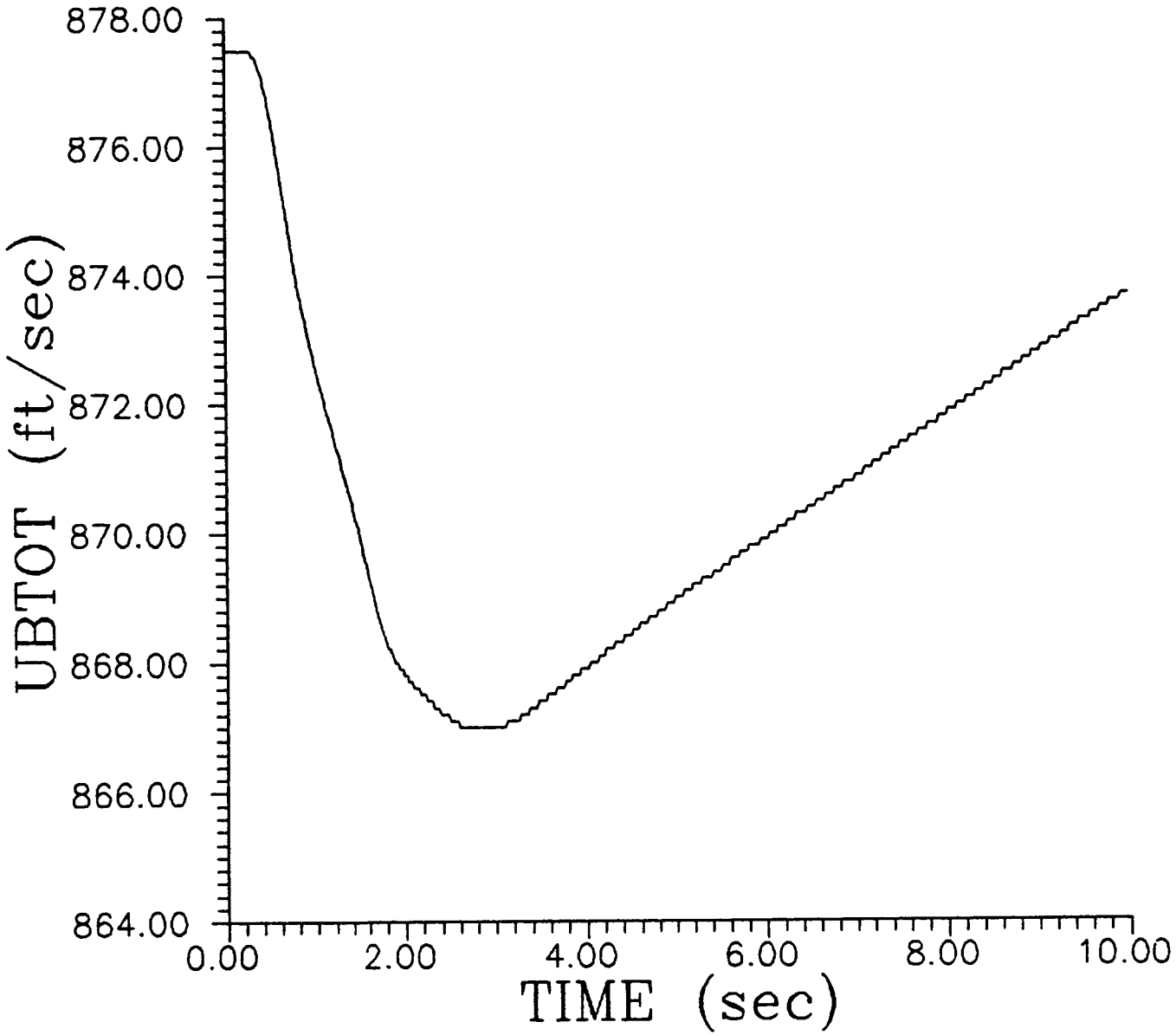

Figure 7.d. Simulation of Centered Left Horizontal Tail and Reconfigured Control Law

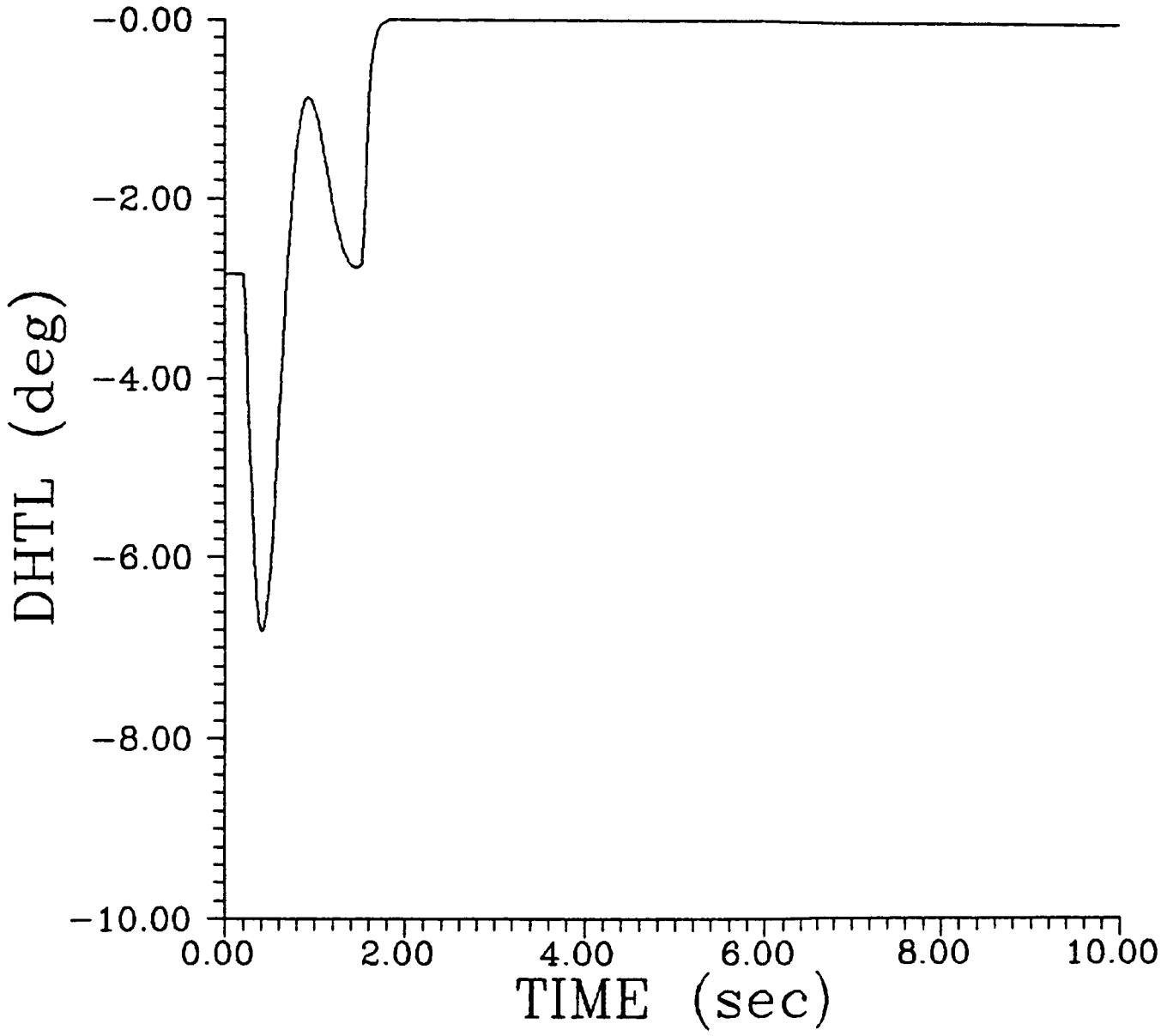

Figure 7.e. Simulation of Centered Left Horizontal Tail and Reconfigured Control Law

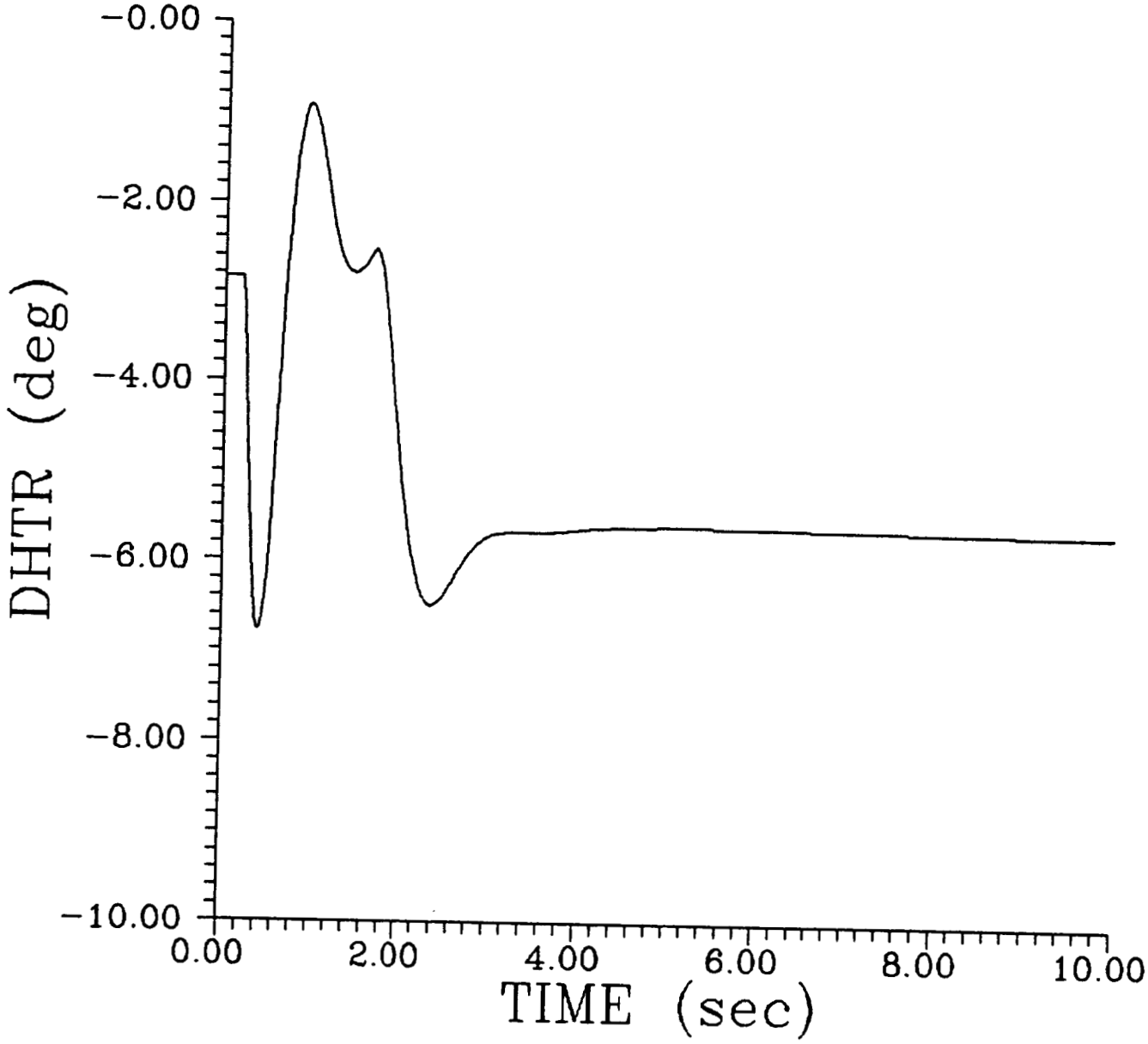

Figure 7.f. Simulation of Centered Left Horizontal Tail and Reconfigured Control Law

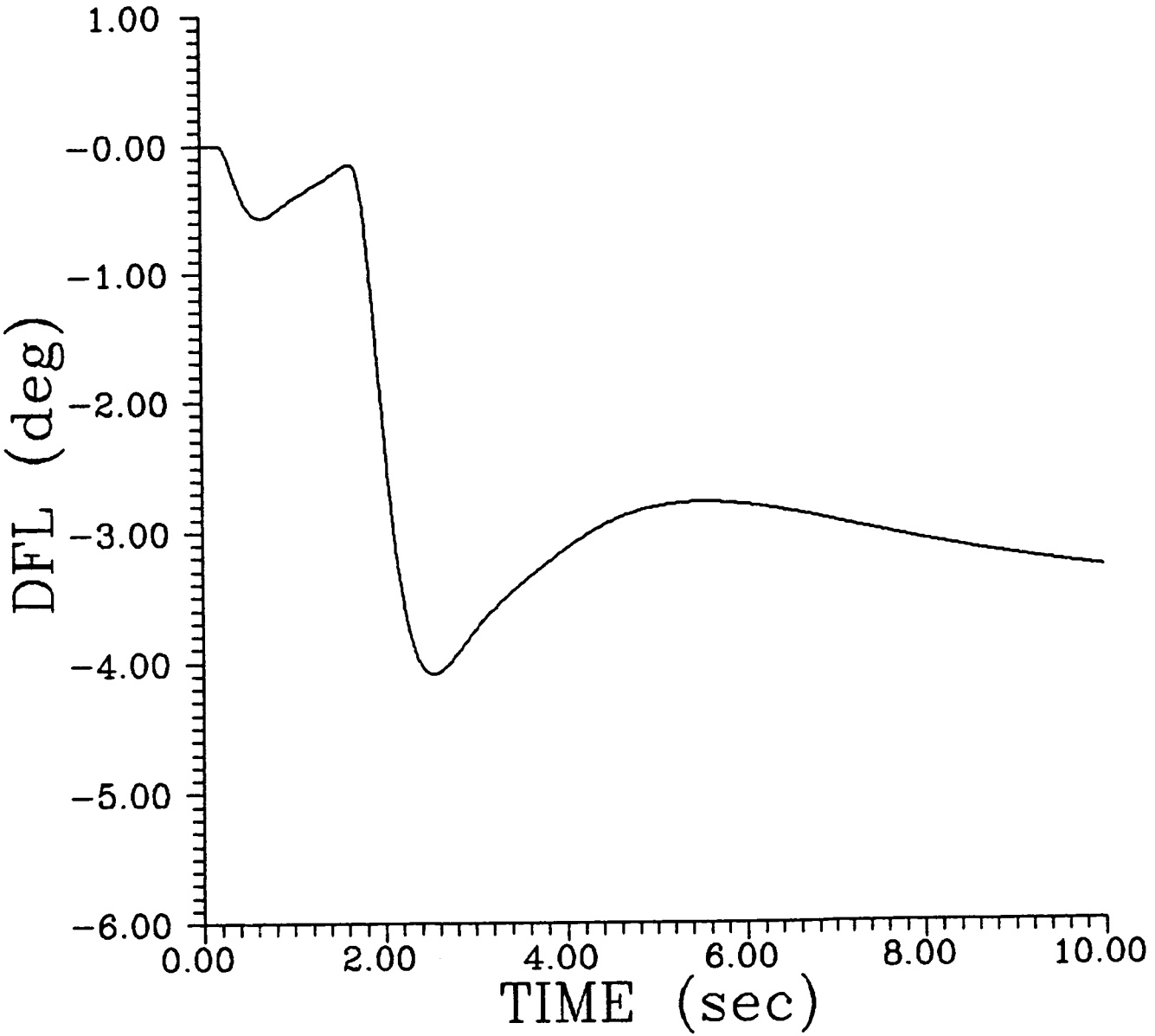

Figure 7.g. Simulation of Centered Left Horizontal Tail and Reconfigured Control Law

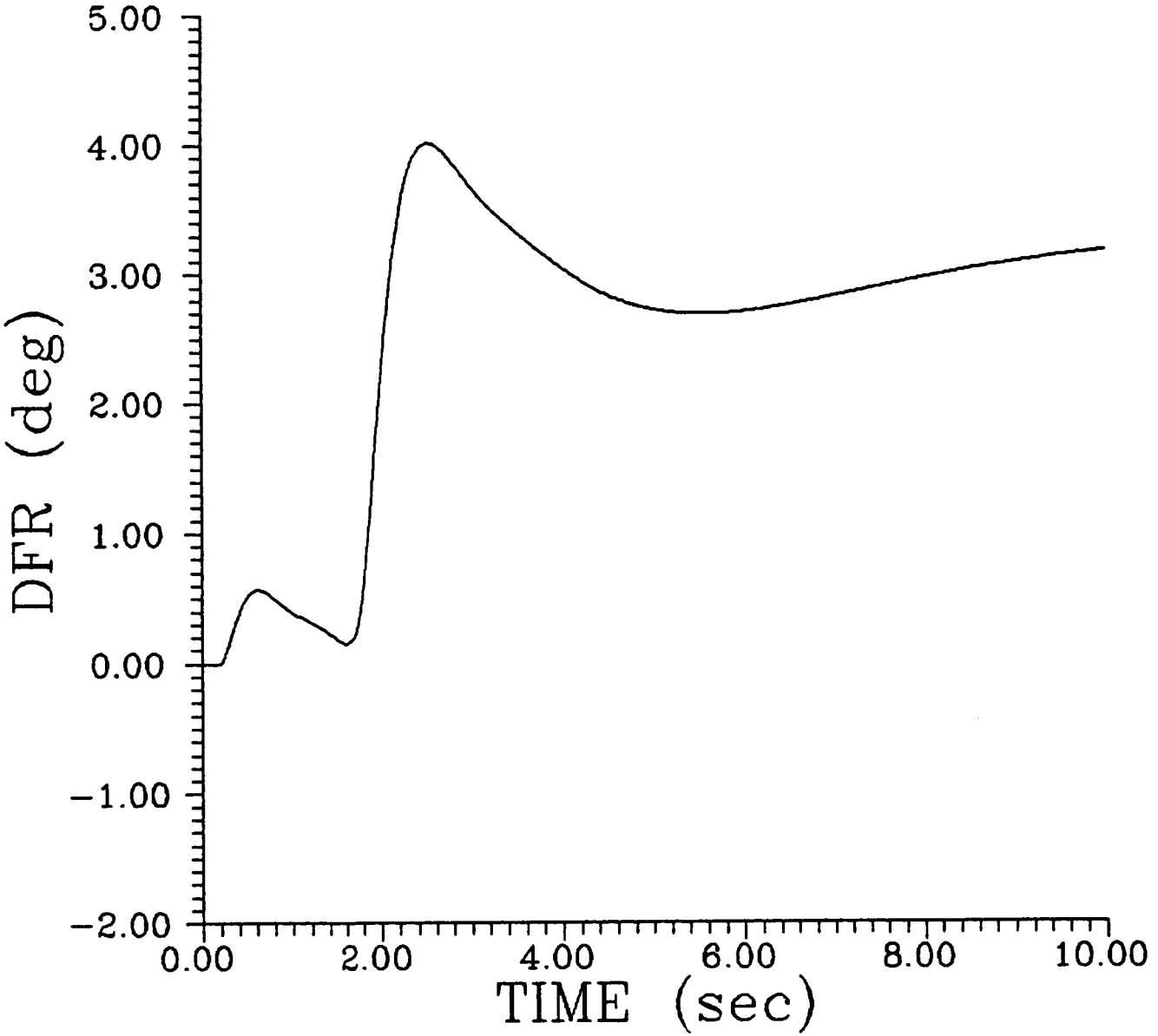

Figure 7.h. Simulation of Centered Left Horizontal Tail and Reconfigured Control Law

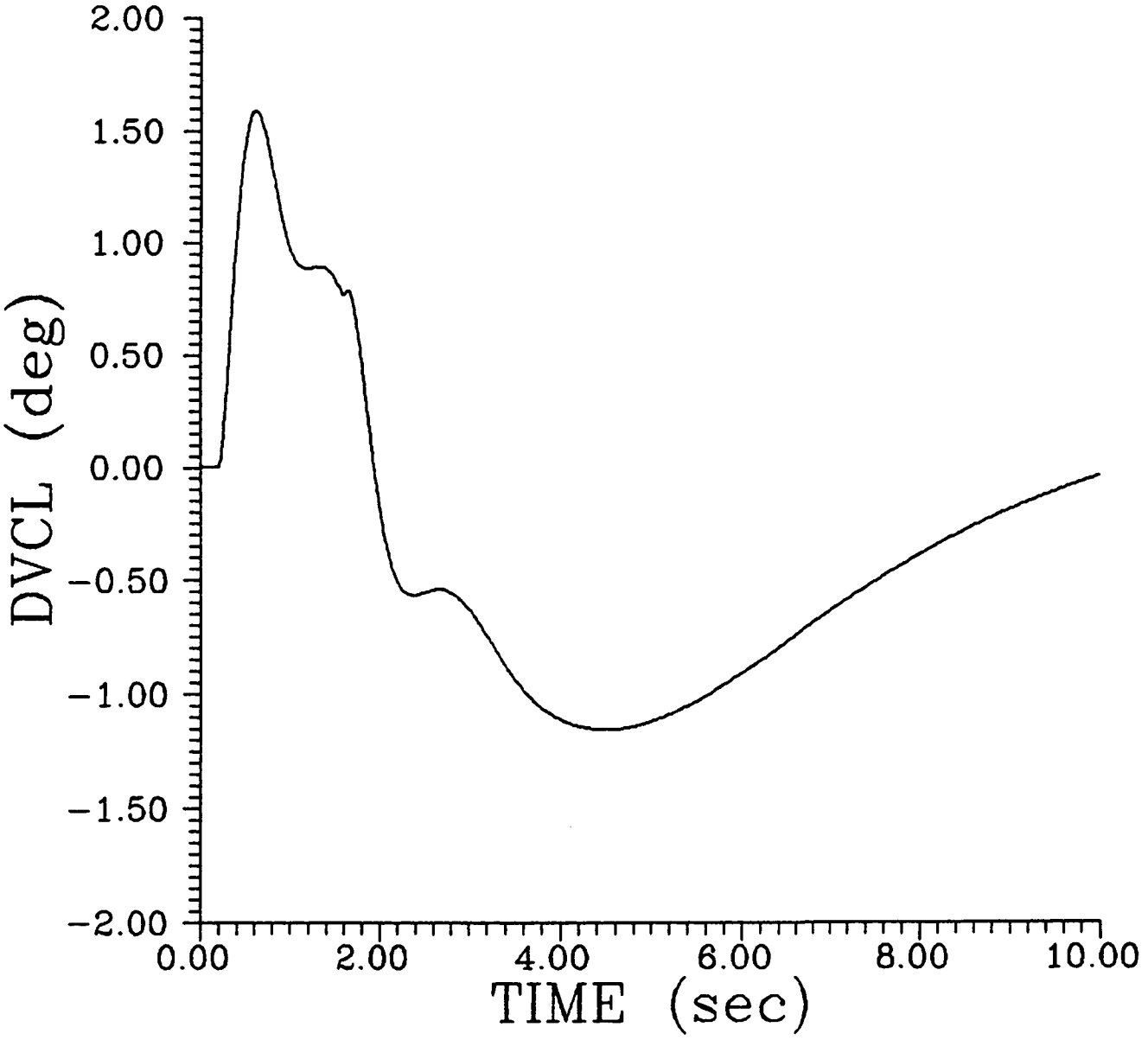

Figure 7.i. Simulation of Centered Left Horizontal Tail and Reconfigured Control Law

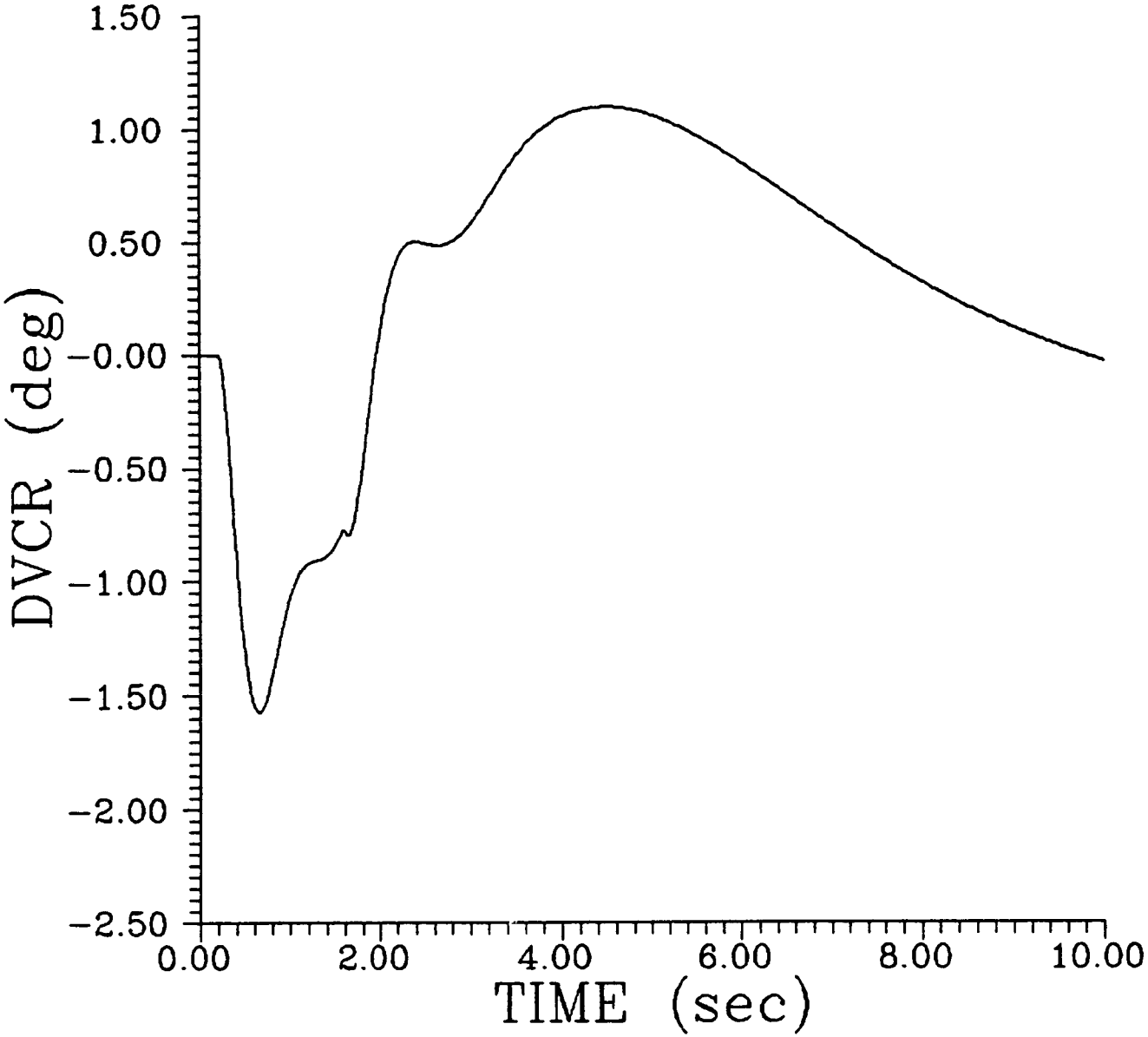

Figure 7.j. Simulation of Centered Left Horizontal Tail and Reconfigured Control Law

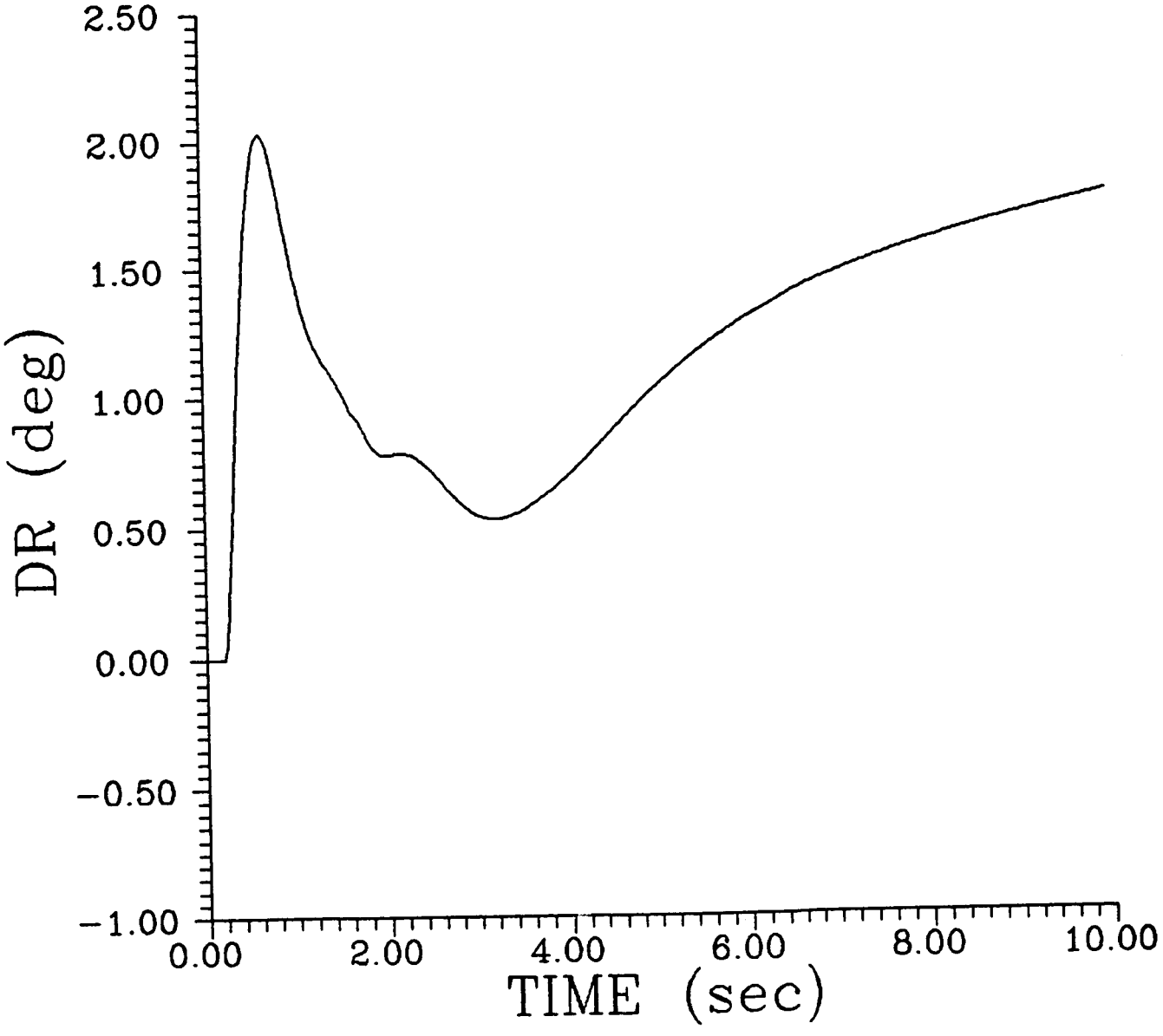

Figure 7.k. Simulation of Centered Left Horizontal Tail and Reconfigured Control Law

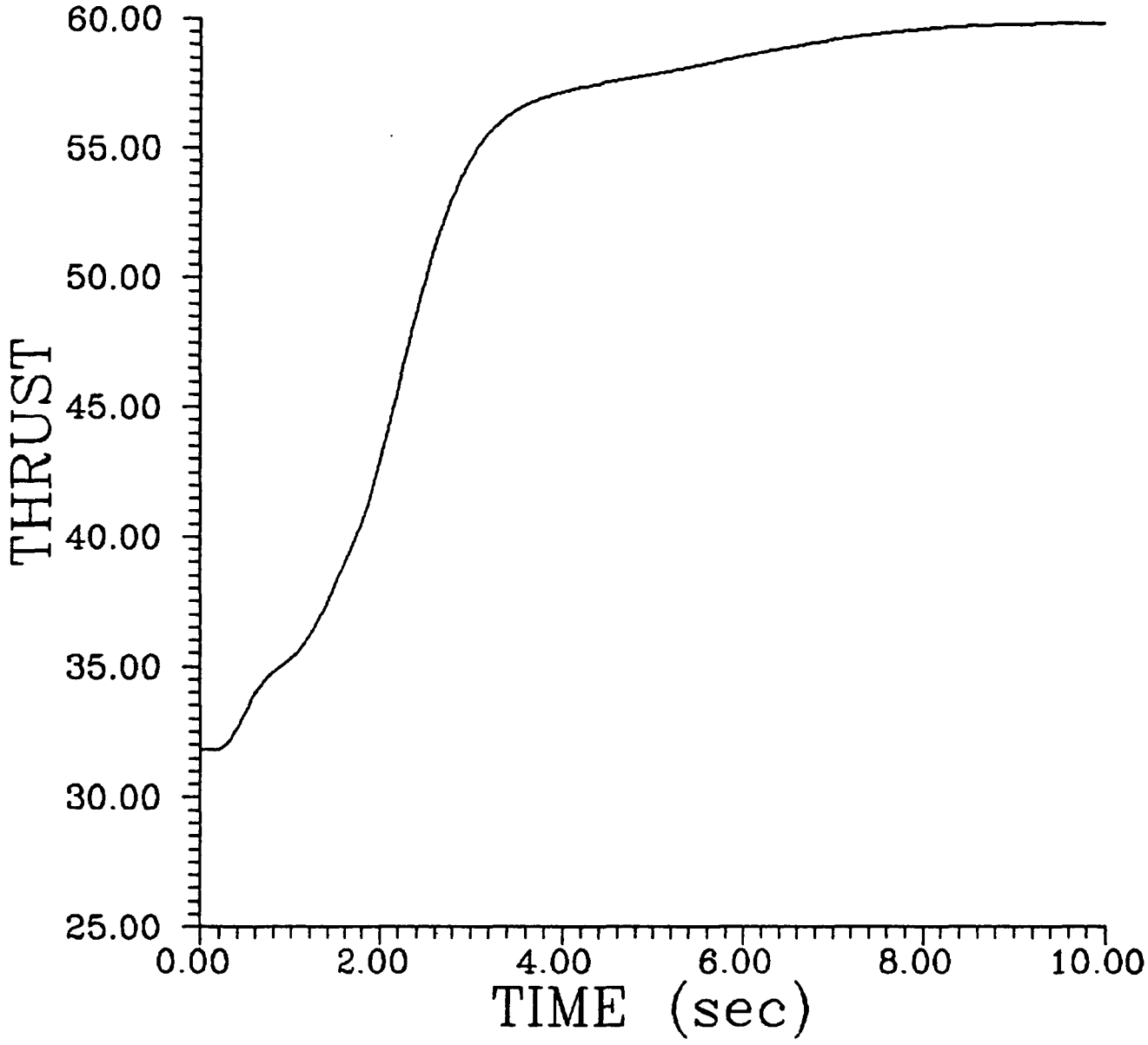

Figure 7.1. Simulation of Centered Left Horizontal Tail and Reconfigured Control Law

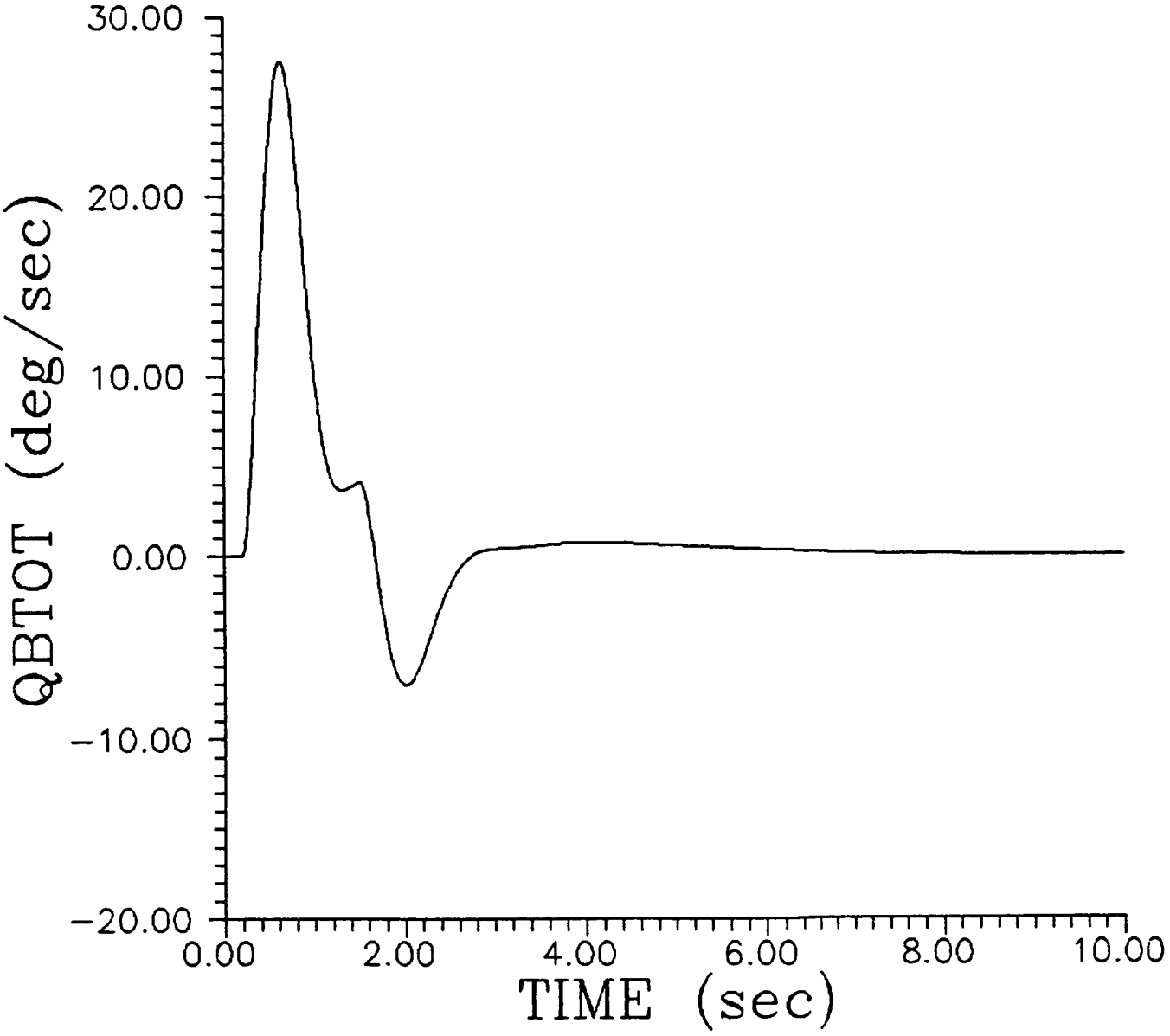

Figure 7.m. Simulation of Centered Left Horizontal Tail and Reconfigured Control Law

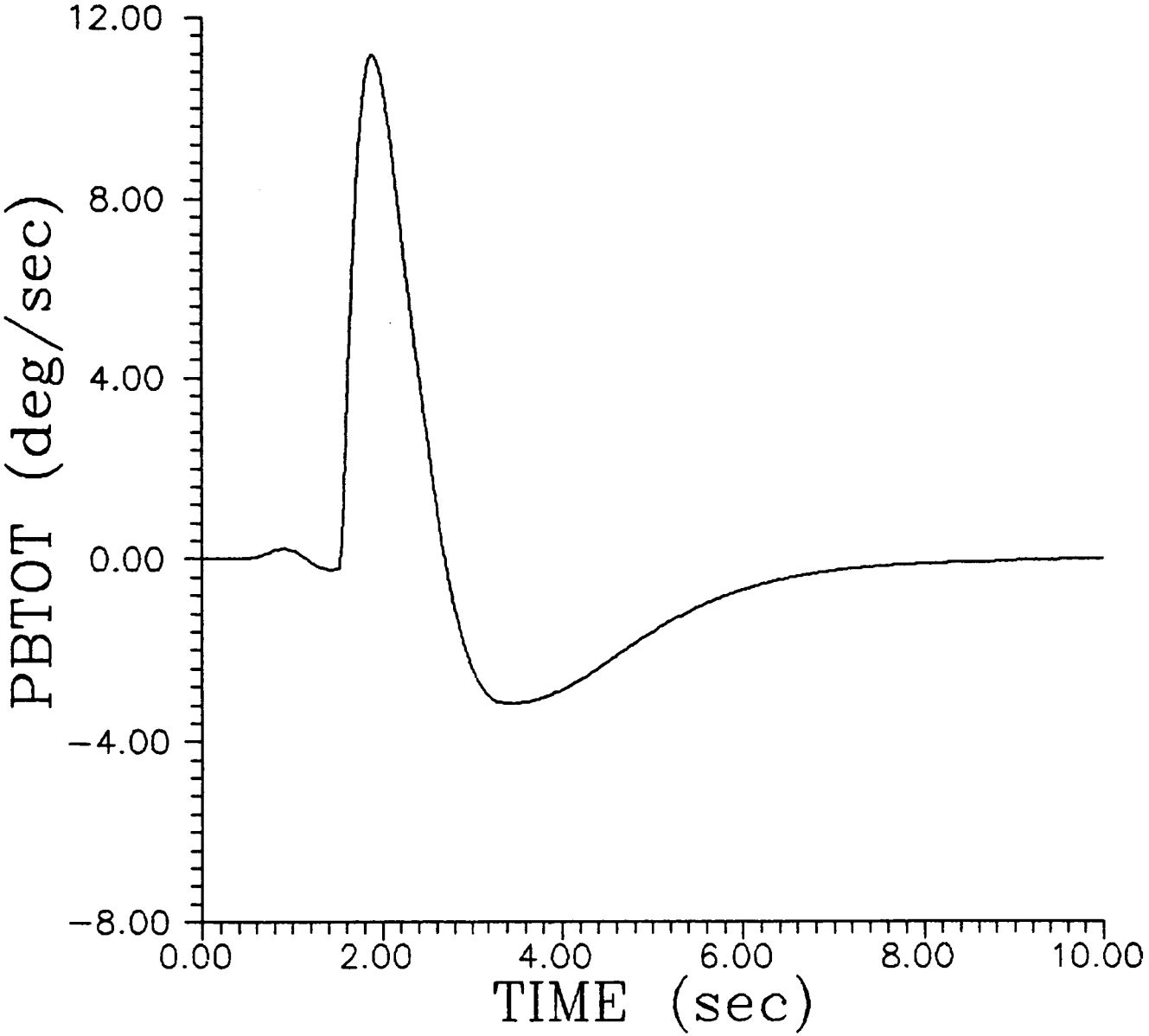

Figure 7.n. Simulation of Centered Left Horizontal Tail and Reconfigured Control Law

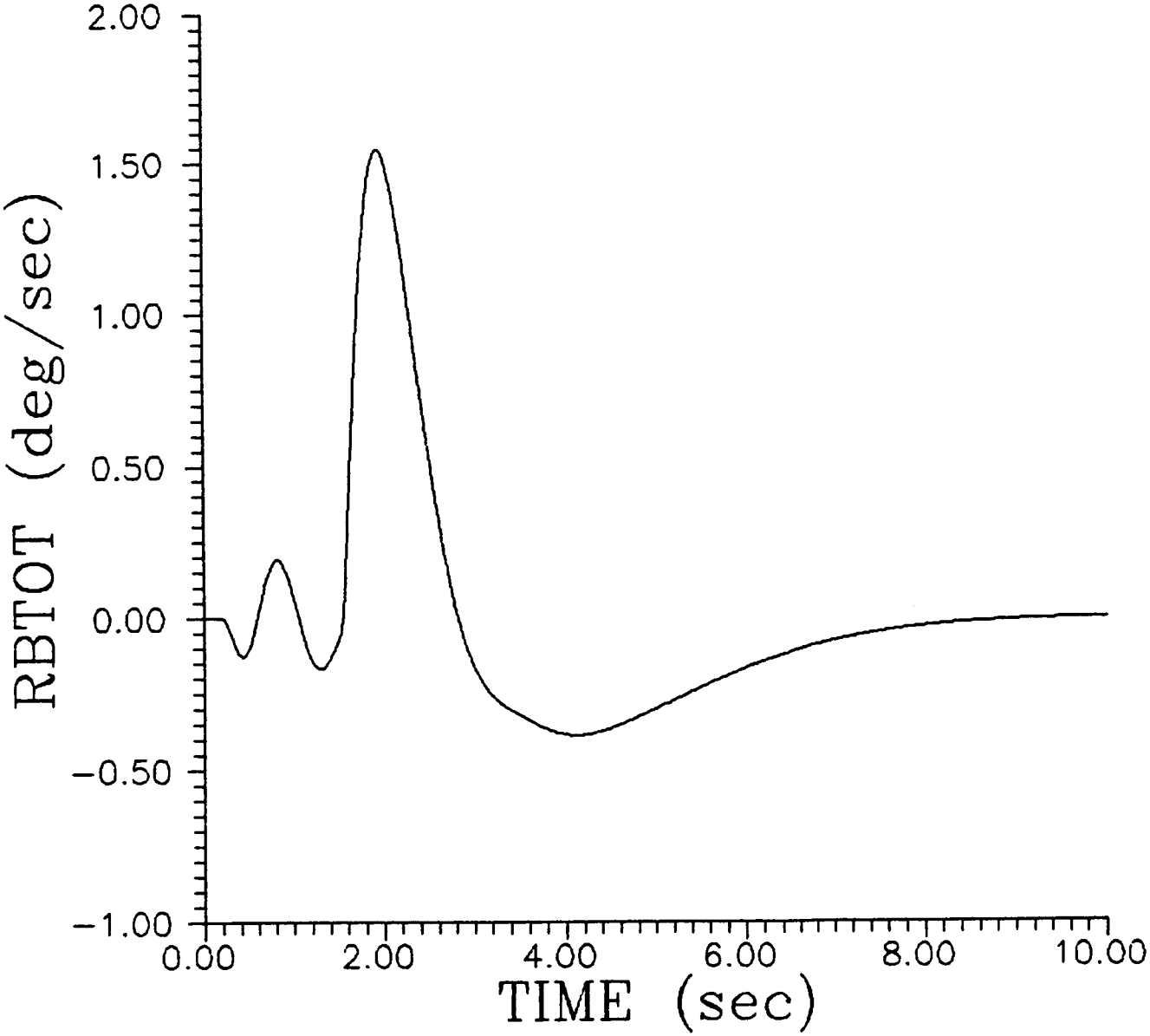

Figure 7.o. Simulation of Centered Left Horizontal Tail and Reconfigured Control Law

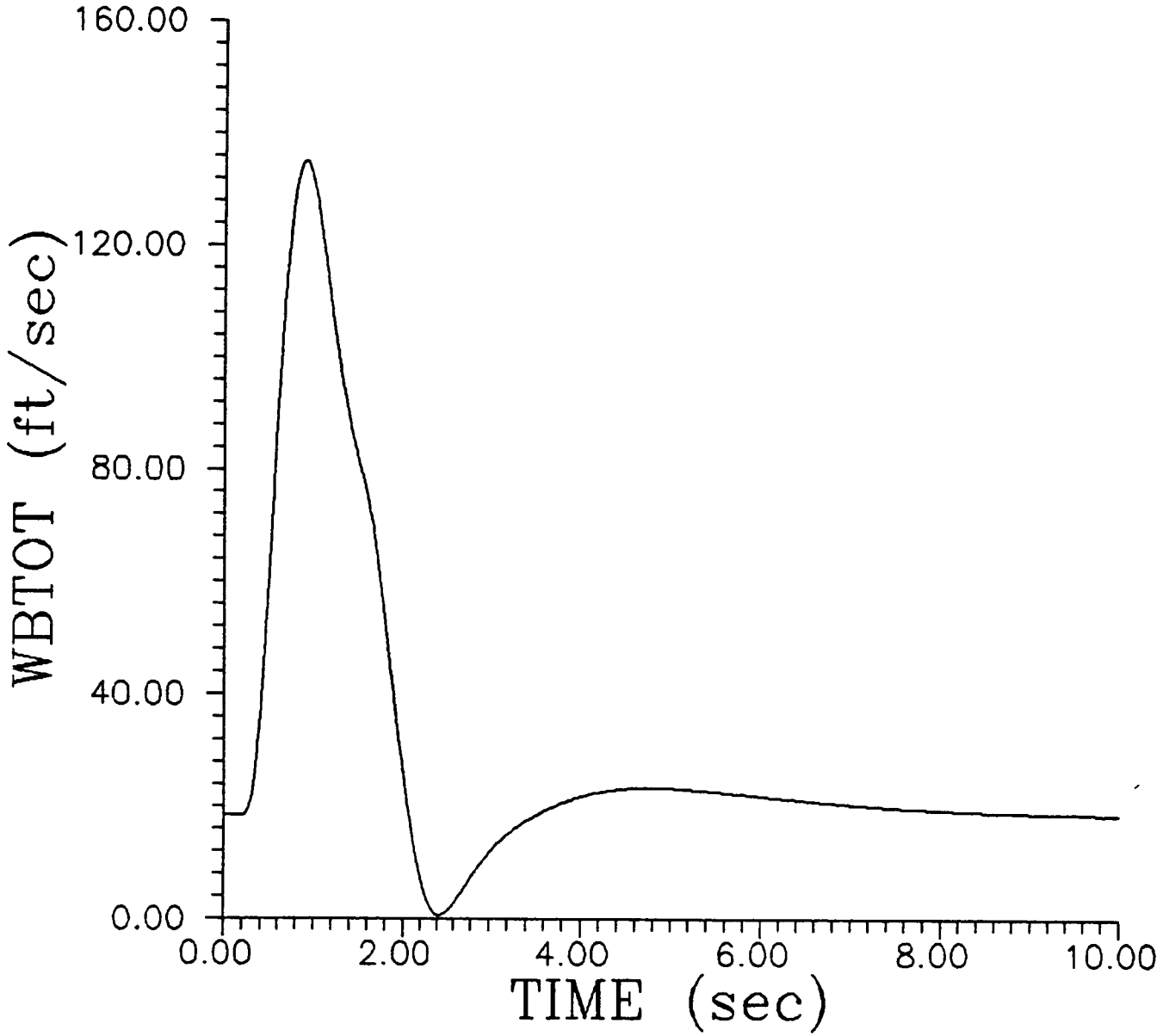

Figure 7.p. Simulation of Centered Left Horizontal Tail and Reconfigured Control Law

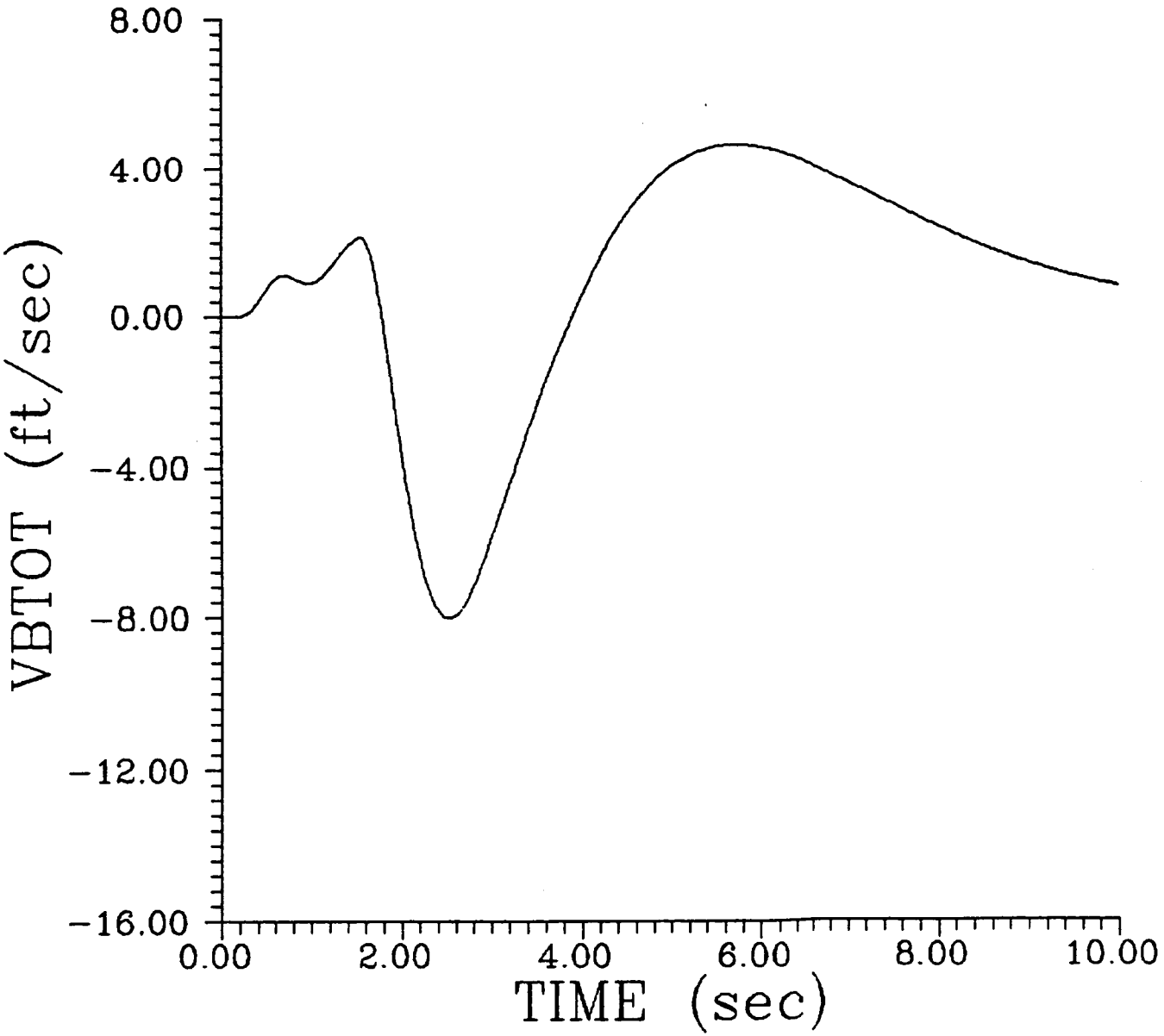

Figure 7.q. Simulation of Centered Left Horizontal Tail and Reconfigured Control Law

Table 1. A and B Matrices at 0.8 Mach and 5000 ft. Altitude

ORIGINAL PAGE IS OF POOR QUALITY

A

	u_B	w_B	q_B	θ	v_B
u_B	0.185276E+01	0.680103E-01	-0.420734E+02	-0.127597E+03	-0.288743E-01
w_B	-0.264915E+01	-0.211069E+01	0.833334E+03	0.111540E+03	0.161393E-01
q_B	-0.870515E-02	0.174956E-02	-0.114709E+01	0.294158E+00	0.426587E-04
θ	0.704352E-02	0.548410E-02	0.630955E+01	0.120452E+01	-0.896722E-03
v_B	0.732773E-01	0.530715E-02	0.303690E+01	-0.258045E+01	-0.489453E+00
p_B	-0.127960E-02	-0.966816E-04	-0.479375E-01	0.438832E-01	-0.821339E-01
r_B	-0.827831E-05	0.349885E-04	0.176224E+00	0.106855E-01	0.114808E-01
ϕ	0.210164E-02	0.108419E-02	0.102725E+01	0.198157E+00	-0.175950E-03
ψ	-0.401382E-03	0.255457E-04	0.384618E-01	0.300838E-01	-0.487672E-05

	p_B	r_B	ϕ	ψ
u_B	0.107470E+01	0.857338E+01	0.534983E+01	0.000000E+00
w_B	-0.149213E+01	-0.113102E+02	-0.754023E+01	0.000000E+00
q_B	-0.391754E-02	-0.187347E+00	-0.197997E-01	0.000000E+00
θ	0.316213E-02	-0.181205E-01	0.239754E-01	0.000000E+00
v_B	0.185952E+02	-0.873939E+03	0.323620E+02	0.000000E+00
p_B	-0.451725E+01	-0.148556E+00	-0.370102E-02	0.000000E+00
r_B	-0.519926E-01	-0.616548E+00	0.210881E-05	0.000000E+00
ϕ	0.100104E+01	0.207903E-01	0.675038E-02	0.000000E+00
ψ	-0.235055E-03	0.998068E+00	-0.112015E-02	0.000000E+00

B

	δR	δhtl	δhtr	δfl	δfr
u_B	-0.175500E-11	0.911570E-01	0.911570E-01	-0.150040E+00	-0.150040E+00
w_B	-0.779970E-12	-0.161480E+01	-0.161480E+01	-0.203680E+01	-0.203680E+01
q_B	0.491380E-12	-0.251560E+00	-0.251560E+00	-0.391970E-01	-0.391970E-01
θ	0.000000E+00	0.000000E+00	0.000000E+00	0.000000E+00	0.000000E+00
v_B	0.805140E+00	-0.252320E+00	0.252320E+00	0.424820E-02	-0.424820E-02
p_B	0.238630E+00	0.562860E+00	-0.562860E+00	0.539680E+00	-0.539680E+00
r_B	-0.121790E+00	0.524460E-01	-0.524460E-01	0.139030E-01	-0.139030E-01
ϕ	0.000000E+00	0.000000E+00	0.000000E+00	0.000000E+00	0.000000E+00
ψ	0.000000E+00	0.000000E+00	0.000000E+00	0.000000E+00	0.000000E+00

	$\delta lefhl$	δvcl	δvcr	δsb	δth
u_B	-0.203960E+00	-0.662130E-03	-0.662130E-03	-0.875550E-03	0.341710E+00
w_B	0.401860E+00	0.315980E-01	0.315980E-01	0.417830E-01	-0.216160E-04
q_B	-0.446440E-01	-0.338080E-01	-0.338080E-01	0.655820E-02	0.263690E-05
θ	0.000000E+00	0.000000E+00	0.000000E+00	0.000000E+00	0.000000E+00
v_B	-0.927860E-13	0.307940E+00	-0.307940E+00	0.990900E-26	0.516990E-25
p_B	0.519310E-11	0.664610E-01	-0.664610E-01	0.000000E+00	0.000000E+00
r_B	-0.413760E-13	0.648400E-01	-0.648400E-01	0.000000E+00	0.000000E+00
ϕ	0.000000E+00	0.000000E+00	0.000000E+00	0.000000E+00	0.000000E+00
ψ	0.000000E+00	0.000000E+00	0.000000E+00	0.000000E+00	0.000000E+00

Table 2. Control Effector Transfer Functions

A. Integrated Servoactuator (ISA) Transfer Function

$$G(s) = \frac{(20.2)(144.8)(71.4)^2}{(2+20.2)(s+144.8)(s^2+2(.736)(71.4)s+71.4^2)}$$

NOTE: The ISA is used to drive
Rudder
Horizontal Tails
Flaperons
Vertical Canards

B. Leading-Edge Flaps Transfer Function

$$G(s) = \frac{7.38}{s+7.38}$$

C. Speed Brake Transfer Function

$$G(s) = \frac{27.28}{s}$$

D. Percent Throttle Transfer Function

$$G(s) = \frac{2}{s+2}$$

Table 3. Control Effector Rate and Position Limits

Control	Rate Limit	Max. Positive Deflection	Max. Negative Deflection
Rudder	120 deg/s	30 deg	30 deg
Left Hoizontal Tail	60 deg/s	25 deg	25 deg
Right Hoizontal Tail	60 deg/s	25 deg	25 deg
Left Flaperon	52 deg/s	20 deg	23 deg
Right Flaperon	52 deg/s	20 deg	23 deg
Leading Edge Flaps	30 deg/s	25 deg	2 deg
Left Vertical Canard	108 deg/s	27 deg	27 deg
Right Vertical Canard	108 deg/s	27 deg	27 deg
Speed Break	27.28 deg/s	60 deg	0 deg
PLA	N/A	100%	0%

Table 4.a. Control Gain Matrices

K_o

	1	2	3	4	5	6
1)	0.73641E-01	0.24068E-02	0.93686E+01	0.43346E+02	-0.83852E+00	0.16631E+02
2)	0.15767E+00	-0.76792E-01	-0.16571E+03	-0.28171E+03	0.72877E-02	-0.20960E+01
3)	0.13515E+00	-0.76745E-01	-0.16321E+03	-0.27[illegible]E+03	0.93282E-02	-0.94502E+00
4)	-0.35132E-01	-0.86939E-03	-0.16678E+01	-0.99714E+01	-0.96873E+00	0.55640E+02
5)	0.17492E-01	0.11124E-02	0.33197E+01	0.13349E+02	0.96729E+00	-0.54266E+02
6)	0.54345E-01	0.30727E-02	0.17691E+02	0.34307E+02	0.41028E+00	0.12003E+01
7)	-0.50495E-01	-0.11095E-02	-0.10371E+02	-0.23758E+02	-0.40381E+00	-0.26346E+01
8)	0.57152E+01	0.15239E+00	0.63362E+02	0.95326E+02	-0.16045E+00	-0.87354E+02

	7	8	9	10	11	12
1)	-0.19058E+03	0.55522E+02	-0.32064E+03	0.90036E+01	-0.31316E+02	0.30987E+02
2)	0.14594E+01	0.55759E+00	0.90308E+00	0.40612E-01	-0.65742E+01	0.25137E+02
3)	-0.13970E+01	0.30788E+01	-0.14079E+01	0.10895E+00	-0.13686E+02	0.32237E+02
4)	0.12576E+03	0.17253E+03	0.12477E+02	0.12592E+01	0.15764E+02	-0.15728E+02
5)	-0.12714E+03	-0.16915E+03	-0.10800E+02	-0.11691E+01	-0.14666E+02	0.14579E+02
6)	0.13237E+03	0.11600E+02	0.40012E+03	-0.32923E+01	-0.25977E+02	0.25448E+02
7)	-0.13243E+03	-0.13816E+02	-0.39908E+03	0.32638E+01	0.21974E+02	-0.21605E+02
8)	0.11242E+03	-0.14603E+03	-0.12246E+03	-0.73755E+01	-0.16460E+03	0.16024E+03

	13	14	15	16	17	18
1)	0.25665E+02	0.22088E+02	-0.26795E+02	-0.21145E+02	0.26878E+00	0.23923E-01
2)	0.22356E+02	0.22263E+02	0.28842E+02	0.28669E+02	0.40306E-01	0.26146E-01
3)	0.21040E+02	0.20967E+02	0.32378E+02	0.32216E+02	0.21017E-01	0.22973E-01
4)	0.85805E+01	-0.69334E+01	0.81713E+01	0.48482E+01	-0.85306E-01	-0.92146E-02
5)	0.18889E+01	0.17295E+02	-0.76165E+01	-0.43678E+01	0.81679E-01	0.68934E-02
6)	0.22057E+02	0.19849E+02	-0.10067E+02	-0.16157E+02	0.22682E+00	0.20237E-01
7)	-0.19782E+02	-0.17488E+02	0.20228E+02	0.26312E+02	-0.21288E+00	-0.18790E-01
8)	0.58001E+02	0.62297E+02	-0.13271E+03	-0.12820E+03	0.50906E+01	0.81901E+00

	19	20	21
1)	0.31767E+02	0.24407E+02	-0.17952E+03
2)	-0.13558E+03	0.33354E+00	-0.94566E+00
3)	-0.13429E+03	0.15288E+01	-0.29494E+01
4)	-0.77459E+01	0.90349E+02	0.14058E+02
5)	0.94923E+01	-0.88879E+02	-0.14607E+02
6)	0.25568E+02	-0.16730E+01	0.15683E+03
7)	-0.20501E+02	0.58241E+00	-0.15602E+03
8)	0.11784E+03	-0.39753E+02	0.45097E+02

Table 4.b. Control Gain Matrices

K_1

	1	2	3	4	5	6
1)	0.11623E-01	-0.12344E-01	-0.23636E+02	-0.38633E+02	-0.29761E-01	-0.22253E+01
2)	0.70292E-01	-0.71743E-02	-0.38208E+02	-0.38568E+02	0.70986E-01	-0.36963E+01
3)	0.86695E-01	-0.14252E-01	-0.53903E+02	-0.61478E+02	0.68675E-01	-0.41924E+01
4)	0.95837E-01	-0.35579E-01	-0.79592E+02	-0.12993E+03	0.24385E-01	-0.85037E+00
5)	-0.95840E-01	0.35501E-01	0.80391E+02	0.12939E+03	-0.32682E-01	0.73964E+00
6)	0.50823E-01	-0.28044E-01	-0.55922E+02	-0.88649E+02	-0.19151E-01	-0.20851E+01
7)	-0.36825E-01	0.22171E-01	0.41859E+02	0.68137E+02	0.19149E-01	0.23659E+01
8)	0.17922E-01	-0.24255E-01	-0.28319E+02	-0.32904E+02	-0.60214E-02	0.18175E+02

	7	8	9	10	11	12
1)	0.96270E+01	0.61853E+00	-0.76022E+01	-0.44604E+00	-0.14212E+02	0.12774E+02
2)	-0.53722E+01	-0.18157E+02	-0.16478E+02	-0.32667E+00	0.13433E+02	-0.18080E+02
3)	-0.50274E+01	-0.18485E+02	-0.17555E+02	-0.34716E+00	0.13289E+02	-0.17560E+02
4)	-0.12587E+01	-0.73106E+01	-0.57668E+01	0.70134E-01	0.10239E+02	-0.10026E+02
5)	0.39297E+01	0.72919E+01	0.61282E+01	-0.12676E+00	-0.11059E+02	0.10748E+02
6)	0.83712E+01	-0.76862E+00	-0.85144E+01	-0.38940E+00	-0.10185E+02	0.94617E+01
7)	-0.76370E+01	0.14190E+01	0.85841E+01	0.36677E+00	0.94104E+01	-0.85034E+01
8)	0.69648E+01	0.10119E+02	0.57591E+01	0.19953E+00	-0.27535E+02	0.26724E+02

	13	14	15	16	17	18
1)	-0.23606E+02	-0.23611E+02	0.22750E+02	0.23099E+02	-0.53025E-01	-0.50283E-03
2)	-0.40255E+02	-0.39027E+02	-0.46715E+02	-0.46323E+02	-0.57352E-02	0.39174E-02
3)	-0.42399E+02	-0.41209E+02	-0.47958E+02	-0.47574E+02	-0.59811E-02	0.55964E-02
4)	0.14278E+02	0.14790E+02	-0.10344E+02	-0.10175E+02	0.31140E-01	0.12729E-01
5)	-0.17948E+02	-0.18537E+02	0.11489E+02	0.11339E+02	-0.38843E-01	-0.13078E-01
6)	-0.18393E+02	-0.18297E+02	0.15515E+02	0.15839E+02	-0.37016E-01	0.43426E-02
7)	0.15402E+02	0.15276E+02	-0.17779E+02	-0.18127E+02	0.35547E-01	-0.29878E-02
8)	-0.28926E+01	-0.33628E+01	0.32071E+02	0.31624E+02	-0.22888E-01	-0.75131E-03

	19	20	21
1)	-0.20370E+02	0.24216E+01	0.21633E+01
2)	-0.13056E+02	-0.97765E+01	-0.59828E+01
3)	-0.23156E+02	-0.99537E+01	-0.63238E+01
4)	-0.61187E+02	-0.39131E+01	-0.25182E+01
5)	0.60316E+02	0.42002E+01	0.36309E+01
6)	-0.42381E+02	0.13781E+01	0.84332E+00
7)	0.33304E+02	-0.10702E+01	-0.75548E+00
8)	-0.72420E+01	0.99118E+00	0.72366E+00

Table 4.c. Control Gain Matrices

K_2

	1	2	3	4	5	6
1)	0.28055E-01	-0.10437E-01	-0.25769E+02	-0.38613E+02	-0.15195E-01	-0.59126E+01
2)	0.64091E-01	-0.11685E-01	-0.48597E+02	-0.54468E+02	-0.80714E-01	0.77247E+01
3)	0.62921E-01	-0.96608E-02	-0.44219E+02	-0.47954E+02	-0.77544E-01	0.73335E+01
4)	-0.85724E-01	0.42491E-01	0.87270E+02	0.14243E+03	0.20682E-01	0.20436E+01
5)	0.95530E-01	-0.47533E-01	-0.10009E+03	-0.16093E+03	-0.23937E-01	-0.12309E+01
6)	0.44433E-02	0.50035E-02	0.42506E+00	0.29204E+01	-0.58835E-02	-0.49877E+01
7)	0.72951E-02	-0.82478E-02	-0.10386E+02	-0.17424E+02	0.81472E-02	0.49873E+01
8)	0.35154E-02	-0.11520E-01	-0.48780E+02	-0.36218E+02	0.30400E-01	-0.15905E+02

	7	8	9	10	11	12
1)	0.21181E+01	-0.16727E+02	-0.17517E+02	-0.25931E+00	0.15035E+02	-0.14692E+02
2)	0.17104E+02	0.12112E+02	0.88924E+01	-0.36029E-01	0.34843E+02	-0.39255E+02
3)	0.17095E+02	0.10783E+02	0.82661E+01	-0.68824E-01	0.35608E+02	-0.40314E+02
4)	-0.45096E+01	0.16432E+01	0.14132E+01	0.13749E+00	0.59341E+01	-0.54995E+01
5)	0.58128E+01	-0.11593E+01	-0.24778E+01	-0.14469E+00	-0.18731E+01	0.16782E+01
6)	-0.11983E-02	-0.15350E+02	-0.15205E+02	-0.19484E+00	0.15224E+02	-0.15015E+02
7)	-0.79779E+00	0.14488E+02	0.13272E+02	0.20403E+00	-0.11528E+02	0.11435E+02
8)	-0.24121E+02	-0.49503E+01	-0.15780E+02	0.52899E+00	0.25081E+02	-0.23403E+02

	13	14	15	16	17	18
1)	0.13939E+02	0.14362E+02	0.17898E+02	0.18456E+02	-0.15682E-01	0.78637E-03
2)	-0.25684E+02	-0.26703E+02	-0.53270E+02	-0.53329E+02	-0.15723E-01	0.24257E-02
3)	-0.25345E+02	-0.26289E+02	-0.54338E+02	-0.54363E+02	-0.15157E-01	0.20023E-02
4)	0.26402E+01	0.30095E+01	-0.70058E+01	-0.69185E+01	0.30952E-02	-0.10306E-01
5)	-0.26790E+01	-0.30365E+01	0.66669E+01	0.66248E+01	-0.79153E-02	0.11026E-01
6)	0.13394E+02	0.13889E+02	0.11357E+02	0.11883E+02	-0.82860E-02	-0.12939E-02
7)	-0.12223E+02	-0.12653E+02	-0.15192E+02	-0.15683E+02	0.11027E-01	0.24316E-02
8)	0.84441E+02	0.85995E+02	0.43571E+02	0.44180E+02	0.55960E-01	0.53491E-02

	19	20	21
1)	-0.19524E+02	-0.59684E+01	-0.28047E+01
2)	-0.21033E+02	0.64186E+01	0.70304E+01
3)	-0.18055E+02	0.58237E+01	0.71050E+01
4)	0.66526E+02	0.42415E+00	-0.34980E+00
5)	-0.75201E+02	0.27114E-01	0.31192E+00
6)	-0.40916E+00	-0.57249E+01	-0.27857E+01
7)	-0.62301E+01	0.52436E+01	0.19007E+01
8)	-0.21157E+02	0.15089E+01	-0.26167E+01

NASA
National Aeronautics and Space Administration

Report Documentation Page

1. Report No.	2. Government Accession No.	3. Recipient's Catalog No.
NASA CR-4226		

4. Title and Subtitle
A Variable-Gain Output Feedback Control Design Methodology

5. Report Date
March 1989

6. Performing Organization Code

7. Author(s)
Nesim Halyo, Daniel D. Moerder, John R. Broussard, and Deborah B. Taylor

8. Performing Organization Report No.
FR-688106

10. Work Unit No.
505-66-01-02

9. Performing Organization Name and Address
Information & Control Systems, Incorporated
28 Research Drive
Hampton, VA 23666

11. Contract or Grant No.
NAS1-17493

13. Type of Report and Period Covered
Contractor Report

12. Sponsoring Agency Name and Address
National Aeronautics and Space Administration
Langley Research Center
Hampton, VA 23665-5225

14. Sponsoring Agency Code

15. Supplementary Notes
Richard M. Hueschen, Technical Representative, Langley Research Center
Final Report

16. Abstract

A digital control system design technique is developed in which the control system gain matrix varies with the plant operating point parameters. The design technique is obtained by formulating the problem as an optimal stochastic output feedback control law with variable gains. This approach provides a control theory framework within which the operating range of a control law can be significantly extended. Furthermore, the approach avoids the major shortcomings of the conventional gain-scheduling techniques.

The optimal variable-gain output feedback control problem is solved by embedding into the Multi-Configuration Control (MCC) problem, previously solved at ICS. An algorithm to compute the optimal variable-gain output feedback control gain matrices is developed. The algorithm is a modified version of the MCC algorithm improved so as to handle the large dimensionality which arises particularly in variable-gain control problems.

The design methodology developed is applied to a reconfigurable aircraft control problem. A variable-gain output feedback control problem was formulated to design a flight control law for an AFTI F16 aircraft which can automatically reconfigure its control strategy to accommodate failures in the horizontal tail control surface. Simulations of the closed-loop reconfigurable system show that the approach produces a control design which can accommodate such failures with relative ease. The technique can be applied to many other problems including sensor failure accommodation, mode switching control laws and superagility.

17. Key Words (Suggested by Author(s))	18. Distribution Statement
variable-gain output feedback, output feedback, stochastic optimal control, Multi-Configuration Control (MCC), gain scheduling, reconfigurable control, failure accommodation	Unclassified - Unlimited Subject Category 08

19. Security Classif. (of this report)	20. Security Classif. (of this page)	21. No. of pages	22. Price
unclassified	unclassified	96	A05

NASA-Langley, 1989